universität wien

MASTERARBEIT / MASTER'S THESIS

Titel der Masterarbeit / Title of the Master's Thesis

„Qualitative- and quantitative analysis of the metabolome of sweat sampled from the fingertips“

verfasst von / submitted by

Max Feuerstein, BSc

angestrebter akademischer Grad / in partial fulfilment of the requirements for the degree of

Master of Science (MSc)

Wien, 2018 / Vienna 2018

Studienkennzahl lt. Studienblatt / degree programme code as it appears on the student record sheet:	A 066 862
Studienrichtung lt. Studienblatt / degree programme as it appears on the student record sheet:	Masterstudium Chemie
Betreut von / Supervisor:	Univ.- Prof. Dr. Christopher Gerner
Mitbetreut von / Co-Supervisor:	----

Acknowledgements

First, I want to thank Univ. Prof. Mag. Dr. Christopher Gerner for the opportunity to write my master thesis under his supervision.

Then, I want to thank all members of the AG Gerner for their support during this work, their patience, collegiality, friendship and for being good examples on the human- and scientific level. Special thanks to Laura Niederstätter and Dr. Samuel Meier-Menches for their support during the practical work and the writing process, as well as to Rupert Mayer for his organizational support. Additionally, I want to thank Dr. Astrid Slany, Dr. Besnik Muqaku, Dr. Johanna Mader, Dr. Denise Wolrab, Dr. Andrea Bileck, Dr. Ammar Tahir, Lukas Janker, Benjamin Neuditschko, Peter Frühauf and Andrea Hilbert for the support and good advice during my time at the Department of Analytical Chemistry of the University of Vienna.

Most of all, I want to thank my family whose support allowed me to start- and finish my studies at the University of Vienna and made my journey into the world of chemistry possible.

Vienna, 2018

Table of contents:

Introduction:

Metabolomics:

The metabolome is defined as the entity of small molecules present in a biological sample, e.g. an organism, a cell or a biofluid, under certain experimental conditions (1). Therefore, metabolomics can be seen as a global approach to enlighten an organism's metabolome, which is connected to its development-, as well as to its physiological- and pathological states (2). The rapid technologic progress of the last decades led to the development of the so called -omics- type disciplines genomics, transcriptomics, proteomics and, more recently, metabolomics. The combined analysis of the genome, transcriptome, proteome and metabolome, whereas the metabolome has the closest relationship to the phenotype of an organism, allows deeper insights into the molecular mechanisms inside living organisms. Therefore, metabolomics can be seen as a valuable tool in modern systems biologic research (3; 4). Small changes in the expression patterns of proteins can have large effects on the concentrations of the related metabolites allowing a more accurate analysis and evaluation of metabolic pathways on the metabolomics level than on the protein- or RNA-level (1). Until recently, academic effort mainly focussed onto the genetic origin of chronic diseases, but, even though large genome profiling studies and the characterization of single nucleotide polymorphisms allowed gaining some fundamental biological insights, fewer diseases than expected could be explained by solely genomic centred research (2). Genome wide association studies were able to identify several genetic risk loci, but only superficial understanding of the biologic mechanisms behind many investigated diseases could be obtained. Hence, integration of metabolic characteristics into genomic data is a promising approach to overcome these drawbacks (5). Investigations of the metabolome, microbiome and epigenome suggest that environmental effects on states of health and disease might be more severe than previously expected. Moreover, there are several common diseases, as heart diseases, diabetes or hypertension which are closely related to alterations in the individual's metabolism (2). Metabolites can be defined as small molecules with a molecular weight less than 2000 Da and include peptides, amino acids, lipids, carbohydrates, organic acids, nucleic acids and vitamins of endogenous origin as well as exogenous substances as drugs, pollutants or toxins and all kind of other small molecules that can be absorbed and metabolized by an organism. Defining the human metabolome is a difficult task compared to the definition of the human genome or proteome, because the human metabolome not only depends on the genes of an organism but also on a wide range of environmental contributions, as the diet and the microflora inhabiting a human being (6). The food metabolome, known to contain more than 25000 substances, depends on the individual dietary habit and includes all metabolites digested and absorbed by the intestines, as well as products of biotransformation processes mediated by the gut microbiome (7). The gut microbiome has a great influence on the overall metabolic phenotype of the host organism

through metabolome-metabolome interactions, for example co-metabolism of substrates and metabolic exchange (8; 9). Investigation of dietary contributions to the metabolome allows discovering new dietary biomarkers and bioactive compounds, as well as the association of diseases with dietary factors (7). Metabolomics can be used as a tool to analyse exogenous metabolites as markers for environmental inputs, as well as endogenous, which means host derived-, metabolites being closely connected to the output of the human genotype (2), but depend on an individual's diet as well (7). Therefore, metabolomics approaches enable the investigation of the currently ongoing events in cells and organisms, while genomic approaches for disease related risk evaluation can be used only for the potential range of action of an organism (2). Because metabolomics experiments aim to investigate a wide variety of analytes with different (chemical) properties at different abundance levels, the development of analytical strategies stays challenging in terms of sample preparation, analyte separation- and detection. Metabolic variations, caused by the circadian rhythm or the diet, can add some degree of complexity to the issues opposed during metabolomics experiments (3). Selecting the adequate sample type, e.g. tissues, cells or biofluids, and -sampling procedure depends on the task and is crucial for the success of metabolomics experiments, especially if metabolites with fast metabolic turnover rates are investigated. Ideally, a sampling procedure allows maximum representativeness, while its invasiveness should be kept as low as possible (1). At least 2000 different primary metabolites are expected in human beings, a number that drastically increases, when secondary metabolites are considered as well (3). Currently, the human metabolome database (http://www.hmdb.ca/), which claims to provide the most current and most comprehensive organism-specific metabolomics data base (6), lists a total number of 4460 detected metabolites of which 3582 metabolites are classified to be endogenous (10).

Different analysis strategies can be used to investigate the metabolome: In targeted metabolomics experiments single analytes or a subset of the total metabolome are analysed using a set of best performing, preferably selective methods to allow a quantitative evaluation of the target analyte(s) in the sample material, while untargeted metabolomics allows the identification of unknown analytes or biomarkers in biological samples. The metabolite profiles can then be related to different biological states of health and disease. Typically, a wide range of small molecules including amino acids, organic acids, sugars, lipids, vitamins as well as exogenous substances can be analysed simultaneously in a single analytical run including highly abundant species as well as low abundant ones (4; 2; 11). To enable bias-free in-depth analysis of a wide range of metabolites, untargeted experiments are including non-selective sampling, sample preparation and analysis methods (11). Both, sampling and sample preparation still represent the major limitations as well as the major sources for errors in metabolomics experiments (1). The success of every analytical experiment highly depends on the quality of the sample preparation. While tailor-made procedures depending on the target analyte are recommended

in quantitative metabolomics experiments, all small molecules can be regarded as targets in untargeted methods and sample preparation needs to avoid the discrimination of single analytes. Typically, but not necessarily, sample preparation can include analyte extraction methods including liquid-liquid extraction, solid-phase extraction and others (3).

Until today, several abnormalities in the individual metabolism could be related to pathologic states of subjects, as atherosclerosis or the risk for type-2 diabetes (2; 12; 13). Moreover, it is highly evident, that disturbed metabolism plays a key role in other pathologic states, as Alzheimer disease or tumorigenesis (2). Personalized medicine based on the combination of genotypic- and molecular profiling, including genomics, transcriptomics, proteomic and metabolomics analysis, is expected to improve medical risk evaluation as well as medical treatment of diseases (14). The use of metabolomics in clinical trials allows monitoring drug compliance- and metabolism or adverse responses via toxicity biomarkers more easily and big confidence is set into the possibility of personalized treatment strategies based on the individual metabolic biomarker profile of the patient. For example, evaluating the metabolic profile after the intake of a combination of harmless drugs, the “Pittsburgh Cocktail”, can be used to evaluate individual variations in the activity of the most important enzymes involved in drug metabolism like cytochrome P450 (CYP) (2), whereas CYP is a family of hepatic enzymes being responsible for the major part of the human drug metabolism and allows more accurate drug dosage (15). The large difference of the physical- and chemical properties of possible metabolites investigated makes it difficult to work with single platform instrumentations and often requires an analyte separation step prior to analyte detection (1; 3). Most frequently used techniques in the field of metabolomics are gas chromatography hyphenated to mass spectrometry (GC-MS), liquid chromatography coupled to MS (LC-MS^n) and nuclear magnetic resonance (NMR) based techniques. Capillary electrophoresis (CE) can be used as an alternative for analyte separation and allows the generation of complementary information to that provided by methods based on chromatography (1). Mass spectrometry based techniques are often the methods of choice, because they enable fast, sensitive, quantitative and in-depth analysis of complex samples (2).

High performance liquid chromatography (HPLC):

Methods used for analyte separation allow the reduction of sample complexity and are of special interest for analytical chemists, whereas high performance liquid chromatography (HPLC) is one of the most prominent techniques. In general, a chromatographic system consists of a mobile phase flowing through a stationary phase. Analyte separation is mediated by the differential partitioning of the analytes between the two phases depending on their chemical properties. This leads to a spatial separation and therefore different elution times of the analytes depending on the applied elution method. Several liquid chromatographic techniques can be used to separate the analytes in solution including

reversed phase- (RP), normal phase- (NP) or hydrophilic interaction chromatography (HILIC) besides others. After loading of the sample under aqueous conditions onto a RP-column, the analytes are separated based on their relative hydrophobicity by interacting with hydrophobic residues immobilized to the column material. The analytes are then eluted with a mobile phase that contains an organic solvent (16; 17). The use of small particle size packing materials with particle sizes below 2 µm enabled operating with higher pressures, minimized the drop of separation efficiency caused by elevated flow rates and significantly improved the efficiency of HPLC separations in recent years. This new technical optimization is named Ultra Performance Liquid Chromatography (UPLC). In combination with monolithic capillary columns and fused core particles, UPLC allows the use of shorter columns and increased flow rates leading to optimized separation speed and outstanding chromatographic resolution (18; 4). The development of hyphenation interfaces connecting HPLC to mass spectrometry analyzers as well as the availability of improved bioinformatics tools drastically influenced bioanalytical applications in the recent past (17).

Mass spectrometry

Mass spectrometry is an analytical technique capable of separating and detecting ionized analyte molecules based on their mass-to-charge ratio (*m/*z). Analytical useful signals arise from interaction of the separated molecules with a mass detector followed by computational data analysis. The resulting mass spectrum is composed of the relative abundances of the detected molecular ions and the corresponding *m/z* values (19). Mass spectrometric signals are proportional to the analyte's concentration. Nevertheless, the use of an internal standard (IS) is highly recommended to compensate analyte loss during sample preparation and variations caused by the mass spectrometer itself. The IS should possess high structural similarity to the target analyte. Therefore, the ideal IS can be obtained by synthesis isotopically labeled molecules of interest (19). Mass spectrometry is the most frequently used technique for high throughput analysis due to its high sensitivity and stability, its wide dynamic range and the short analysis time (4). Because of its applicability to a wide range of target analytes, the possibility of multi target analysis and fast assay development tandem mass spectrometry (MS/MS) hyphenated to HPLC has become an important technique in clinical analytical chemistry within the last 10-15 years (20; 21), especially when it comes to therapeutic drug monitoring, the diagnosis of metabolic disorders (21), microbiology, toxicology and endocrinology, besides others (20). The introduction of electrospray ionization (ESI) technique allowed "soft" and relatively non-specific ionization of molecules from solution with high ionization efficiency, whereas generated analyte ions are relatively stable and less prone to decay events when compared to other ionization techniques. Today, ESI is one of the most frequently used techniques for the analysis of liquid samples and, especially due to its compatibility to

chromatography based separation techniques, provides a powerful tool for the (bio-) analytical chemist (22).

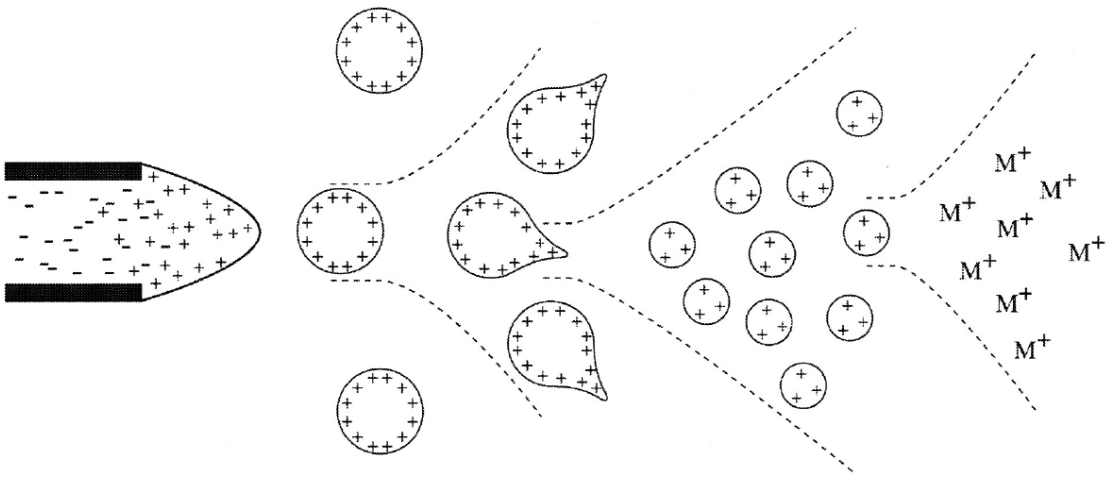

Figure 1: The principal of electrospray ionization (ESI) (19).

Figure 1 shows the principles of the ESI-ionization mechanism schematically. During the ESI process a potential is applied to a liquid inside the tip of a stainless steel capillary (20). While coulomb attraction forces pull the liquid towards the counter electrode, surface tension tends to hold the liquid within the tip of the capillary. After a specific voltage threshold is reached, the liquid surface at the end of the nozzle changes its elliptical shape, forms a so-called Taylor cone and a spray is emitted from its tip. The resulting spray is composed of fine dispersed and charged liquid droplets close to their Rayleigh limit (22). The size of the droplets decreases continuously due to evaporation of the solvent caused by elevated ESI-source temperatures and nitrogen gas flow, whereas the application of an inert nebulizing gas allows the use of higher flow rates (19). Because droplets are not perfectly symmetrically the Rayleigh limit is reached locally and Taylor cone formation starts again. Smaller secondary droplets are ejected and analyte ions are released from the surfaces of charged droplets with radiuses in the nanometer range (22; 17). After entering the gas phase analyte ions are accelerated into the mass analyzer (19). High resolution mass spectrometers, as time of flight- (TOF) or Orbitrap detectors, can generate data with (sub-) ppm mass accuracy and allow the calculation of the analyte's elemental composition based on its mass-to-charge ratio (*m/z*). Recent instrumental developments of high resolution mass spectrometers, i.e. smaller Orbitrap mass analyzers, enable faster cycling times and therefore coupling to UPLC with narrow peak widths in the low second range (4).

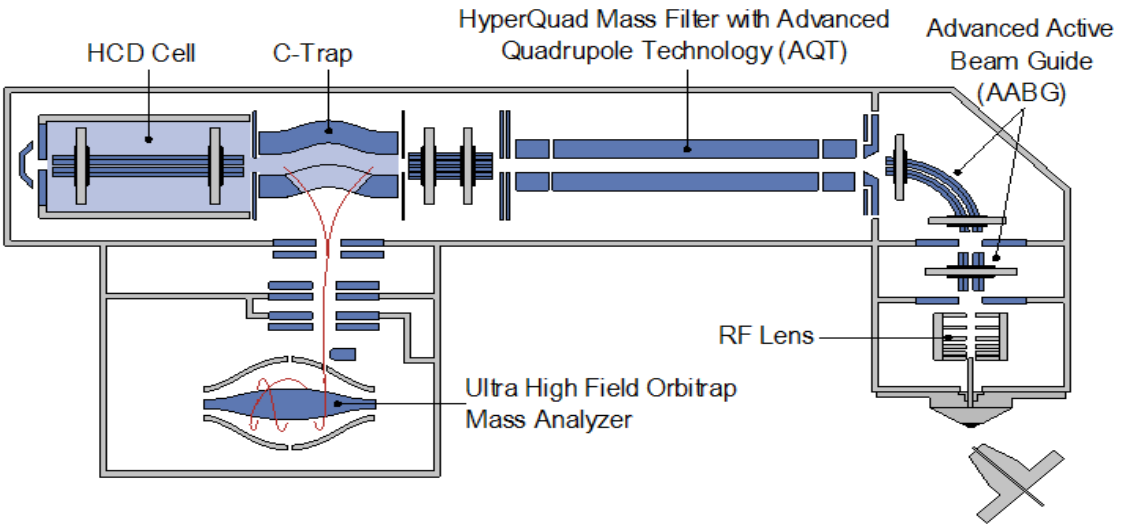

Figure 2: Schematic representation of the Thermo Scientific™ Q Exactive™ HF mass spectrometer (http://planetorbitrap.com (23)).

The Thermo Scientific™ Q Exactive™ HF mass spectrometer consists of a quadrupole, a high field orbitrap mass analyzer, a C-Trap and a collision cell (HCD cell) (24) and allows a MS^1-resolving power of 240000 (25). The orbitrap analyzer is an alternative type of ion trap that is able to bring ions onto stable orbits around a spindle electrode in the centre of the orbitrap. Radial oscillation depending on the *m/z*-ratio of the analyte ions can be observed, whereas electrodes at the endcaps of the detector prevent lateral loss of the oscillating ions. The current induced by the oscillating ions can be detected by an external electrode and yields, after fourier transformation of the initial signal, a mass spectrum (17). Although elemental composition can be calculated precisely based on high resolution full MS data, unambiguous identification of metabolites can only be reached by analysis of the fragmentation fingerprints obtained from multistage-, or tandem MS experiments (4). In tandem MS a parent ion is selected based on its *m/z* and enters a collision cell, where the target analyte ion collides with a collision gas, for example nitrogen, resulting in fragmentation of the parent ion. Later on, fragment ions can be analyzed using a second mass detector (20). Searching tandem mass spectra against reference databases is the fastest and most comprehensive approach for meaningful interpretation of mass spectrometric data in metabolomics experiments. In recent years several databases could be established providing measured- as well as computationally generated reference spectra of highly structurally diverse metabolites. Collision induced dissociation (CID) and higher energy collision-induced dissociation (HCD), used for orbitrap-type mass spectrometers, are the most common ion activation modes for high resolution tandem MS, both typically with collision energies in a range between 0-100eV. Stepped or ramped collision energies can ease compound identification and annotation in MS/MS database searches significantly. In automated search algorithms candidate molecules are selected based on the *m/z* of the precursor ion followed by scoring the similarities of the generated fragment spectra regarding mass accuracies of the fragments, as well as their intensity distribution. Natrium- or ammonium

adduct formation, as well as water loss of the target analytes can be considered in the interpretation of the generated mass spectra (25). In recent years improvements of bioinformatics tools eased processing of mass spectrometric data, a lot. Fully automated data interpretation algorithms in combination with reviewed mass spectrometry databases are allowing fast interpretation of complex datasets with minimal effort (4). With mzCloud (https://www.mzcloud.org) a tool to overcome the lack of publicly available and curated spectral-tree databases was introduced recently. In addition to an extensively curated tandem MS database, including high- and low resolution mass spectrometric data obtained under various experimental conditions (collision energies and isolation widths, e.g.), it offers the possibility to find structures of yet unknown metabolites based on known fragment patterns of structural subunits using the Precursor Ion Fingerprinting technique (4).

Coffee and cocoa products:

Coffee is the second most consumed drink after water worldwide and its consumption was demonstrated to affect the human health in several ways (26; 27). Although about 70 species of *coffea* are known to exist only the beans of c*offea arabica* and c*offea canephora* are of commercial interest. Green coffee beans are mainly composed of carbohydrates (about 60% of the dry weight), followed by lipids, proteins, peptides and amino acids, a variety of polyphenols, as well as nitrogen containing compounds, as caffeine (CF) or trigonelline (27). Cultivation of the coffee plant has a long history. It was first discovered in Ethiopia (27) and is known to be cultivated since the 15th century (28). After being harvested, the coffee beans are dried, roasted and powdered, whereas its typical taste and fragrance develop during the roasting process. The harsh reaction conditions during the roasting process lead to the transformation of the chemical composition of the coffee bean via pyrolysis of organic compounds, caramelization or the Maillard reaction, leading to a wide variety of volatile substances especially important for the odour of roasted coffee (27). Beneficial effects of coffee consumption on the human health have been described, including a reduced overall mortality as well as a reduced risk for several types of cancer and chronic diseases, like cardiovascular diseases, Parkinson's disease, Alzheimer's disease, type-2 diabetes and depression (27; 26). Accumulation of the effects of several phytochemicals present in coffee, including improved insulin sensitivity, improved glucose metabolism, as well as delayed intestinal absorption and reduced storage of glucose, seems to be responsible for the negative correlation between type-2 diabetes and coffee consumption (29). Overall, more than 1000 compounds have been detected in coffee beverages with caffeine, the chlorogenic acids (CGAs), trigonelline, the diterpenes cafestol and kahweol or melanoidins formed during the roasting process being discussed as the main classes of bioactive compounds in coffee (26; 27; 28). Most of the beneficially properties of coffee consumption are related to the antioxidative potential of the bioactive compounds found in the brew, as well as their protective properties against diseases related to subclinical

and chronic inflammation processes. Coffee consumption seems to attenuate the release of several mediators of the inflammatory response, such as interleukine 6 or tumor necrosis factor alpha, although the data is somewhat inconsistent (26). More recently, *in vitro* and *ex vivo* experiments using isolated peripheral blood mononuclear cells could show that coffee consumption either activated or deactivated inflammatory response significantly depending on the investigated individual. Nevertheless, the reasons for differing influence of coffee ingestion onto the response to inflammatory activation could not be revealed (30). Another study indicated strong interindividual differences in the activation of the antioxidative response in humans after the consumption of coffee (31). Independent from their possible beneficial effects on human health, the bioactive compounds found in coffee beans may have different fates during processing of the coffee bean and absorption, metabolism, distribution and secretion by the human organism (32). The time of a phytochemical's maximum plasma concentration is closely related to the investigated compound's molecular properties, especially its lipophilicity, polar surface area and molecular mass, whereas absorption can occur either in the upper- or lower intestine. Dietary intake form, for example solid, semi-solid or liquid, is another major factor influencing a compound's absorption peak (33). Additionally, the molecular size, the possibility to accumulate in tissues, the rate of metabolic conversion or the rate of urinary elimination are highly influencing the bioavailability of exogenous substances and can lead to a large divergence between the concentrations of a target molecule in nutritional sources and its concentration in the target tissue (34). While CF is very thermostable, the CGAs and trigonelline are substantially degraded during the roasting process yielding caffeoyl quinide (4-caffeoylquinic-1,5-lactone), caffeic acid and catechol as major degradation products in the case of the CGAs, while the main products of trigonelline degradation are niacin and N-methyl pyridinium (32). Although nicotinic acid is highly abundant in coffee, it was not detected in human plasma after coffee intake while plasma levels of less abundant nicotine amide increased (35). Referring to literature the amino acid content of coffee beans is dominated by asparagine, glutamic acid, alanine, aspartic acid and lysine (27).

The use of cocoa beans, the ground seeds of the *Theobroma cacao* tree's fruits, has a history exceeding three millennia. Originally cocoa was consumed as a tart-tasting and, most likely, slightly alcoholic beverage by Olmec, Maya and Aztec societies. Its consumption was associated with strength and virility by the Aztecs (36) and played an important role as status symbol, currency or in rituals (37). Although processing of cocoa has changed drastically, chocolate and cocoa products are still associated with well-being and health benefits (36). Cocoa contains several bioactive phytochemicals, mainly flavonoids and other phenols, as well as the methylxanthines CF and theobromine (TB) (34) with TB being the mayor purine alkaloid (38). Cocoa products have an antioxidant potential that exceeds most other flavonoid containing foods or drinks due to the high abundance of radical scavenging flavonoids (34). Epidemiological studies could reveal a connection between the consumption of polyphenol-rich food

and cardiovascular health (39). Besides cocoa, consumption of flavonoid rich comestibles as red wine, black tea or grape juice has been associated with improved endothelial vasodilation (39; 40; 41; 42). Procyanidins, polymers formed of epicatechin subunits (43), are the most abundant species of biological active compounds in chocolate, but due to their low concentrations in human plasma bioavailability tends to be low compared to highly bioavailable TB, CF or (-)-epicatechin (34). TB, which can act stimulatory onto the central nervous system, is responsible for the bitter taste of cocoa (36). Several studies are indicating a beneficial role of chocolate and cocoa for the cardiovascular health. Chocolate consumption can lower LDL cholesterol abundance, while it tends to increase HDL cholesterol levels in human plasma. Anti-inflammatory properties combined with inhibition of platelet activation can lead to a reduced risk for arterial thrombosis (34; 44). Additionally, regular chocolate consumption is associated with a decreased risk for insulin resistance (45).

Xenobiotics in coffee and cocoa and related metabolites:

Caffeine and its metabolites:

CF, the most frequently consumed physio-stimulating substance, is mainly ingested as a component in beverages like coffee, tea or energy drinks (28). Typically, a cup of coffee contains between 50 mg and 100 mg CF, but the amount can vary significantly depending on the coffee beans, the roasting-, as well as brewing technique used (27). Its biosynthesis in the coffee plant is a four-step process. First xanthosine is methylated yielding 7-methylxanthosine, which is hydrolysed yielding 7-methylxanthine (7-MX). N-methyltransferase converts 7-MX via a two-step methylation and TB into CF (38). The purine alkaloid CF as well as its primary metabolites TB, paraxanthine (PX) and theophylline (TP) are highly bioavailable in human beings and able to distribute freely within the whole body (46). After oral administration CF is absorbed nearly completely in the gastrointestinal tract without significant first pass effect (47), reaches its maximum concentration in the body within 60 min and distributes to all kind of tissue including the brain, whereas its moderate lipophilicity allows CF to pass all biological membranes. Typically, CF possesses a half life time of approximately 5 hours in human plasma, but elimination is delayed in neonates, during pregnancy or in case of hepatic diseases (27; 47). The main part of the ingested dose of CF is absorbed by the small intestine, while approximately 20% of the overall CF uptake takes place in the stomach (46). After passing the blood-brain barrier CF non-specifically antagonises the adenosine receptor subtypes A_1 and A_2, causing the well-studied physiologic effects associated with CF consumption (27; 48). The interaction of CF with adenosine receptor associated pathways influences vasodilation, smooth muscle contraction, as well as the heart rate (28). Adenosine receptor antagonism increases levels of the neurotransmitter dopamine, which reduces fatigue and enhances perception and alertness. Heart rate increases and the blood pressure rises leading to several possible

adverse reactions including headache, nervousness, palpitations, insomnia or tremor, in case of extensive consume. Nevertheless, the dose-response relationship is highly variable between individuals and depends on the consumer's behaviour regarding CF intake (27; 49). CF consumption was associated with reduced risk for suffering type-2 diabetes and may play a protective role against cardiovascular diseases (28) and Parkinson's disease. On the other hand, CF consumption, in case of maternal intake during pregnancy, is associated with decreased birth weight and an increased risk of pregnancy loss (26). In the human liver CF is mainly metabolized by several isozymes of cytochrome P450 (CYP), whereas the CYP1A2 isoform, which can be solely found in the liver, plays the dominant role for the demethylation and oxidation of CF (27; 46). The major degradation pathway in humans starts with 3-N-demethylation by CYP1A2 yielding PX as primary metabolite (46; 47). It contributes to approximately 81.5% of the demethylation products of CF followed by TB (10.8%) and TP (5.4%) (46). Besides 1-, 3- and 7-demethylation, CF can be oxidized to 1-, 3-, 7-trimethyluric acid after 8-hydroxylation (47). The three dimethylxanthines TB, TP and PX formed during the first demethylation reaction are further metabolized to 1-, 3-, or 7-MX. After oxidation to the corresponding methyl-uric acids the conversion into substituted uracil- or allantoin derivatives via ring opening is possible (27; 46). Ratios of the metabolites generated during CF degradation can be used to evaluate the activity of the involved enzymes, as CYP1A1, CYP1A2 or N-acetyltransferase 2 (NAT2) (46; 47). CF has great potential for CYP phenotyping in humans due to its favourable pharmacokinetic properties as well as its safe applicability (47). The CYP1A2 activity is not distributed normally within several investigated populations. Instead, a trimoidal distribution of CYP activity indicating separation into groups of slow-, intermediate- and fast metabolizing individuals is proposed, whereas 50% of the Caucasians are slow- or intermediate metabolizers (46; 50). Renal clearance dominates the excretion of CF and its metabolites, although only 2% of the ingested CF can be found in human urine in a non-metabolized form due to efficient reabsorption of CF in the renal tube in combination with intense metabolism in the liver. The pharmacokinetic behaviour of CF as well as its metabolites can be influenced by diseases, especially of the liver, pregnancy, or the use of oral contraceptives as well as components found in the diet, including broccoli or alcohol (46). Correlation of the CF concentrations in serum and saliva (46), as well as concentrations found in blood and sweat obtained from a fingerprint have been demonstrated (51; 52). The possible metabolic routes of CF and its metabolites are extensively resumed in Figure 3.

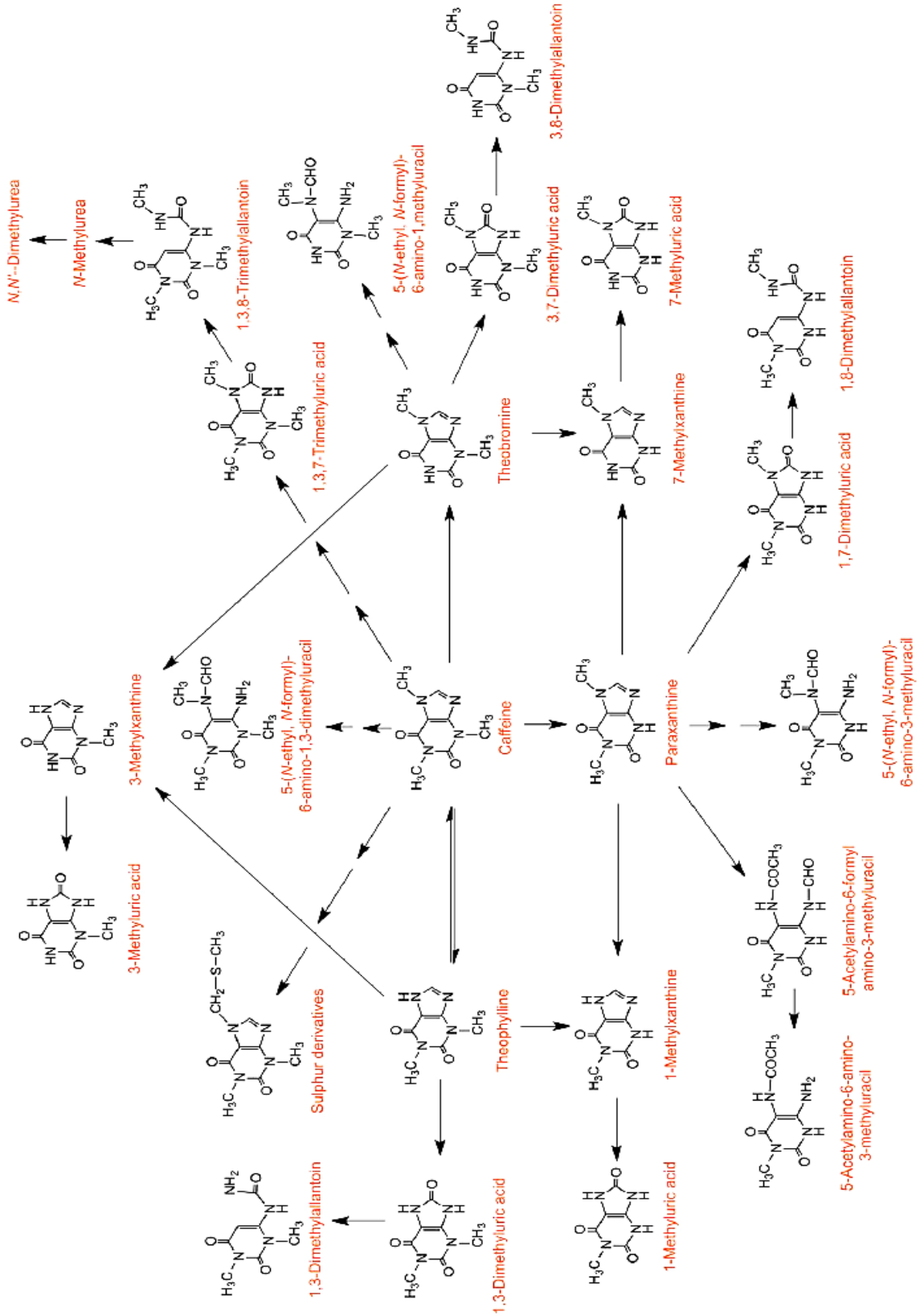

Figure 3: Possible metabolic routes for the degradation of CF in humans (27).

Trigonelline:

The pyridine alkaloid trigonelline is discussed to have potential diabetes preventing properties and represents about 1% of the dry weight of green coffee beans (27). It is a phytohormone present in several other comestibles, as legumes (53) and might act as a neuroprotective agent (54). During the roasting process of coffee beans trigonelline is partially degraded yielding nicotinic acid (niacin) and other pyridins (27; 35). Studies indicated a half-life time in humans of approximately five hours, whereas trigonelline can be found 15 min after coffee intake in human plasma reaching its maximum concentration approximately 2.5 hours after the ingestion of coffee (27; 32). Most of the ingested amount of trigonelline is excreted unchanged in human urine (35).

The chlorogenic acids (CGAs):

The chlorogenic acids (CGAs) are a class of biological active organic acids naturally occurring in coffee, pomme-fruits, blueberries and several other fruits. Coffee is the richest dietary source of CGAs for most humans. While roasted coffee beans contain 2-5 g/100 g, 20 mg up to 675 mg of CGAs can be found in 200 mL of coffee, depending on the coffee bean itself, the roasting process and the brewing technique used (55; 56). Chemically speaking, the CGAs are consisting of the esters of quinic acid with the hydroxycinnamic acids, as caffeic acid, ferulic acid or *p*-coumaric acid. Naturally occurring CGAs include isomers esterified at the 3-, 4- or 5- position of quinic acid, as well as di-, tri- and tetra esters of caffeic acid and mixed di-esters (56). The caffeoylquinic acids (CQAs), dicaffeoylquinic acids and feruoylquinic acids are the most prominent subclasses found in coffee. Together they are accounting for 92-95% of the overall CGAs found in roasted coffee beans, with 5-O-caffeoylquinic acid (5-CQA) being responsible for 35% of the total CGA content (55). CGAs and their degradation products undergo intense metabolism processes yielding a wide variety of metabolites including the (di-)hydroxycinnamic acids as well as their sulfates and glucuronides. Ferulic acid and feruoyl sulfate can be detected in human plasma about one hour after coffee intake (32), while levels of CGA metabolites as dihydro-caffeic acid and dihydro-ferulic acid, most probably formed by the intestinal microflora and absorbed in the colon, show peaks 7-11 hours after coffee ingestion (57). High bioavailability of the major CQA species present in coffee was demonstrated in an intervention study by

Monteiro et al. The pharmacokinetic behavior of the CQAs appeared to be very complex, including high interindividual variability and dual concentration peaks in plasma for all CQAs. This indicates a complex absorption process, with parts of the total CQA content being absorbed in the stomach, while another fraction is possibly absorbed in the small intestine. The plasma extracts were treated with sulafatase- and β-glucuronidase prior to the analysis of CGA-content and the sum of free- and conjugated CGAs was analyzed quantitatively (55). However, later studies showed some contradictory image of the kinetic behavior of CGAs in human plasma after ingestion of coffee: Only a single plasma peak

of CQAs was observed 30-90 min after coffee consumption in a more recent study using a similar experimental design as Monteiro et al. including β-glucuronidase- and sulfatase treatment. The results confirmed the high interindividual variability of the plasma appearance of CGAs, but indicated a low overall bioavailability of CGAs caused by poor absorption in the small intestines (57). In 2014 Lang and co-workers analyzed plasma samples after ingestion of coffee without enzymatic treatment of the samples prior to analysis. Non-metabolized 5-O-caffeoylquinic acid (neochlorogenic acid) could only be detected at trace levels in some individuals approximately one hour after coffee intake, while CGA metabolites formed by the microflora of the intestines were detected in human plasma six hours after coffee intake (32).

(-) Epicatechin:

Flavanols are polyphenolic compounds of the secondary plant metabolism commonly found in most higher plants and represent the major class of antioxidants found in cocoa (36; 39). They are able to reduce platelet- and endothelial cell activation and have a regulatory influence onto the inflammatory response (36). Additionally, flavanol intake can have beneficial effects on the blood pressure, insulin resistance, glucose tolerance and may improve the immune response leading to an overall decreased risk for cardio vascular diseases and reduced overall mortality (39; 44). Epicatechin is responsible for approximately 35% of the total phenolic content present in cocoa. Plasma concentration peaks of monomeric and polymeric flavanols can be observed two hours after cocoa ingestion followed by total elimination within 6 hours (43). Epicatechin is discussed to be the main actor responsible for the beneficial effect of flavanol rich cocoa products on cardiovascular health (36; 39). Epicatechin is metabolized to sulfates, glucuronides and methyl conjugates, whereas 4‘-O-methyl-epicatechin-O-β-D-glucuronide isomers are its main metabolites (43; 39). Glucuronidation can take place either at 3‘-, 5‘-or 7‘-position of the flavanol ring system, whereas 5‘- and 7‘-glucoronide formation is favored (39).

The secretory glands of the skin:

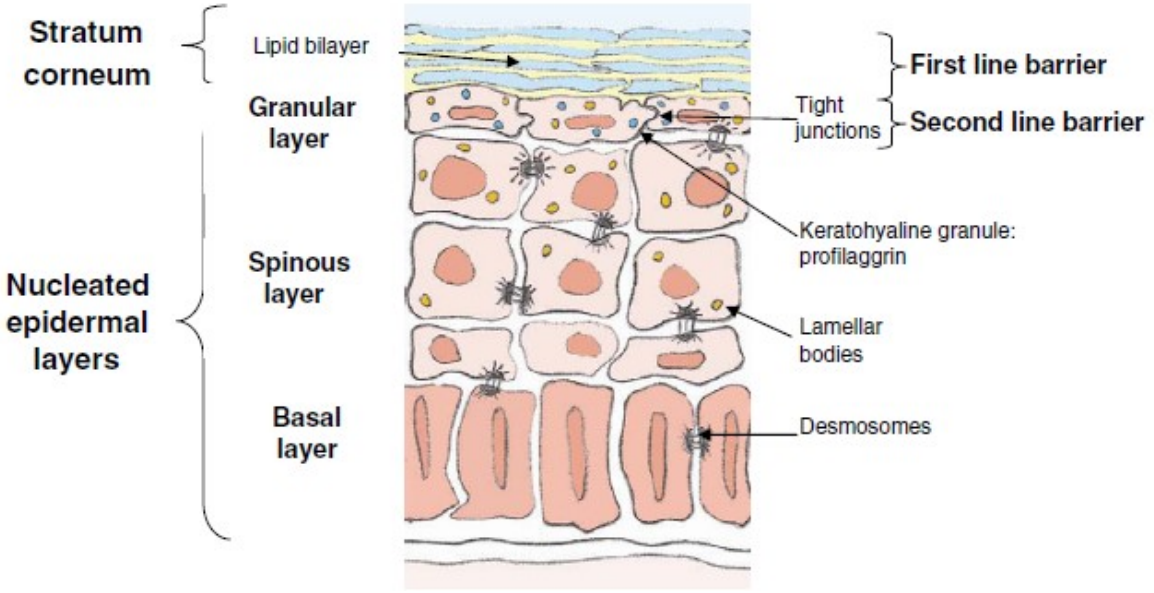

Figure 4: Structure of the human epidermis consisting of several layers. From inside out: basal layer, spinous layer, granular layer and *stratum corneum* (SC) (58).

The human skin, an organ with an overall surface area of 1.5-2 m^2, separates the body's "inside" from the "outside" (59). It consists of the dermis and the epidermis, whereas the *stratum corneum* (SC), part of the epidermis and outermost layer of the skin, represents the interface to the surroundings and a first barrier. It prevents the body from excessive water loss as well as from infiltration of unwanted exogenous materials. Keratinocytes, the most abundant cells within the epidermis, are responsible for the secretion of most structural proteins, as filaggrin, and the lipid content. Lipids are forming the protective layer of the SC *t*ogether with structural proteins, hydrolytic enzymes, acids, antimicrobial peptides and several layers of corneocytes (58; 60). A detailed view onto the structure of the epidermis is given in Figure 4. The dermis is situated between the epidermis and the innermost part of the skin, the fat compartment of the hypodermis. It is composed of several different cell types, elastic fibres and collagen. Additionally, the dermis possesses a strong net of blood- and lymphatic vessels and hosts sweat- and sebaceous glands (58). The secretory glands of the skin can be classified into two groups: the holocrine glands, namely sebaceous- and meiboniam glands, and the merocrine-, or sweat glands, which can be further subdivided into eccrine-, apocrine glands and, described more recently, the apo-eccrine glands (61). Eccrine sweat glands can be found all over the human body except at the lips, clitoris or the external ear canal (62). Apocrine sweat glands exist already in new-borns and are activated during the adolescence. In embryos they are localized all over the body, but are solely present at hairy body areas, e.g. the axillae or the genital area, in adults (63; 64). After bacterial decomposition, apocrine secretion gets its characteristic odour and becomes the major contributor to the odour of the human skin (64). Sebum, a complex mixture of lipids, including triglycerides, free fatty acids, squalene,

cholesterol and wax esters, is secreted by the sebaceous glands (65; 66). Normally, sebaceous glands are distributed over the majority of the body's surface, except the palms and the soles, with high glandular densities found at the face, the scalp and the upper trunk. Sebum plays an important role in preventing bacterial or fungal infections of the human skin and maintaining its moisture (65).

An individual's total water loss through the surface of the skin can be divided into active sweating and insensible perspiration. Insensible perspiration is caused by a combination of water diffusion following the vapour pressure gradient within the SC and basal sweat flows provided by non-activated sweat glands. Its extent varies between different parts of the human body with water losses from the hands and feet being approximately two to four times higher than losses from other parts of the body's surface (61). Although insensible, due to low flow rates and reabsorption of water in the sweat duct, sweating in resting thermoneutral individuals is still mediated via impulses of the vegetative nervous system (61; 67). The average palmar sweat rate of resting individuals at room temperature was determined to be approximately 100 nL/cm^2/min (68). Other authors measured basal sweat rates of approximately 180 nL/cm^2/min at 25 °C and similar basal palmar sweat rates at temperatures up to 34 °C (69). Nevertheless, it should be noted that absolute quantities can vary considerably depending on the investigated individual as well as the experimental method used, whereas the amount of water lost can be determined either gravimetrically or using hygrometry (61). Although palmar sweat glands can be activated thermally, powerful stimulation by a wide variety of non-thermal signals (61), including physical exercise, sensory- and mental stimuli or skin pressure, is possible (67). Sweat secretion from the surface of the palms can be induced by mental or emotional stress as well as noxious stimuli and is thought to be mediated by either the central sympathetic nervous system or the sympathetic reflex (68). Differences between sweat secretion rate and the rate of its reabsorption during the passage of the sweat duct as well as differences in the cholinergic sensitivity and glandular densities lead to regional variations of sweat rates. Highest glandular densities (approximately 350 glands per cm^2) in combination with lowest glandular flow rates can be found on the palms and soles of the feet with the volar surface of the finger providing even higher glandular densities exceeding 500 glands per cm^2 (61). In general, sweat is a clear and hypotonic fluid produced by the secretory glands of the epidermis. It is a slightly acidic highly diluted aqueous solution with a pH ranging from pH 4 to pH 6.8. Although its main component is water (about 99%), several electrolytes, metabolites as urea, pyruvate, or lactate, xenobiotics and their metabolites, amino acids, peptides and even proteins can be found in sweat. Sweat rates are naturally increasing due to nervousness, stress, exercise and high ambient temperatures, but can also be influenced by relative humidity, hormonal imbalances or ingested foods and medication (70). Sweating is essential for the regulation of human body temperature and closely related to both, human brain- and skin temperature. Because heat loss mediated by sweat evaporation

is crucial for human survival, approximately two million eccrine sweat glands can be found on a standardized individual of 170 cm height and 70 kg weight (61; 71). Aquaporins, membrane channel proteins for the transport of large amounts of water, have been identified in the apical membranes of human sweat glands (71).

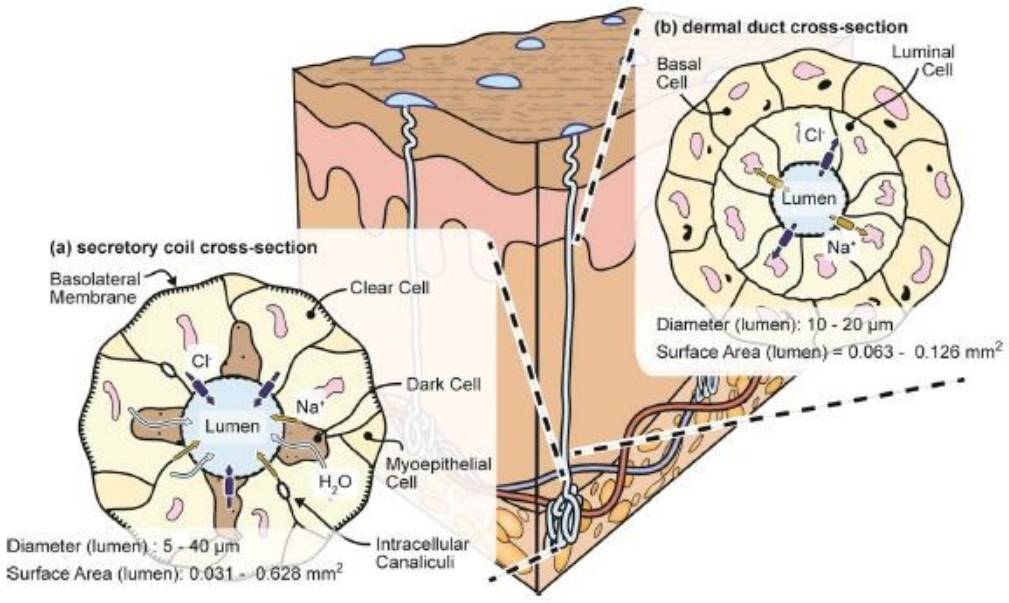

Figure 5: Structure of the human skin and human eccrine sweat glands, including cross sectional illustration of (a) the secretory coil and (b) the dermal duct (72).

Figure 5 shows the structure of human eccrine sweat glands including cross sectional views onto the secretory coil and the dermal duct of the gland. It consists of a secretory coil, a dermal duct and an upper coiled duct with an expanding diameter, penetrating the skin and forming a sweat pore (61; 72). For an optimized blood supply, the secretory coils are encompassed by capillary cages (61). Each coil is composed of three different types of cells, the clear cells, which are the origin of the secreted *preliminary* or *primary* sweat, dark cells, which are discussed to play a major role in the membrane cellular transport of sweat constituents and the supporting myoepithelial cells. The dermal duct consists of a bilayer of basal- and luminal cells, which form microvilli for improved absorption and secretion properties due to an enhanced surface (72). The sweat rates of active eccrine sweat glands are naturally not exceeding 5-10 nl/min/gland, but can be increased yielding up to 20 nl/min/gland, in case of sweat induction using pilocarpine. On the other hand, swelling of the SC can reduce the diameter of the upper coil, resulting in reduced flow rates, especially, where the SC is thick (e.g. the fingertips) (72). Regarding natural sweat secretion, the neural pathway of sweating has its starting point in the primary thermoregulatory centre, which is located in the hypothalamus (71). It reacts to changes of the body temperature detected by central or peripheral thermoreceptors (61). Eccrine sweat secretion is then induced by the release of acetylcholine by the cholinergic terminals of the sympathetic nerves connected

to the eccrine sweat gland. Additionally, sweating can be stimulated locally by the release of acetylcholine after an axon reflex. Especially at low- and medium sweat rates the rapid degradation process of acetylcholine via hydrolysis by the acetylcholinesterase plays a key regulatory role (71). The mechanism of sweat secretion is discussed to rely on a Na^+-K^+-Cl^- co-transport model. After stimulation of the cholinergic nerve ends, intracellular Ca^{2+} concentrations in sweat gland cells increase due to extracellular input from the interstitial fluid as well as intracellular Ca^{2+} release from the endoplasmic reticulum. Following this activation step, K^+ is pumped across the basolateral membrane into the stroma, while Cl^- enters the secretory lumen. The now formed chemical gradient induces Na^+, K^+ and Cl^- co-transport into the cell followed by recycling of Na^+ and K^+ into the interstitium, while Cl^- enters the secretory lumen. Afterwards charge neutrality is re-established by Na^+ fluxes via intracellular junctions and finally, due to the high osmolality of the lumen, water derived from the surrounding cells flows into the secretory coil. The resulting *preliminary* sweat is pumped through the dermal duct, where Na^+ and Cl^- ions are reabsorbed by specific transmembrane proteins (72; 73). Cholinergic sensitivity of sweat glands can be used to evaluate the enervation of the investigated skin area. Recently a quick and easy test for the diagnosis of diabetic neuropathy has been developed using the amount of secreted sweat from the feet to estimate sudomotor dysfunction and therefore cholinergic enervation of the feet (74). Small molecules can enter eccrine sweat using various transport mechanisms, depending on the molecular properties. In case of intermediate hydrophobicity combined with sufficient solubility in water, molecules, for example ethanol, are able to diffuse passively across membranes leading to a good correlation of the ethanol concentration in blood and sweat. Although passive transport mechanisms for both, weakly acidic and weakly basic compounds have been suggested, amplified sweat levels of basic compounds can be observed, while the levels of acidic compounds appear to be suppressed. Caused by differences in the pH of blood and sweat, weak bases, which are uncharged in blood, will protonate in the more acidic environment of preliminary sweat. Hence, the diffusion velocity from sweat to blood is restricted, resulting in amplified concentrations of weak bases in secreted sweat. Additionally, molecules produced by the sweat glands themselves, e.g. lactate, can be found in secreted sweat, further encumbering the interpretation of metabolomics data obtained from sweat analysis. (72). A wide variety of sampling- and sample preparation methods, as well as analytical instrumentations was used to analyse human sweat. The sampling procedures can be very time consuming (70) and include direct extraction of human sweat components from the palms using 10% ethanol and tissue culture dishes (75), sampling of sweat from the axillae directly after formation using a Gilson pipette (76), sweat collection using the Macroduct® sweat collecting device after sweat induction via pilocarpine iontophoresis (77), gauze sponge patches (8) as well as special self-made tools as glass rollers and pipettes with reverse capillaries (78). The first sweat sampling devices were rather crude systems composed of several layers of filter paper, cotton or towel. More recently smaller and more

comfortable swat patches have been developed consisting of a transparent surgical dressing and an absorbent pad which are attached to the forearm (70). A frequently used tool for the collection of sweat is the Macroduct® sweat collector with a capacity for 15 µL sweat. This concave disk with a spiral tube is used to sample the minimum amount of sweat sufficient for cystic fibrosis testing. Additionally, a bigger version is available for experiments requiring larger amounts of sweat. With the so called Megaduct, it is possible to sample up to 0.5 mL sweat (70). Typically, sweat is sampled after induction of sweating either thermally or chemically using pilocarpine (70). Although most authors stated to have collected pure eccrine sweat, sebaceous- and/or apocrine impurities originating from the sweat collection procedure of choice can't be avoided by using the techniques described above.

The metabolome of eccrine sweat:

Non-invasiveness is a major- but still challenging- goal in clinical diagnostic research. Human sweat is discussed as a possible source of potential biomarkers and, due to the possibility of non-invasive sampling, a lot of effort has been spent on the investigation of the potential and possible clinical applications of sweat (72). Especially for patient groups for which sampling of blood can be connected with severe health risks, as elderly people, new-borns or haemophiliacs, sweat sampling could be an interesting alternative due to its completely non-invasive character. Additionally, it offers a less complex sample matrix compared to blood or plasma and therefore requires only simple sample preparation steps prior to analysis. The main drawbacks of conventional sweat analysis are time consuming sampling procedures depending on the analyte of interest, problems due to evaporation, the need for trained staff for successful sampling and possible contamination of sampled sweat caused by the sampling technique applied (70). While the composition of several biological matrices, as serum, plasma or tissues, is very stable and regulated by homeostasis mechanisms, there are large inter- and intra-individual variabilities in others, as urine (1) or sweat, depending on the physiological conditions (8). A major issue in sweat metabolomics, especially when quantitative information is required, is the normalization of the amount of sweat sampled. Additionally, electrolyte concentrations in sweat samples increase in the case of dehydration compared to states of euhydration. Therefore, it is likely that metabolite concentrations in sweat samples may vary in a sweat rate- and hydration state dependant manner, which complicates the issue of sample normalization even further (8). Until today, using sweat as specimen in routine testing is still restricted to the determination of the sweat chloride level in cystic fibrosis testing and screening for drugs of abuse (72; 77), while blood and urine are used most frequently as specimen for clinical routine analysis (78). Cystic fibrosis is an autosomal recessive disease that is caused by a defect gene encoding for the cystic fibrosis transmembrane conductor regulator (CFTCR), a chloride channel present on the membranes of mucus and sweat producing cells. A dysfunctional CFTCR protein accelerates the loss of sodium and chloride through epithelial secretory cells

and leads to several severe complications such as lung diseases and hepatic and pancreatic insufficiency due to an abnormal secretion of mucus (79). In the human metabolome database (HMDB) 90 metabolites are classified as originating from human sweat. This list includes amino acids, organic- and fatty acids, amines, sugars, creatine and creatinine (80). The pattern of free amino acids in sweat differs from the composition of other biofluids. Serine is the most abundant amino acid in sweat (>20%) followed by glycine (ca. 15%), the glutamic acid derivative pyrrolidone 5-carboxylic acid (PCA, also known as pyroglutamic acid), alanine, citrulline and threonine. The relative abundance pattern of amino acids in sweat resembles the amino acid pattern found in profilaggrin, a major epidermal protein found in corneocytes. Besides glycerol, urea, lactic acid and other components (78), hygroscopic amino acids obtained from the degradation of filaggrin play an important role as part of the natural moisturizing factor (NMF) (76) necessary for epidermal hydration, pH-homeostasis, skin elasticity and the maintenance of the barrier function of the skin (78; 76). The analysis of the amine/phenol submetabolome revealed high interindividual differences in the metabolite composition of human sweat in general, as well as differences between the sweat composition of male and female individuals (8). The sweat metabolome can be affected by the occurrence of diseases, leading to altered concentrations of sweat compounds or even the presence of new compounds in sweat. Therefore, further research could lead to new sweat-based biomarkers for states of health and disease (70). First interesting achievements in the field of sweat metabolomics pointed out possible applications. For example, based on a panel of metabolites, including sugars, amino acids and certain lipids, a prediction model able to discriminate between healthy individuals and individuals suffering from lung cancer has been developed using high resolution mass spectrometry (77). In 2015 a method for the non-invasive estimation of plasma concentrations of levodopa, used as medication to treat Parkinson's disease, by analysing its sweat concentration in samples obtained from the palms was published (75). Assuming that small, but sufficient amounts of drugs are excreted via sweat following their absorption, distribution and metabolism, sweat can be used as an alternative biological sample for drug testing (81). Hence, sweat is, besides urine, the favoured biofluid used for doping controls, mainly due to the possibility of non-invasive sampling (70). Nevertheless, the mechanisms of the transport of most drugs and their metabolites from blood to sweat can't be explained sufficiently yet. Usually, sweat patches are used for sweat collection followed by analyte extraction methods as liquid-liquid extraction or different types of solid phase extraction depending on the target analyte(s). The combination of high resolution separation techniques as gas- or liquid chromatography with mass spectrometry allowed sweat analysis to enter the field of metabolomics and screening for drugs or drugs of abuse (70). A wide variety of drugs has been detected in sweat, ranging from opiates over cocaine, amphetamines and cannabinoids, to pre-

scription drugs (70; 81; 82). Instrumentations used to enlighten the composition of the (sub-) metabolome of human sweat include cation chromatography using an automated amino acid analyser after ninhydrin derivatization (76), GC-MS (76), LC-MS/MS (77) and methods based on NMR (78).

Fingerprints and finger-mark residue:

For more than a century, fingerprints have been used as an important and robust source of information for criminalists (83; 66). Hence, numerous techniques for the visualization of latent fingerprints have been developed, including ninhydrin staining (84). Latent fingerprints are deposited at surfaces after contact with an individual's fingertip and consist of natural secrets of the secretory glands found in the skin of a fingertip. Besides endogenous compounds, these depositions can contain exogenous substances, e.g. CF or drugs of abuse, as part of the secrets from epidermal glands, as well as external contaminations such as dirt, cosmetics, blood or grease (83; 85; 86; 51; 87; 84). The molecular composition of the human fingerprint depends on several factors, including the microbiome, skin cells, as well as personal habits, as diet, medication or the use of care products (59). Although the palms including the fingertips contain solely eccrine sweat gland, secrets of other types of epidermal glands, as sebum, can be found in fingerprints and might originate from contact with other sebum rich parts of the body, e.g. the face (88; 89). Porous surfaces, as paper or cotton, allow the rapid absorption of eccrine constituents in a fingerprint, while sebaceous components are only slowly absorbed (87; 90). Additionally, duration- as well as the pressure applied during the contact between a finger and the surface can have an influence onto the amount of the compounds transferred to the object's surface (90). Besides the possibility to identify a suspect based on the unique pattern of ridges found at the fingertips' surfaces, finger-mark residues can yield a lot of other useful information. DNA, metabolites, peptides and proteins have been detected in fingerprints allowing the determination of several donor characteristics, such as information about age, diet or drug abuse (66). These lifestyle-related chemicals are transferred to objects as part of the residues left at the surface after contact and allow some extent of insight into the personal habits (85). The chemical composition of fingerprint residue has been analysed using a wide variety of analytical techniques, including CE-MS (84), LC-MS (91) and GC-MS (89), and can vary between individuals (84; 66). For example, the total amino acid content of latent fingerprints varies between 20.7 ng and 345.1 ng. There is high confidence within the reviewed literature, that serine is the most abundant amino acid present in fingerprints. However, when it comes to other major amino acids, some extend of disagreement was found within the reviewed literature. Other abundant amino acids present in fingerprints are glycine, alanine and asparagine, whereas relative and absolute amounts are differing within the reviewed literature (84; 89; 91; 87). Additionally, there might exist considerable variation within the amino acid composition of different individuals' fingerprints, e.g. when it comes to the amounts of glutamic acid, histidine or ornithine detected in fingerprints (91).

The lipid content of the fingerprints includes different fatty acids, squalene and cholesterol (89; 87). The lipid composition of latent fingerprints varies between children and adults, whereas fingerprints of children contain more volatile compounds resulting in a reduced longevity of infants' fingerprints. Age related variations in fingerprint composition are affecting the concentration of fatty acids, cholesterol and carbonyl esters (87). In 2013 Kuwayama et al. published a targeted metabolomics workflow for the time course measurement of CF and its primary metabolites using sweat sampled from a single fingertip within one minute. The sampling devices were based on filter paper and a LC-MS/MS method was used for the analysis of the extracts. CF levels in blood samples peaked 1 h after consumption of coffee, while a delayed CF peak was observed in fingerprint samples of the investigated individuals. However, kinetics of CF in the fingerprints varied within the individuals and showed maxima 1 h, 3 h or 5 h after consumption of coffee. Levels of CF and its major metabolite PX in samples obtained prior to coffee ingestion showed some variations that were related to differences in the individuals' consumer behaviour (51). In later research work 9 drugs including ibuprofen, dihydrocodeine and acetyl salicylic acid, as well as four drug metabolites were analysed in blood, urine, saliva and sweat obtained from a fingerprint using LC-MS/MS. A correlation of the time courses of several analyte concentrations between blood and saliva and between urine and fingerprint, respectively, was stated. Nevertheless, some metabolites showed delayed appearance in sweat compared to urine, an effect that could not be related to the chemical properties, as the pK_a or log*P* of the target analytes. The authors reported difficulties to identify the more acidic analytes, which might be related to a decreased overall sensitivity in the negative ionization mode (86). A lot research effort has been spent on the development, validation and application of targeted metabolomics methods for the quantitation of CF and its metabolites in blood, plasma, saliva and eccrine sweat derived from the fingertips in this research group. In his master thesis, Clemens Langbauer developed and validated fast and simple methods for the extraction and quantitation of CF and its metabolites using a chip-based nano-LC-MS platform for blood, saliva and sweat sampled from the fingertips. Due to the high hydrophilicity of the target molecules the chromatographic separation of the analytes with the used LC-system appeared to be challenging. While CF could be baseline separated from all three dimethylxanthines, the separation of the isomers TB, PX and TP was only partly successful. PX and TP were regarded as an analyte group, because the separation of both analytes was insufficient. Time course measurements were performed and different types of CF metabolism in a cohort of 5 individuals could be stated (52). During two subsequent bachelor theses UHPLC methods for the chromatographic separation and quantitation of CF and its primary- and secondary metabolites TB, TP, PX, 1-methylxanthine, 1,7-dimethyluric acid as well as for cumaric acid were developed. TP and PX could be separated using an UHPLC system and a different eluent system compared to the nano-LC method developed by Langbauer. However, TP and the

secondary metabolites of CF 1-MX and 1,7-dimethyl uric acid stayed below the lower limit of quantification in most samples analysed by the authors (92; 93). The laps of time between coffee intake and occurrence of the maximum level of CF in the fingerprints showed interindividual variation, which was consistent with results from Kuwayama's work. Therefore, Langbauer, Hauser and Langer grouped the subjects into slow- and fast metabolizers, whereas differences in the kinetic profiles were hypothesised to arise from variations in the individual enzymatic activities of CYP in the liver (52; 93; 92).

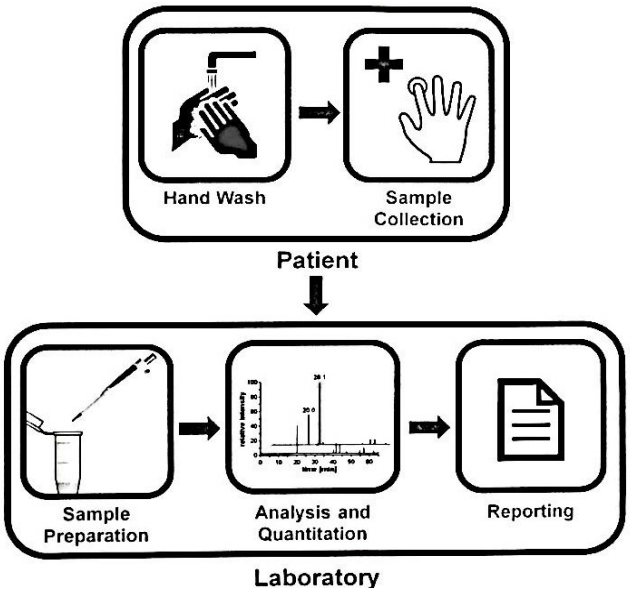

Figure 6: Schematic representation of the workflow used for the analysis of the metabolome of sweat derived from the fingertips (©Dr. Samuel M. Meier-Menches).

The aim of this work was the development of an untargeted UPLC-MS/MS workflow for an Orbitrap HF mass spectrometer hyphenated to an UPLC system for the analysis of the composition of sweat- and blood samples. An extraction method for the sweat secreted within two minutes by the tips of the thumb and the index finger was developed based on a similar method (52). Further, retention time of the identified metabolites were aligned and a full MS method was used during an intervention study to elucidate the effect of coffee and dark chocolate consumption on the composition of the metabolome of blood- and sweat samples. The pharmacokinetic behavior of phytochemicals identified in chocolate and coffee, as well as of their key metabolites, was analyzed. Based on this technique, a shorter full MS method for the chromatographic separation and quantitation of CF as well as its primary metabolites TB, PX and TP was developed and partly validated. The applicability of the developed method was demonstrated by quantifying the amount of CF, TB and PX in eccrine sweat sampled from the fingertips during a three-phase double-blind study. Therefore, sampling devices were sent to external partners who collected the sweat samples, while samples were extracted and analyzed in our laboratory.

Materials and instrumentation:

All solvents used within this work were of HPLC-MS grade. Acetonitrile and methanol were purchased from VWR chemicals while HPLC-MS grade water was obtained from an in-house Millipore water purification system (8.5 MΩ). Formic acid (~98%), used to acidify the eluent system, was obtained from Fluka. Stock solutions were prepared from anhydrous caffeine (>99%, Fluka), theobromine (≤98%), paraxanthine (~98%, SIGMA) and theophylline (>99%, SIGMA), while d9 caffeine (≤98%, Aldrich) was used as an internal standard. All standards used for the calibration curves were diluted from these stock solutions. 1-Methylxanthine (Aldrich) and 3-Methylxanthine (Aldrich) were used for identification of the monomethylxanthine isomers during the development of an internal compound database. A SONOREX DIGITAL 10P (Bandelin) ultrasonic bath was used to overcome insufficient solubilization of the analytes. Kimbersky-Clark® Professional Precision Wipes (Kimtech Science, 11x21 cm, white) were the starting material for the development and mass production of filter-paper based sampling devices and conventional metal tweezers were used to handle the filter devices. Blood was sampled after pricking the fingertips with FreeStyle Lancets (Abbott). During blood sample extraction, solvents were evaporated using nitrogen obtained from a nitrogen-generator. 1.5 mL and 2 mL Eppendorf tubes, 0.5 mL safe lock Eppendorf tubes as well as 10 mL and 50 mL Falcon centrifugal tubes were used for the preparation of standard solutions and during the extraction procedures and stock solutions were stored in glass vials (8 ml, Scherf Präzision Europa GmbH). Prior to analysis extracts were transferred to glass vials (N9, 1.5 ml, Screw Neck (Macherey-Nagel), incl. inserts (15 mm tip, Macherey-Nagel)). Gilson pipettes of different size and the corresponding pipette tips were used to transfer solutions. A Duo Plus Package with miVac Duo, miVac Duo Pump and miVac SpeedTrap (Genevac SP Scientific) was used to dry filter paper devices after sampling, if storage prior to sample extraction and analysis was necessary. Chromatographic separation of the analytes was achieved using a Vanquish UPLC system (Thermo Scientific) with a core-shell C18 column (100 x 2.1 mm, 2.6 µm particle size, Phenomenex) hyphenated to a Q-Exactive HF mass analyzer (Thermo Scientific). Additionally, a Vortex Genie 2 (Scientific Industries, Inc.), a Thermomixer Comfort 1.5 ml (Eppendorf), a Centrifuge 5424 (Eppendorf) and a microcentrifuge (Starlab) were used during sample preparation.

Chocolate bars (70% Cocoa, Lindt Excellence) and Coffee Capsules (Tchibo "Espresso kräftig") were administered during the intervention studies.

Experimental:

All sample preparation steps as well as qualitative- and quantitative analysis of sweat- and blood samples was performed at the Department for Analytical Chemistry of the University of Vienna, while a part of the analyzed sweat samples was sampled at the Centre for Chronobiology of the Psychiatric Hospital of the University Basel (UPK Basel). During the development of the internal compound database and the kinetic studies, all blood- and finger sweat samples were collected with written consent of each donor and approval of the Ethics Committee of the Medical University of Vienna (approval number 2010/349 to Prof. Dr. Christopher Gerner). At the Centre of Chronobiology at the UPK Basel finger sweat samples were collected with the written content of every donor and approval of the Ethics Committee northwest-/central Switzerland (EKNZ).

Untargeted metabolomics and kinetic investigations:

Small molecules in human blood, sweat, coffee and chocolate were investigated during two intervention studies. During a first experiment, three subjects, two males and one female, fasted for CF containing foods and beverages (coffee, chocolate or energy drinks, e.g.) for 24 hours. The three volunteers started the experiment without consumption of any breakfast. First the zero value was investigated under initial conditions. Therefore, sweat was sampled from the fingertips of the left- and right hand's thumb and index finger. Then, blood was sampled by pricking any other fingertip with a lancet and subjects drank a cup of coffee on an empty stomach after the sampling procedure was accomplished. A breakfast composed of different sweet pastries which didn't contain CF or chocolate was then consumed by every individual. Subsequently, blood and sweat from the fingerprints of the left and right hands were sampled in 30 min intervals for two hours. Analytes were extracted and all samples were measured as technical triplicates using the full-MS method described in the methods section. Additionally, samples of one subject 60 min after coffee ingestion were analyzed with the MS^2-method using a fragmentation energy of 30 NCE. In a second intervention study six volunteers were divided into three groups, each composed of one male and one female subject. One group ingested coffee, the second consumed half a bar of dark chocolate (50 g), while the last group didn't ingest any coffee- or chocolate-products and represented the control group. Sweat and blood samples were taken every 20 min during the first hour and every 30 min within an overall time of three hours. Coffee was diluted 1:1000 and chocolate was extracted and analyzed. To increase the analyte coverage for the retention time alignment, all samples were analyzed as triplicates using the dd-MS^2 methods described in the methods section with a collision energy of 60 NCE. Additionally, the corresponding full MS method was used to investigate the kinetics of the key bioactives in ingested coffee and chocolate.

All sampling and extraction techniques-, as well as UPLC-MS methods used are described in more detail in the methods section.

Quantification of caffeine and its metabolites in sweat sampled from the fingertips:

Based on the UPLC-MS method used for untargeted metabolomics experiments, a second UPLC-full MS method with a slightly different elution gradient and a shorter overall runtime was developed and validated. In a double-blind study, CF as well as its primary metabolites PX and TB were quantified in sweat sampled after the ingestion of CF or a placebo. Therefore, filter paper based sampling devices were prepared and sent to the partner group at the Centre for Chronobiology at the UPK Basel. Eight volunteers underwent a three-phase-trial, whereas subjects ingested either CF, a placebo or passed a withdrawal phase. During the whole experiment, subjects were asked to avoid consumption of foods and drinks containing CF, alcohol, drugs and drugs of abuse. The compliance was controlled by quantitation of CF and its primary metabolites in sweat sampled from the fingertips, as well as entries in a sleep-wake diary. Every phase started and ended with an ambulatory part lasting eight days, with a two-day laboratory part in between. Placebos, as well as CF were both administered on a daily basis in form of three capsules that either contained solely mannitol or 150 mg of CF in mannitol. During the withdrawal phase CF was ingested during the first eight days and consumed the last CF containing capsule on the ninth day, followed by administration of placebo during the rest of the experiment. Within the first- and the last 8 days subjects were treated ambulatory and sampled themselves right before bedtime and therefore several hours after intake of the last capsule, while during the laboratory part sweat was sampled in two-hour-intervals during day time. Usually a brake of three days up to four weeks was situated in between the three phases of the double-blind study. After each phase, samples were sent back to Vienna where analyte extraction and -quantitation was carried out in our laboratory. Sample identities were cyphered, amounts of CF, PX and TB were plotted against time and sample batches were related to the corresponding phases of the trial.

Method evaluation:

Extraction efficiency was determined for CF, TB, PX and TP by analyzing extracts of filter paper sampling devices spiked with 1 µL of multi-standards containing 1 ng and 10 ng of all four analytes, respectively. The relative peak areas of the analytes in the filter paper extracts were compared to their counterparts determined in aqueous standard solutions. Three individual extractions were used to determine the mean efficiency, its standard deviation as well as the corresponding coefficients of variation (CVs). CVs were then used as measure for the extraction reproducibility. For the evaluation of the technical reproducibility standards extracted from filters spiked with 1 ng and 10 ng of CF, TB, PX and TP were analyzed. The measurements were triplicated and technical reproducibility was determined as CVs of the technical triplicates. Matrix effects were evaluated by spiking sweat extracts obtained from an

individual fasting for any methylxanthine rich food or beverage for the last 24 hours with multistandards to overall amounts of 1.2 ng, 12 ng and 24 ng of CF, TB, PX and TP in the extract. Then, relative peak areas (relative area under curve (rAUC)) were compared with rAUCs found in aqueous multistandards with corresponding analyte concentrations. However, some amount of TB was detected in the sweat samples and the analytes' rAUCs found in the "blank" sweat extract before spiking were subtracted from every sample before the matrix effects were calculated.

Sampling reproducibility was evaluated by sampling index finger and thumb of the left and right hand of a single individual, three hours after the ingestion of two cups of coffee. The sampling procedure was repeated three times successively and differences of the amounts of CF, PX, TB and TP between the left and right hand, within the extraction replicates as well as the overall variation were evaluated. Experimental stability and comparability of the results of the high throughput analysis were controlled by monitoring mean values and CVs of the AUCs of the IS.

Methods:

Preparation of stock solutions:

Stock solutions were 1 µg/µl solutions of CF, d9-CF, TP and PX in methanol. Due to its poor solubility in methanol the concentration of the TB stock solution was 10 ng/µL. All calibration standards were freshly prepared from the stock solutions at the date of the corresponding experiments. All stocks were stored in the fridge at 4°C until use and analyte stability in solution was checked regularly.

Filter preparation:

During the whole preparation of the filter paper based sampling devices used for sweat collection fresh latex gloves were used to minimize contamination. First, a hollow punch of a diameter of 1.2 cm was rinsed three times with Milli-Q water and ethanol. Then, several sheets of low-lint laboratory paper were folded and placed in a clean and new plastic bag in a way that multiple layers of filter paper could be stamped out at once. Round pieces of filter paper with an area of 1.13 cm^2 were cut out using the hollow punch and a hammer. Tweezers were cleaned by rinsing with ethanol and the two layers of plastic foil which were imbedding the densely packed filters were removed. The filters were checked for integrity and completeness of separation from each other and were then transferred into a fresh and clean plastic bag. Single filters were placed in 0.5 mL safe lock Eppendorf tubes and stored in the dark at room temperature until further use. Prior to the sampling process each filter was humidified using 3 µL of Millli-Q water.

Sampling and sample preparation:

Hands were washed with soap and warm water, whereas special attention was given to the complete removal of the soap at the end of the washing procedure. The hands were dried using fresh paper towels and, to obtain an appropriate amount of sweat, sweat secretion at the fingertips was allowed for one minute at room temperature. Filter paper sampling devices were placed between the fingertips of the thumb and the index finger and removed after another minute. The filter papers were returned to the 0.5 mL Eppendorf tube, dried and stored at 4°C until extraction. During the sampling procedure, filters were handled with clean tweezers only. The sweat- and blood samples for the qualitative analysis, as well as for the kinetic studies were sampled in our lab, while sweat samples analyzed during a double-blind study were collected by external partners. The study was composed of three phases where subjects ingested CF, a placebo containing lactose, or underwent a withdrawal phase. Therefore ready-to-use filter sampling devices in labeled 0.5 µL safe lock Eppendorf tubes were sent to UPK Basel where our partners sampled sweat from the subject's fingertips or subjects sampled themselves at home. More detailed information concerning the design of the double-blind study is given in the experimental section. The extraction method was kept as simple as possible. Because eccrine sweat mainly consists of water, analytes were extracted from the filter papers by a simple solid-liquid extraction using water as extractant. 120 µL of 1 pg/µL d9-CF were added to the filters, the solution was then pipetted up and down 10 to 15 times and the filter was "pelleted" at the bottom of the tube by applying pressure with the pipette tip. Finally, the supernatant was removed and transferred into a v-shaped insert in a glass vial. Blood was sampled from the fingertips using disposable lancets and an Eppendorf pipette. A finger was pricked and 20 µL of blood were transferred into an Eppendorf tube containing 480 µL acetonitrile. The mixture was vortexed for one minute and shaken on a thermomixer with maximum speed at 40°C for 10 min. After three repetitions of the overall procedure, the samples were centrifuged at 14000 rpm for 10 min to pellet the protein content. 250 µL of the supernatant were then transferred to a glass vial, dried under nitrogen and redissolved in 250 µL 1 pg/µL d9-CF in water containing 0.2% formic acid. For the extraction of analytes from chocolate 2 g of dark chocolate were melted and dissolved in 70 mL 60°C hot MS grade water using an ultrasonic bath. The solution was cooled down and stored overnight in the fridge at 4°C to separate hydrophobic constituents from the aqueous content. The fatty layer was deposited and the solution was centrifuged at maximum speed for 20 min to obtain particle freeness. Coffee samples were prepared by 1:1000 dilution of the same freshly cooked coffee ingested by the subjects during both intervention studies. To avoid damages of the HPLC system during analysis, samples were centrifuged prior to analysis to guarantee particle freeness.

HPLC-MS-Methods:

Based on results of previous research we decided to use UPLC instrumentation and a gradient system. First, a method for untargeted metabolomics experiments with an overall run time of 7.5 min was developed. 0.2% formic acid (FA) in H_2O was used as eluent A, while 0.2% FA in methanol (MeOH) was used as eluent B. The gradient started with 1% phase B. After quickly reaching 5% B, the main separation gradient started and eluent B reached 40% of the mobile phase after 4.5 min. 80% B was used to remove hydrophobic contaminants from the column and finally the column was re-equilibrated using 1% B. A detailed representation of the gradient system is given in Figure 7.

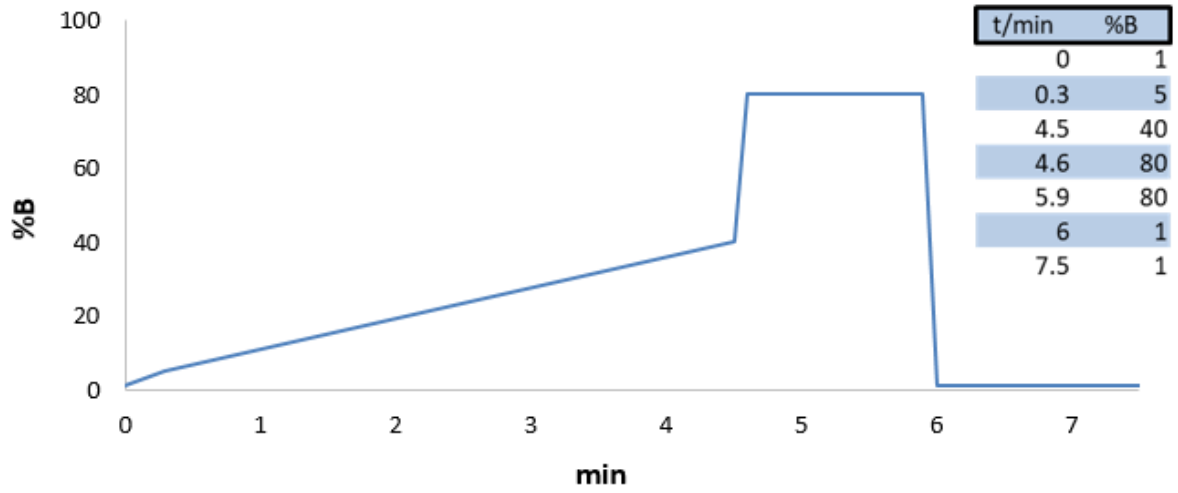

t/min	%B
0	1
0.3	5
4.5	40
4.6	80
5.9	80
6	1
7.5	1

Figure 7: Schematic and tabular representation of the gradient system used for the chromatographic separation during untargeted metabolomics experiments. Eluent A was 0.2% FA in H_2O, while eluent B was 0.2% FA in MeOH.

To reduce the overall analytical runtime during high throughput analysis, a 6.5 min UPLC method was developed for the quantitation of CF and its primary metabolites using the same eluents, but a slightly different gradient system. Because complete separation was only necessary for CF and its metabolites TB, PX and TP, the separation gradient stopped at 20% B after 2.9 min. Then, a washing step using 80% B followed by re-equilibration similar to the method developed in the first place were applied. A detailed view onto the resulting chromatographic method can be obtained from Figure 8.

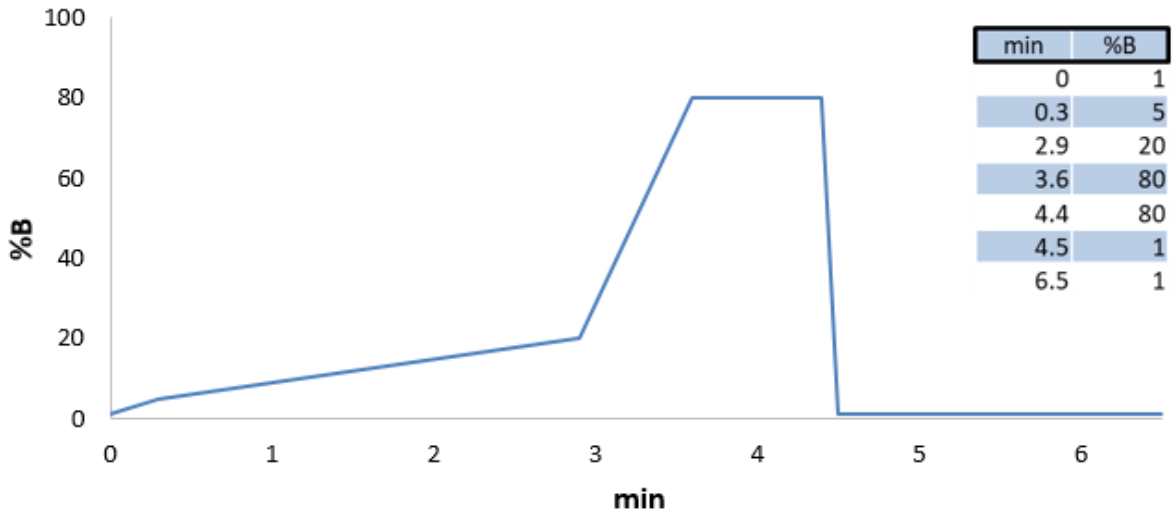

min	%B
0	1
0.3	5
2.9	20
3.6	80
4.4	80
4.5	1
6.5	1

Figure 8: Schematic and tabular representation of the gradient system used for the chromatographic separation in targeted metabolomics experiments. Eluent A was 0.2% FA in H_2O, while eluent B was 0.2% FA in MeOH.

To evaluate potential carry over events, blank samples were injected in periodic intervals, however no relevant carry over effects were observable during the experiments.

Several methods for the mass spectrometric detection after chromatographic separation were developed. All methods described in the following were operating in the positive ionization mode. In preliminary experiments the negative ionization mode was used as well, but due to a low overall analyte coverage it was not used in the studies described in this work. In combination with the longer UPLC method (7.5 min total runtime) two data dependent (dd) top 4 MS^2-methods with a dynamic exclusion time of 2 s, as well as a full MS method were developed. Analytes were identified using the MS^2-methods with scan ranges of 100-260 m/z and 250-1000 m/z, respectively and a resolution of 30000 at the MS^1 level and 15000 at the MS^2 level. With this approach we tried to face the high density of small molecules with m/z below 250 compared to molecules with higher mass in the analyzed samples. The maximum IT was set to 50 ms and the isolation window was 1.2 m/z. The collision energy was set to 30 or 60 NCE, respectively. The list of putatively identified analytes was used to develop a retention time alignment later on used to semi-quantitatively analyze the samples with a full MS method. The full MS method had a scan range of 100-1000 m/z and a resolution of 60000. For the quantitation of CF and its primary metabolites TB, PX and TP a full MS method with a scan range of 150 to 1000 m/z, a maximum IT of 50 ms and a mass resolution of 60000 in combination with the shorter UPLC method with a total runtime of 6.5 min was applied.

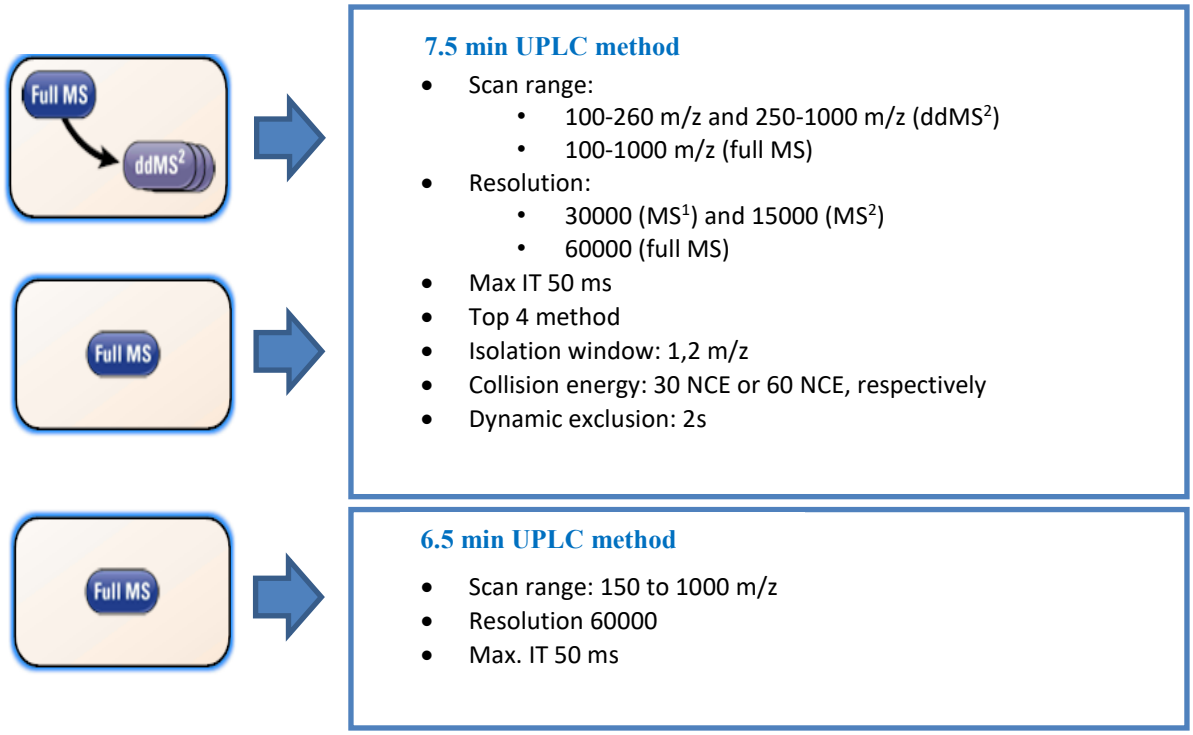

Figure 9: dd-MS² and Full MS methods used to analyze sweat sampled, blood samples as well as coffee and cocoa extract.

Processing of MS² data:

The Compound Discoverer™ 2.1.0 software (Thermo Scientific™) was used to identify metabolites from generated MS² data. A template untargeted metabolomics workflow already implied in the software package was adapted for our purposes. It included automated selection of spectra from raw files, creation of mass traces, retention time alignment, detection and grouping of unknown compounds, identification of background compounds and searching against the mzCloud database. Retention times were aligned allowing a maximum retention time (RT) shift of 0.05 min, while product- and fragment mass spectra were matched to reference spectra with a mass tolerance of 5 ppm. The integrated filter function was used to simplify the evaluation of the obtained results. Therefore, only identification with a mzCloud best match greater than or equal to 80 and a minimum area of 50000 in at least one of the analyzed samples were included in the data analysis. The settings used were based on a pragmatic approach of trial and error. Identifications with mzCloud best match of less than 80 were assessed to be most likely false positives. The IS solution containing 1 pg/µL d9 CF showed an average AUC of 1e6. Therefore, chromatographic peaks with AUCs of less than 50000 were only present in trace amounts in the analyzed samples, or probably arose from noise events and were excluded from further data analysis. The MS² spectra were manually compared with reference spectra in the mzCloud database.

Unambiguous identification was not possible in several cases. For example, four CGA isomers and two urocanic acid isomers were present in the sample set and distinction between isomers was not possible based on the MS^2 spectra. Therefore, the compounds were merged to groups of compounds in the internal library and the retention times of the isomers were added to the names, e.g. "Urocanic acid isomer 0.533 min". Other analyte peaks were matched to two different isomers in case of identical reference fragment spectra, as in the case of catechin/epicatechin or threonine/homoserine. Figure 10 shows a fragment spectrum for CF measured in a blood sample and the corresponding spectrum obtained from the mzCloud database. Compounds were seen as identified if the exact mass of the precursor matched with mass accuracy better than or equal to 5 ppm. Additionally, similar intensity ratios of the most abundant fragment ions present in the fragment spectrum when compared to the reference spectrum were used as a criterion for positive identification.

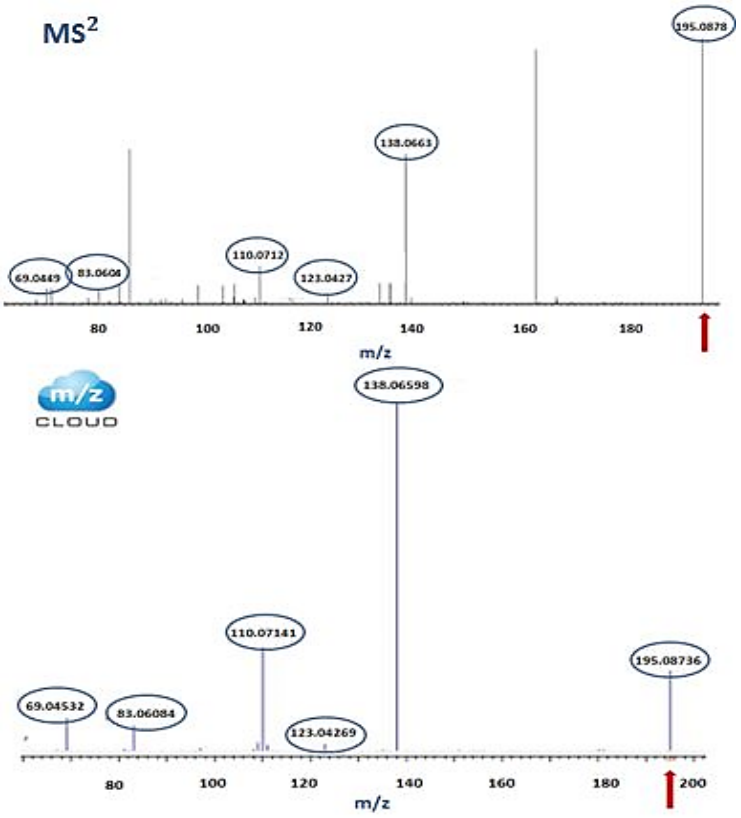

Figure 10: MS^2-spectrum of CF measured in a blood sample (top) compared to the corresponding reference spectrum in the mzCloud database.

Processing of full MS data:

Full MS data was (semi-) quantitatively analyzed using the Tracefinder 4.1™ software using a mass tolerance of 10 ppm. Peaks were detected using the genesis algorithm, whereas the peak with nearest RT was picked in case of a signal noise ratio exceeding a threshold of two. Nevertheless, several samples were reanalyzed, controlled and data was corrected if necessary using the Xcalibur™ software and a mass tolerance window of 10 ppm. Both software packages were obtained from Thermo Scientific™.

Results:

Development of an internal compound library:

An internal molecular library was developed from the MS^2-data obtained from chocolate extracts, 1:1000 dilutions of freshly brewed coffee as well as blood- and sweat samples of a single individual 60 min after the ingestion of coffee and blood- and sweat samples of six individuals. Two individuals consumed coffee and two individuals consumed chocolate, while the remaining two individuals avoided consumption of any comestibles known to contain CF or its metabolites. Samples were taken before- and 20 min, 40 min, 60 min, 90 min, 120 min and 180 min after the ingestion of coffee or chocolate. The library contained retention times and molecular masses of the target analytes and was used later on to detect chromatographic peaks automatically via the Tracefinder software during two intervention studies. The list was extended by 1-MX, an analyte that was not identified by MS^2-data. Three peaks with a molecular mass corresponding to 1-, 3- or 7-MX were detected but only 3-MX and 7-MX could be identified based on their fragment spectra. Peaks were confirmed using standard solutions and 1-MX was added to the internal library. Overall, the internal database was composed of 95 analytes, including amino acids derivatives- and derivatives, contaminants as PEG-polymers, xenobiotics as CF, TB, catechin/epicatechin or trigonelline and other potentially interesting molecules as betaine, acetylcholine, nicotinic acid, histamine, adenosine, uracil or uric acid. The complete internal compound library can be reviewed in more detail in the appendix (Table 7).

Figure 11 shows an example chromatogram of the three MX isomers. 3-MX and 7-MX were identified by MS^2-spectra matches, while RT of 1-MX was confirmed by analysis of a 1-MX standard solution.

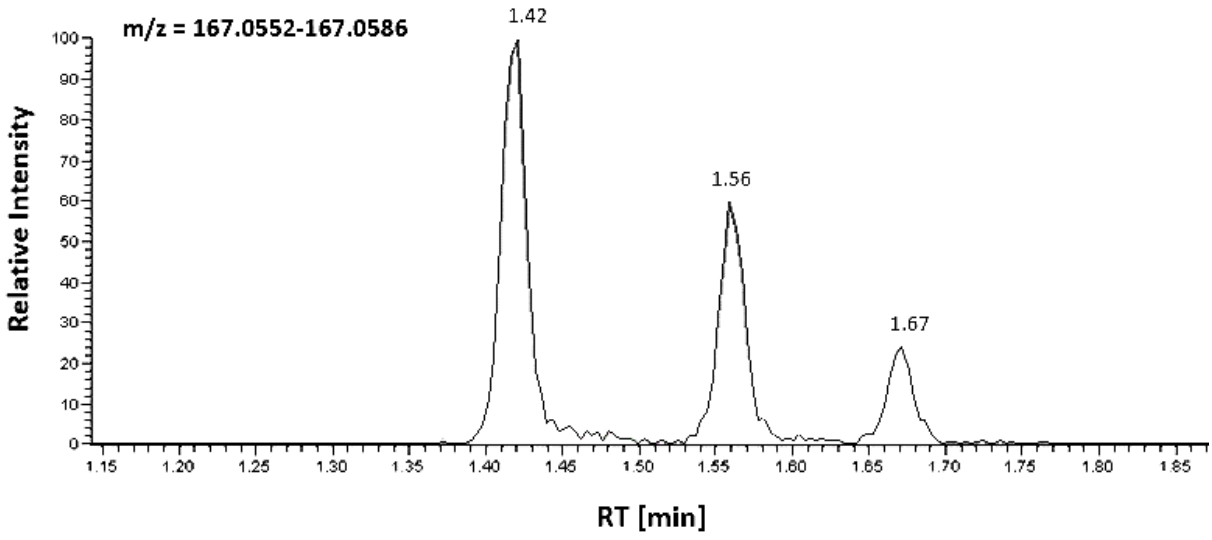

Figure 11: Example chromatogram for 7-MX, 3-MX and 1-MX in a blood sample.

Figure 12 shows the extracted ion chromatogram of ions with m/z of 355.1029 ± 10 ppm in a 1:1000 dilution of coffee. The peaks were identified as CGA using the compound discoverer software and the m/zCloud database. However, 5-CQA is the only caffeoylquinic acid isomer present in the library. The compound peaks were treated as an analyte group, because distinction between the position-isomers of CQA was not possible without using standard solutions of the isomers. Therefore, the peaks are listed as CGA isomers, whereas the retention time of the corresponding peak was used as label to allow unambiguous assignment of the chromatographic peaks.

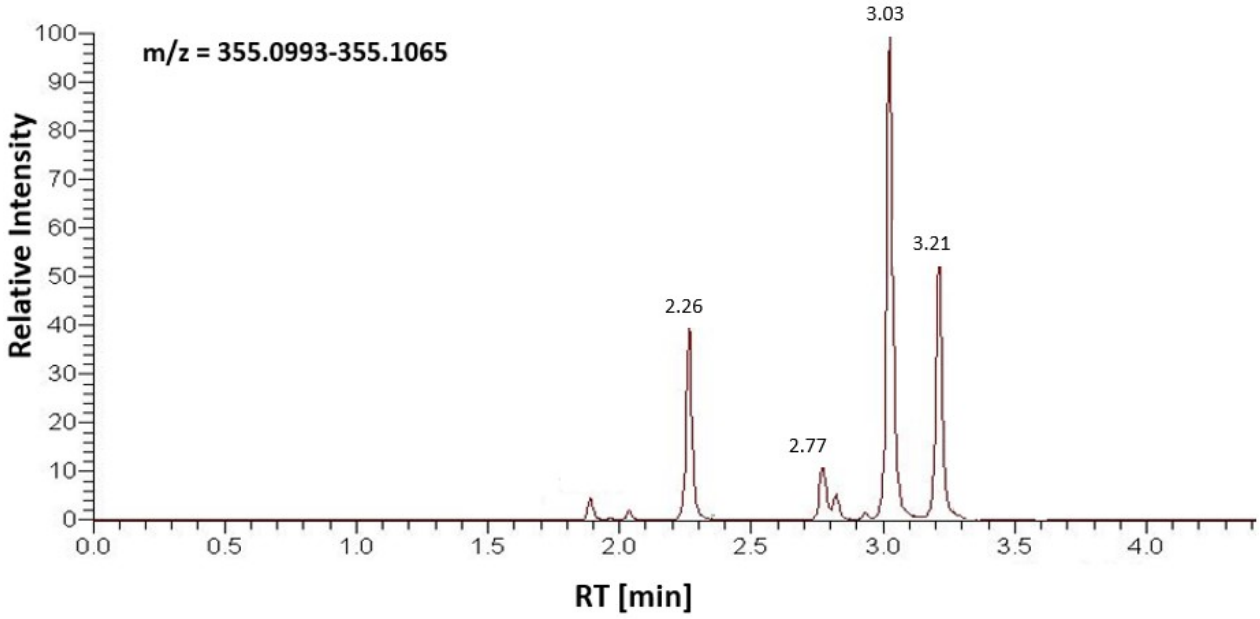

Figure 12: Chromatogram of potential CQA isomers obtained from UPLC-MS analysis of a 1:1000 of coffee.

Intervention study No. 1: Ingestion of coffee

Donor	Age [years]	Sex	Consumer's Behaviour
A	40-50	m	Intense consumption of coffee
B	20-30	f	Moderate consumption of coffee
C	20-30	m	Intense consumption of coffee

Table 1: Table of participants taking part in intervention study 1.

During an intervention study, three individuals were fasting for CF containing beverages and foods for 24 hours before they ingested a single cup of coffee. A classification of the three volunteers is given in Table 1. Blood and sweat derived from the fingertips of the thumb and the index finger of the left and right hand were sampled in accordance to the sampling methods described within the experimental section. Biofluids were sampled before- and 30 min, 60 min, 90 min and 120 min after ingestion of coffee. Samples, as well as a 1:1000 dilution of the ingested coffee were analyzed using a UPLC-MS platform. The full-MS-method used are described in detail within the methods section.

AUCs of the analytes included in the internal compound database were determined using an automated Tracefinder method. The limit of detection (LOD) of every single analyte was calculated as the average AUC of blank samples plus three times the corresponding standard deviation. Only analytes yielding chromatographic peaks exceeding the LOD were accepted as detected. 80 substances were detected in blood samples, 83 substances in fingerprints, of which 41 were detectable in the filter matrix as well. Therefore, only substances with significantly higher AUCs in the average sweat sample compared to the filter matrix were accepted to originate from sweat. Significances were calculated using an unpaired two tailed t-test, whereas p-values equal or lower to 0.05 indicated significant differences between the relative AUCs found in sweat samples and in the filter matrix. 77 substances surpassed this threshold and were accepted to originate from secreted sweat. Nevertheless, several compounds, as PEG 5, PEG 7 or caprolactam, which can be seen as probable contaminants, were still part of the dataset of analytes found in sweat. Caprolactam, the monomer of nylon-6, is able to migrate into foodstuff from plastic packaging (94). 51 substances were detected in the coffee samples, whereas CF and trigonelline were the dominant compounds identified. Choline, quinic acid, pyroglutamic acid, CGA isomers, nicotinic acids as well as decanamide were other-, abundant metabolites identified in diluted coffee. Relative AUCs of the ten most intense compound peaks found in coffee are depicted in Figure 13.

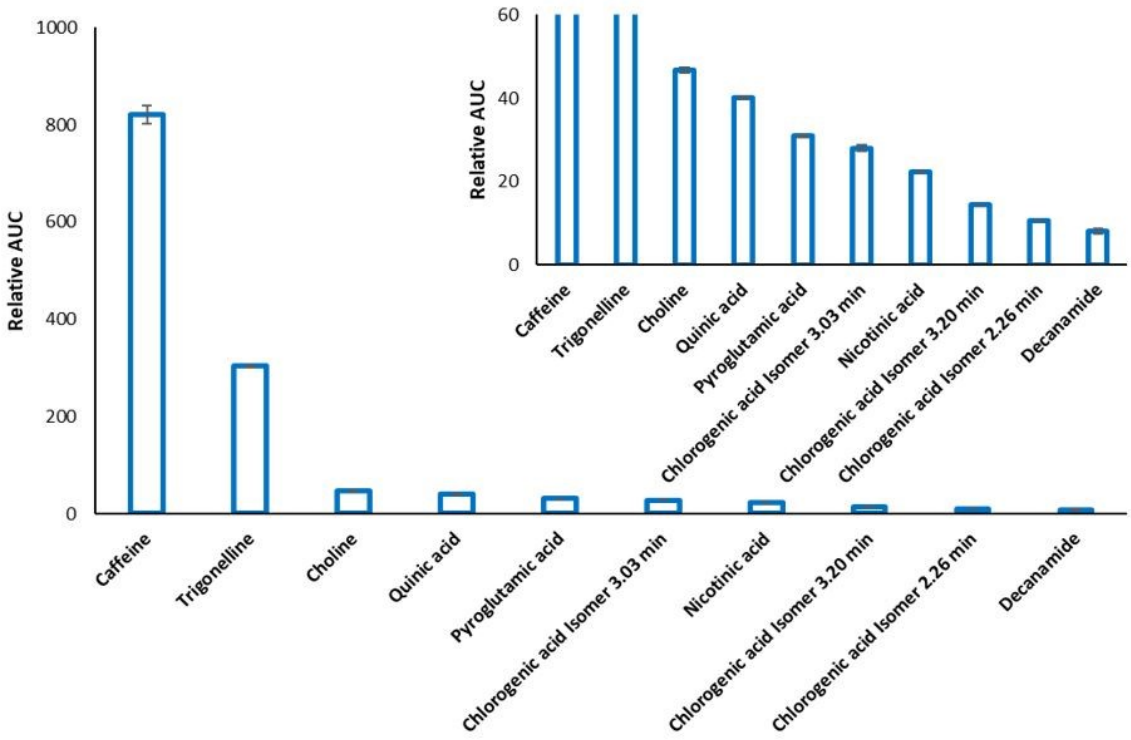

Figure 13: Ten compounds with highest rAUCs in a 1:1000 dilution of coffee during intervention study 1.

79.5% of the metabolites identified during untargeted metabolomics analysis were present in both biofluids, while only 8% and 12.5% of the analytes were characteristic for sweat samples and blood samples, respectively. A Venn diagram showing the distribution of detected metabolites within both biofluids is given in Figure 14. Analytes found exclusively in sweat extracts were the isomers of CQA, EDTA, pyrogallol and sorbic acid, while 3-hydroxypicolinic acid, 4-indolecarbaldehyde, decanamide, decanoylcarnithine, dibutyl phosphate, diethylphthalate, ergothioneine, N-methylhydantoin, palmitoylcanitine, PEG n8 and spermidine were solely present in extracted blood samples. PEG n8 and diethyl phthalate are most likely arising from contaminations during the sampling- and extraction procedures. Then, blood- and sweat kinetics of the most abundant metabolites found in coffee, as well the metabolites of CF, namely TB, PX, TP, 1-MX, 3-MX and 7-MX were investigated. The results are discussed in the section below, whereas the discussion is restricted to analytes whose abundances showed at least

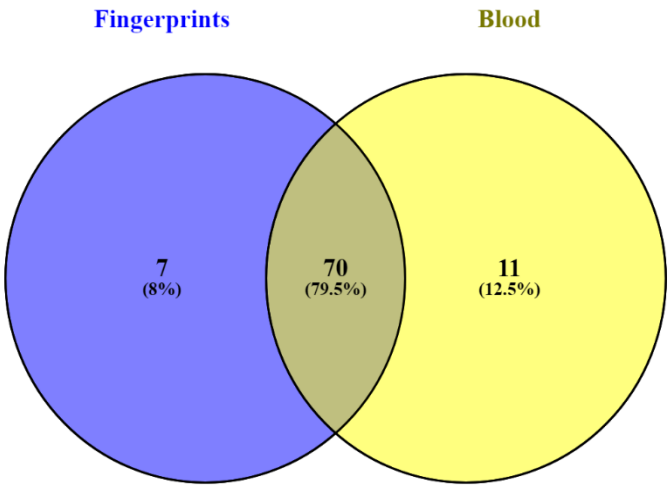

Figure 14: Venn diagram showing the number of metabolites detected in sweat from the fingerprints (blue), blood (yellow) or both (dark yellow) during intervention study 1.

some response to the ingestion of coffee. Because analytes were not quantified, the resulting kinetic profiles are discussed on a semiquantitative basis as rAUCs. Interindividual variation was calculated as the coefficient of variation (CV) of a target analyte in blood, or sweat, respectively, sampled from every individual at the same time point of the experiment. CVs were determined as ratio of the standard deviation and the corresponding average rAUCs of the target analyte within a group of samples. Intra-individual variations were calculated analogous from analytes' rAUCs found in sweat sampled from the left- and the right hand's fingertips of a single individual at a distinct time point.

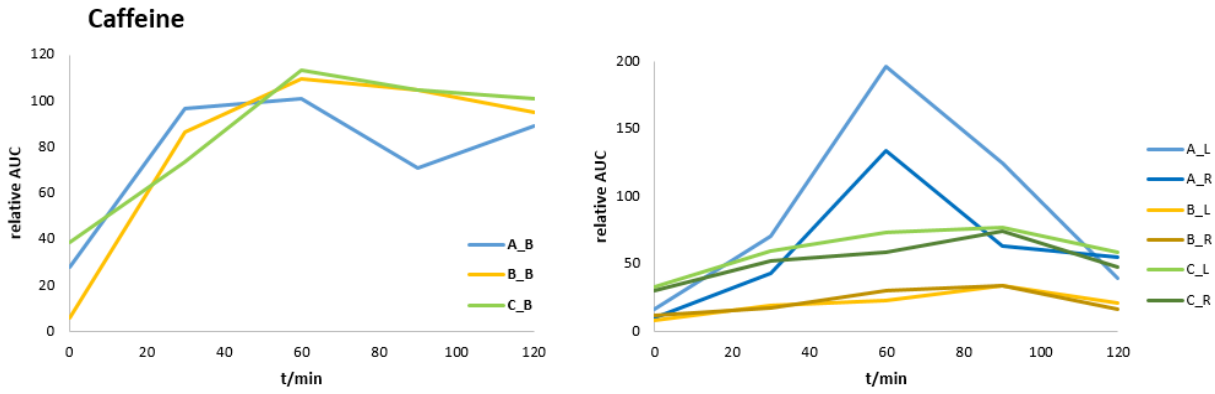

Figure 15: Kinetic profiles of CF in blood-(left) and sweat samples (right) analyzed during intervention study 1.

Figure 15 and Figure 16 are showing the kinetic profiles of CF in blood- and sweat. CF increased drastically within the first 20 min after coffee ingestion in sweat- and blood samples and peaked 60 min after coffe intake in all blood samples. The maximum rAUC occurred after 60 min in sweat samples obtained from individual A, while peaks were shifted and occurred after 90 min in samples of subjects B and C. CF levels under starting conditions showed an interindividual variation of 59%, especially because rAUCs of CF found in sweat of individual C was approximately three times higher compared to the other subjects. The rAUC of the CF peak in sweat samples of individual A was approximately two times and five times higher compared to rAUCs of CF in sweat samples of individuals B and C, respectively, with an overall interindividual variability of 69%. Interindividual variability was 44% 120 min after coffee intake with lowest CF levels found in sweat sampled from individual B. The kinetic profiles of CF in blood samples were highly similar for all three investigated subjects with CF maxima observed 60 min after coffee intake. Interindividual variability was 68% before consumption of coffee and diminished to 6% in blood sampled 60 min and 120 min after coffee intake. The higher variation

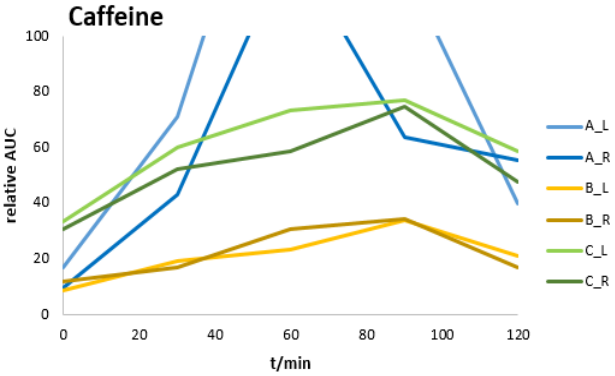

Figure 16: Kinetic profiles of CF in sweat samples analyzed during intervention study 1 (zoomed in).

found under starting conditions was most likely caused by differing consumer's behavior within the group of subjects and should be avoidable by the application of more stringent dietary restriction in future experiments, especially a longer period of CF abstinence. Qualitative similarities of time courses of caffein in blood and sweat samples were observed for individuals B and C, while kinetics in blood and sweat seemed to be more distinct for individual A. In general, it can be stated that sweat samples showed higher interindividual variability when compared to the highly similar timecourses of CF found in the blood samples of all three individuals investigated.

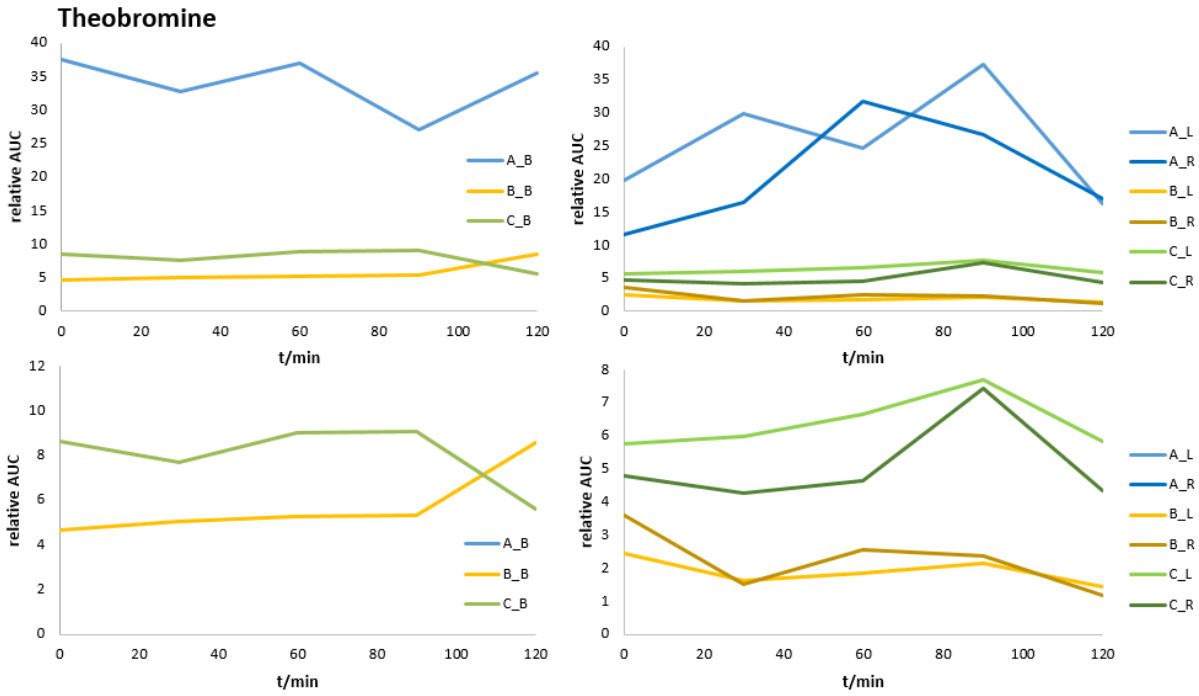

Figure 17: Top figures: kinetic profiles of TB in blood-(left) and sweat samples (right) analyzed during intervention study 1. Bottom figures: magnifications focused onto samples with lower analyte abundances.

Kinetic profiles of TB showed a different picture (compare Figure 17): the rAUCs of TB tended to decrease in sweat sampled from individual B, while an increase of TB was observed in sweat sampled from individuals A and C with peak levels observed 60 min to 90 min after the ingestion of coffee. Meanwhile, no clear trend was observed for the analyzed blood samples: variations of the TB content found in blood samples from individual A, which in general showed high TB levels compared to samples obtained from individuals B and C, seemed to occur randomly. Only individual B showed increasing TB levels during the last 30 min investigated, while TB levels decreased in blood sampled from individual C during the same time period. Interindividual variability of TB exceeded 84% in blood sampled under starting conditions as well as 90 min and 120 min after ingestion of coffee. Similar as for TB levels in blood, interindividual variations of TB levels in sweat samples exceeded 84% at all investigated time points. Especially high TB levels observed in samples obtained from individual A before consumption of coffee were indicating that this phenomenon might be explained by the consumer's behavior of the

three volunteers, e.g. consumption of TB rich foods or drinks by individual A prior to the 24 h abstinence of methylxanthine rich comestibles. Therefore, it should be possible to reduce interindividual variability by elongated and more stringent dietary restrictions, including TB containing foods and drinks, prior to similar intervention studies. Concluding, high TB levels observed in blood samples under starting conditions were associated with high TB levels present in sweat samples. TB levels found in sweat are likely to rather depend on accumulation of TB than on a direct relation to its kinetic behavior in blood upon coffee consumption. Anyway, to allow meaningful kinetic investigations of TB in sweat samples and its correlation to blood kinetics, further experiments with high doses of TB containing comestibles, e.g. chocolate, seem to be necessary. Additionally, an extended sampling time should be considered in future experiments.

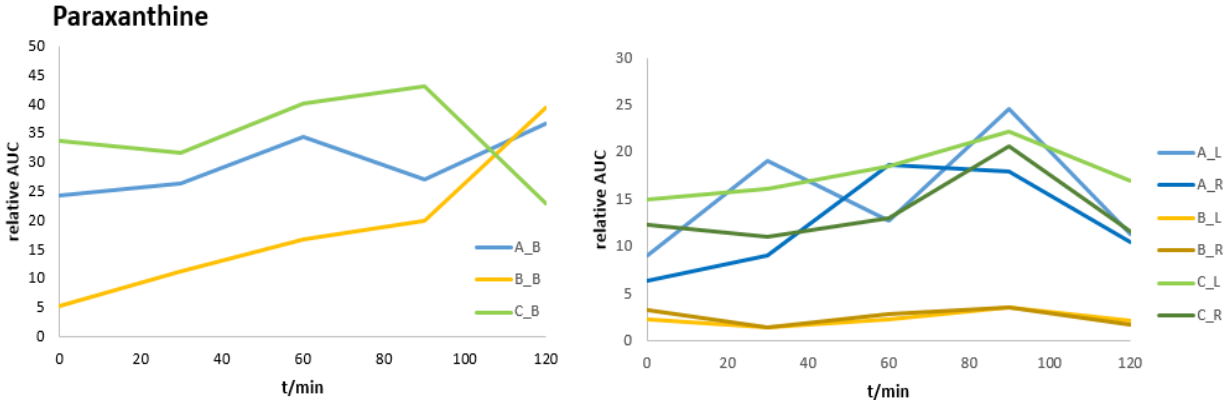

Figure 18: Kinetic profiles of PX in blood-(left) and sweat samples (right) analyzed during intervention study 1.

Figure 18 and Figure 19 are showing the time courses of PX in sweat- and blood sampled before and after consumption of coffee. Time courses were qualitatively similar to the kinetic profiles determined for TB, although blood levels tended to increase in all investigated individuals. PX peaked 90 min after ingestion of coffee in blood sampled from individual C, while highest PX levels were detected after 120 min in blood samples of individuals A and B. PX peak levels were detected in sweat samples of all three individuals 90 min after coffee intake. Only sweat sampled from the right hand of individual A showed an earlier PX peak 60 min after coffee intake, while PX determined in sweat from the left hand showed a local minimum 60 min after coffee ingestion. Kinetic behavior of PX in sweat of individual B was slightly different to kinetics in sweat of both other volunteers. After levels decreased during the first 30 min of the experiment a PX maximum was observed after 90 min. A maximum intraindividual

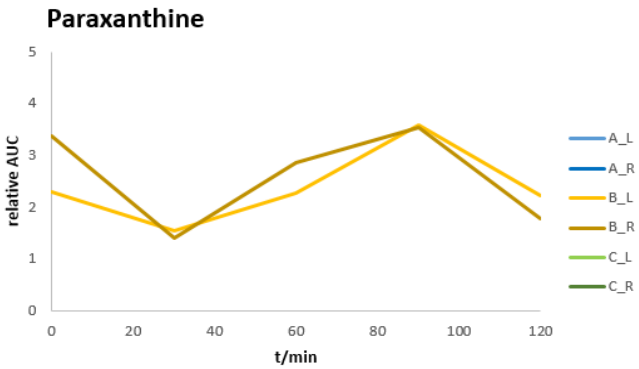

Figure 19: Kinetic profiles of PX in sweat samples analyzed during intervention study 1 (zoomed in).

variability of 50% was observed in sweat sampled from individual A 30 min after the ingestion of coffee while it stayed below 27% for all other data points in all subjects. The interindividual variability in sweat samples unambiguously exceeded variabilities found within every volunteer with CVs between 61% and 75% for any time point of the experiment. Interindividual variability of PX in blood decreased from 68% under initial conditions to 27% in blood sampled two hours after ingestion of coffee. Although kinetic profiles of PX showed a similar pattern as profiles determined for TB, a trend indicating increasing amounts of PX in blood- and sweat from the fingertips, with peaks occurring 90 min after the ingestion of CF or later, was observed. Generally, PX levels found in blood under initial conditions were associated with high levels found in sweat, as was already described for TB in the section above.

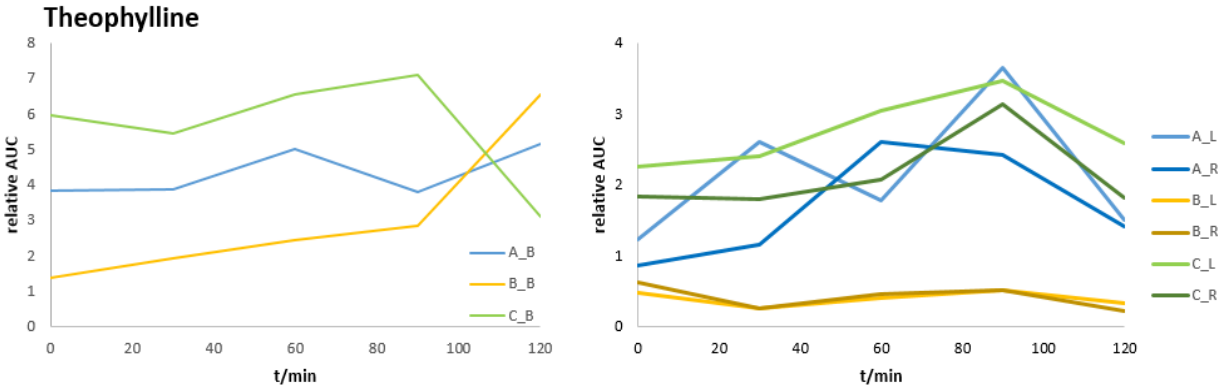

Figure 20: Kinetic profiles of TP in blood-(left) and sweat samples (right) analyzed during intervention study 1.

Kinetics of TP followed a similar pattern as kinetics of TB and PX described in the sections above (compare Figure 20 and Figure 21). Blood levels of TP showed peak levels 90 min after ingestion of coffee in blood sampled from individual C, while levels increased in samples of individuals A and B during the whole experiment. Sweat levels of TP peaked after 90 min in samples from individuals A and C, whereas TP generally decreased in sweat sampled from subject B and showed the same, rather random fluctuation pattern observed for TB and PX with a minimum detected 30 min- and a local maximum 90 min after coffee intake. The maximal intraindividual variability was observed in sweat sampled from individual A 30 min after coffee ingestion with a CV of 54%, while CVs didn't exceed 30% in any other pair of samples.

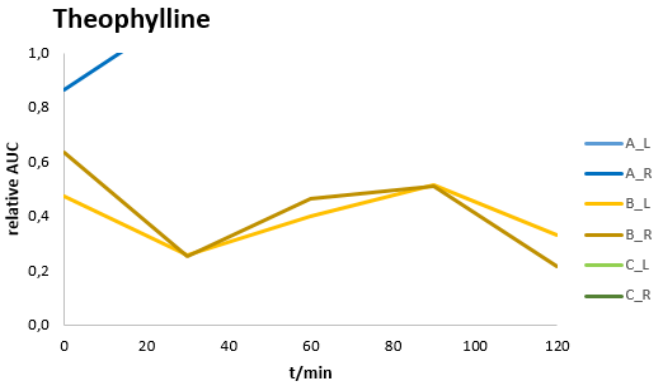

Figure 21: Kinetic profiles of TP in sweat samples analyzed during intervention study 1 (zoomed in).

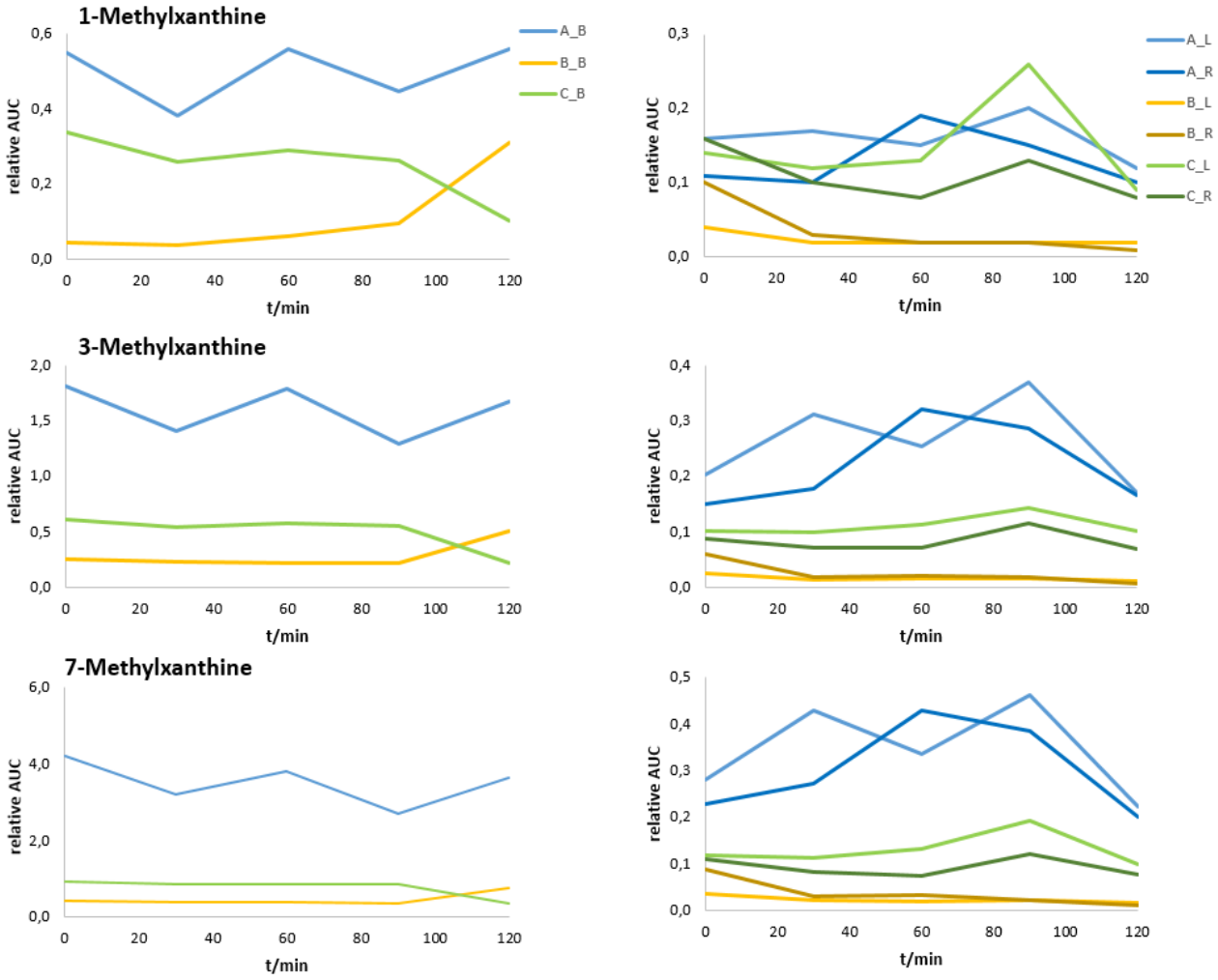

Figure 22: Top to bottom: kinetic profiles of 1-MX, 3-MX and 7-MX in blood-(left) and sweat samples (right) analyzed during intervention study 1.

Figure 22 shows the kinetic profiles of 1-MX, 3-MX and 7-MX observed in blood- and sweat samples. The rAUCs of 1-, 3- and 7-MX, the secondary metabolites of CF, were lower than rAUCs of its primary metabolites TB, PX and TP. In general, the three MX iomers showed similar time course patterns in blood and sweat. 1-MX levels showed rather random variations in blood samples from individual A, while its content nearly sextupled in samples of individual B and in samples of individual C during the investigated period. Again, high variability within the group of volunteers was observed with peak levels detected 90 min after coffee intake in sweat obtained from individuals A and C, while levels decreased in sweat sampled from individual B. Similar to the dimethylxanthines TB, PX and TP, no clear kinetic trend was observed neither in blood, nor in sweat samples. Nevertheless, relatively high 1-MX blood levels observed in samples of volunteers A and C under starting conditions were associated with high levels present in sweat samples. Similar patterns were observed for 3-MX and 7-MX in blood- and sweat. As described for TB, TP and 1-MX in the sections above, levels of 3-MX and 7-MX in blood samples of individual A varied during the whole experiment, while levels increased in blood samples of individual B and decreased in blood samples of individual C. Peak levels of 3-MX and 7-MX were found

90 min after coffee ingestion in individuals A and C, decreasing rAUCs were observed in sweat sampled from individual B.

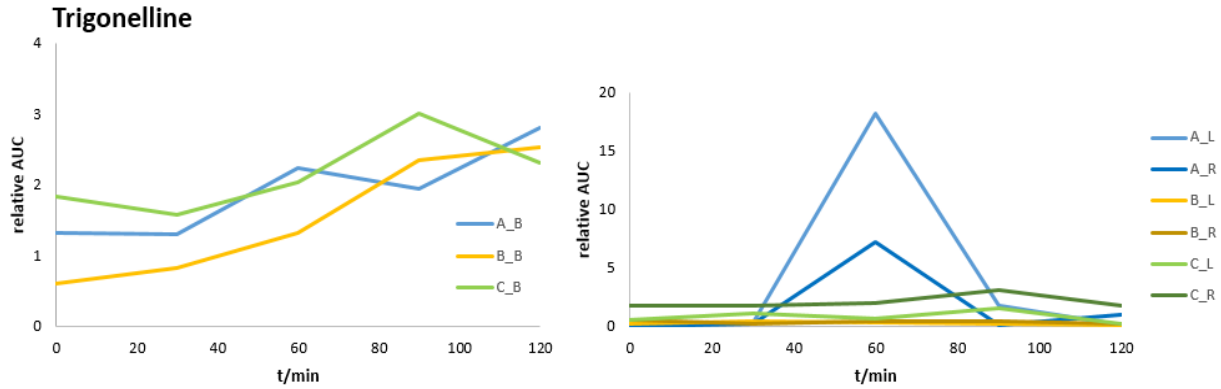

Figure 23: Kinetic profiles of trigonelline in blood-(left) and sweat samples (right) analyzed during intervention study 1.

Trigonelline was present in sweat- and blood samples of all three individuals before- and after ingestion of a cup of coffee (compare Figure 23). Its levels in blood samples under initial conditions showed an overall interindividual variability of 49% with highest rAUCs found determined for samples from individual C. The kinetic behavior of trigonelline in sweat samples obviously differed from the kinetics determined for trigonelline in blood. While trigonelline showed similar time courses in blood samples of all three individuals with maximum trigonelline levels observed 90 min or 120 min after coffee intake, respectively, trigonelline levels in sweat peaked 60 min and 90 min after coffee intake in samples from individuals A and C, respectively, and decreased in sweat obtained from individual B. However, the intense trigonelline peak observed in sweat of individual A 60 min after starting the experiment exceeded the trigonelline levels in all other sweat samples by approximately one order of magnitude.

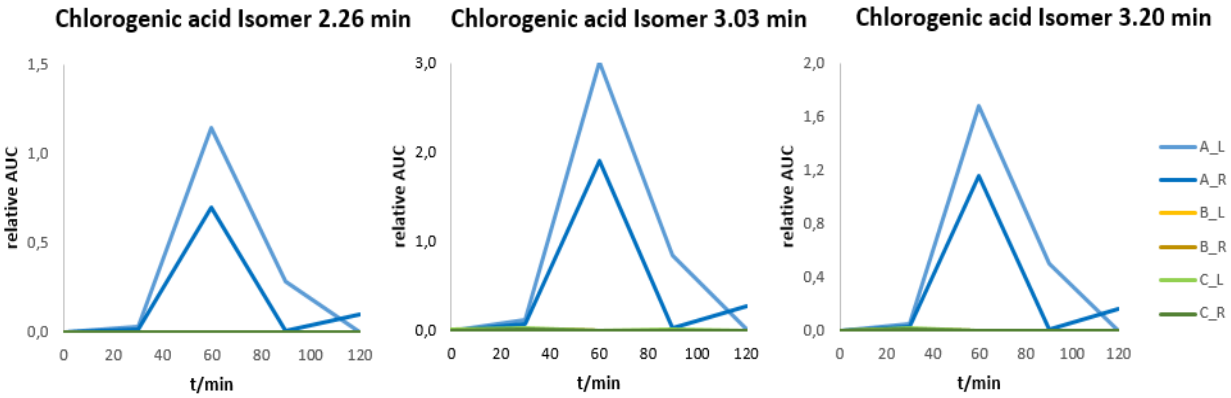

Figure 24: Kinetic profiles of CGA isomers in sweat analyzed during intervention study 1.

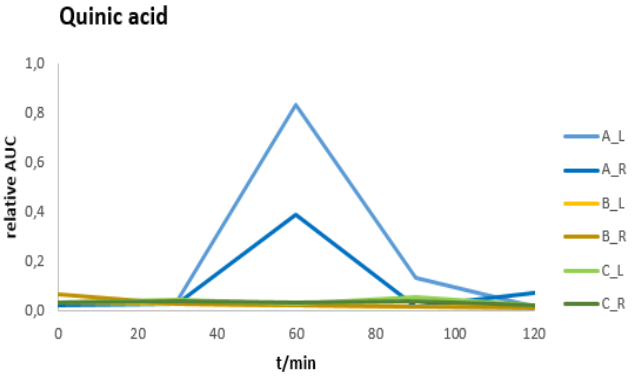

Figure 25: Kinetic profiles of quinic acid in sweat analyzed during intervention study 1.

Substantial amounts of CGA isomers were present in sweat sampled from individual A, while only trace amounts, merely distinguishable from noise, were detected in some single samples of individuals B and C. All CGA isomers, as well as quinic acid showed parallel kinetic behavior resembling the time course of trigonelline in sweat of the same volunteer with peak levels found 60 min after ingestion of coffee. The CGA isomer with retention time 3.03 min had the most intense chromatographic peak followed by isomers with retention times 3.2 min and 2.26 min. Whether peaking CGA and quinic acid levels 60 min after coffee intake determined solely in individual A were caused by distinct individual kinetics due to differing permeabilities of the skin or were originating from contamination of the individual's fingertips, could not be cleared during this experiment and should be subject to further investigations. Kinetic profiles of CGA isomers and quinic acid are shown in Figure 24 and Figure 25, respectively.

Intervention study No. 2: Ingestion of coffee or chocolate

Donor	Age [years]	Sex	Chocolate consume	Coffee consume	Group
A	40-50	m	moderate	intense	Coffee
B	40-50	f	moderate	moderate	Coffee
C	20-30	m	moderate	moderate	Control
D	50-60	f	moderate	rare	Control
E	20-30	m	moderate	rare	Chocolate
F	20-30	f	moderate	moderate	Chocolate

Table 2: Table of participants taking part in intervention study 2. Consumer's behavior regarding chocolate and coffee intake was classified as rare, moderate or intense.

During a second intervention study, coffee and chocolate were used to investigate the kinetic behaviour of the most abundant metabolites identified in both products. Hence, 45 and 50 compounds were detected in 1:1000 dilutions of coffee and cocoa extract, respectively. The pattern of the ten most abundant compounds found in the coffee sample during this experiment was nearly identical to the pattern observed during the first study, but caprolactam was the 10th intense analyte peak in coffee instead of decanamide (compare Figure 26). As described above, caprolactam is a monomer used during the production of nylon-6 and can migrate from package material into foodstuff and therefore might originate from plastic surfaces, e.g. the plastic capsules used during the brewing procedure. The top 10 substances present in chocolate were dominated by TB followed by CF. Choline, the amino acids leucine/norleucine, phenylalanine, valine, proline and isoleucine, as well as betaine and catechin/epicatechin were the next abundant substances detected in the chocolate extract. The data can be reviewed in more detail in Figure 27.

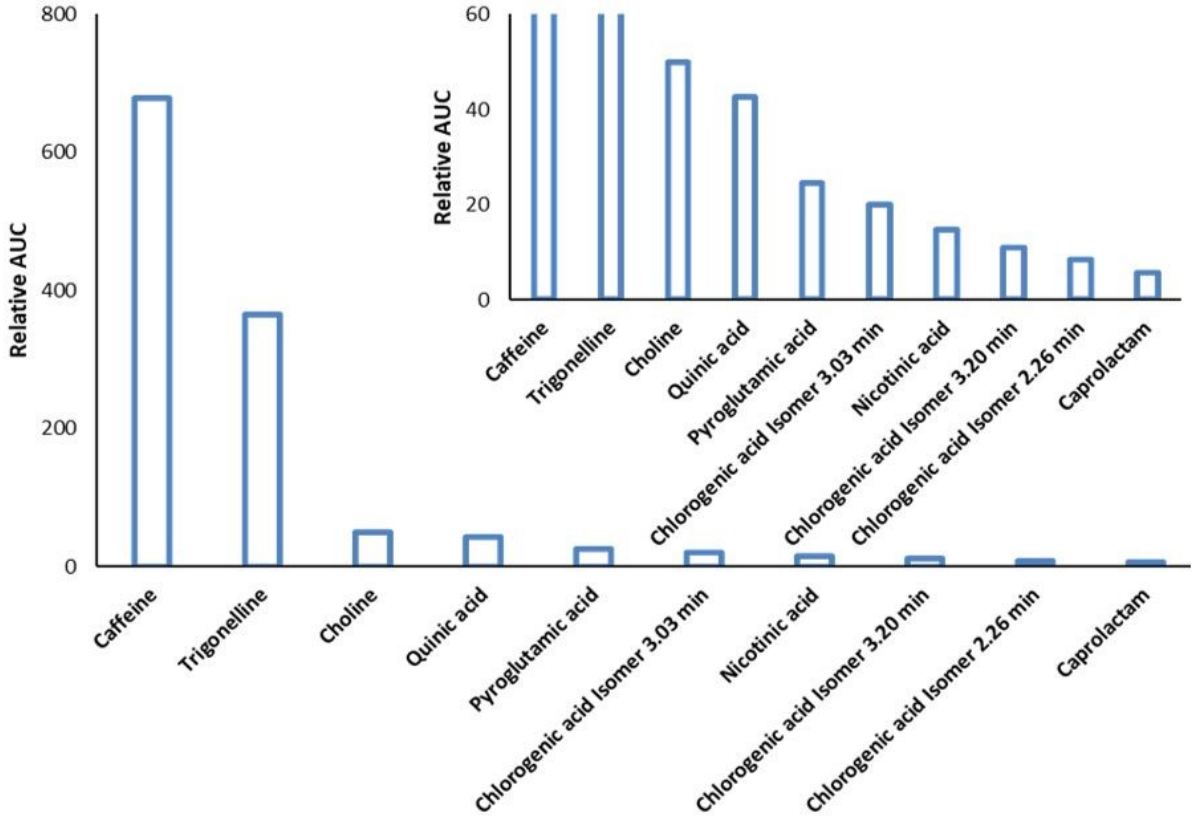

Figure 26: rAUCs of the ten compounds with the most intense chromatographic peaks detected in coffee during intervention study 2.

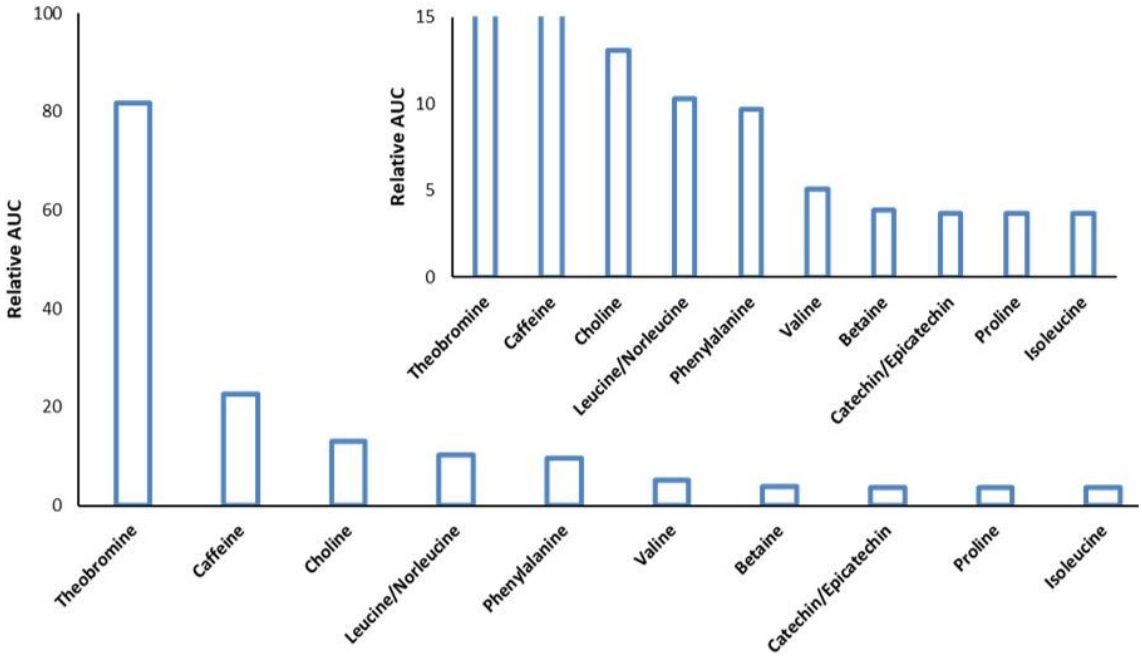

Figure 27: rAUCs of the ten compounds with the most intense chromatographic peaks detected in chocolate extract during intervention study 2.

82 metabolites were detected in extracts of sweat sampled from the fingertips, of which 39 were present in extracted filter paper as well. An unpaired two-sided t-test was used as decision criterion (p-value ≤ 0.05) to determine whether an analyte originates from sweat or the filter paper used during the extraction procedure. Hence, 79 compounds were classified as originating from finger sweat. 17 compounds were solely observed in sweat samples, but not in blood samples, including catechin/epicatechin, the CGA isomers, the amino acids citrulline, glutamic acid and lysine, as well as nicotinic acid, quinic acid, sorbic acid, EDTA and triethanolamine. PEG polymers were found in sweat extracts, but were regarded as contaminations most likely originating from sampling- and sample preparation steps. Overall, six compounds, namely 1-aminocyclohexanecarboxylic acid, decanamide, ergothioneine, spermidine, the antihistamine diphenhydramine and the anti-inflammatory drug mefenamic acid were detected exclusively in extracted blood samples, while all other 62 analytes were found in both sample groups. The anti-inflammatory drug mefenamic acid was only present in blood samples of individual B. In general, it has to be stated that metabolites were identified based on database matches and should be regarded as putatively identified. To exclude the possibility of false-positive identifications, verification of the results using standard solutions would be necessary.

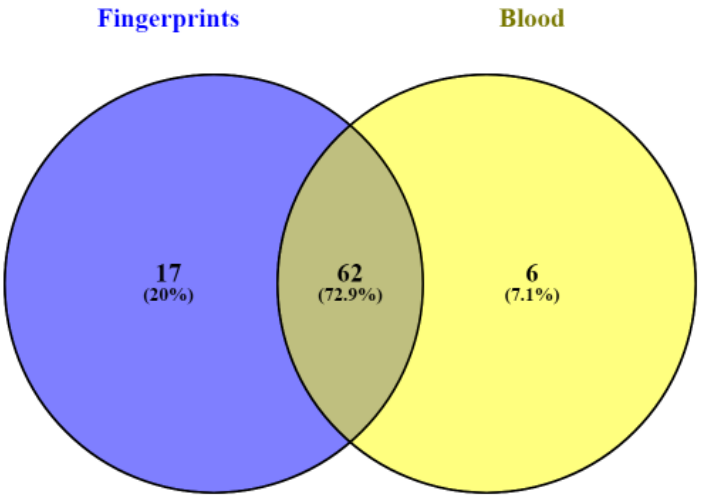

Figure 28: Number of metabolites detected in sweat (blue), blood (yellow) or both (dark yellow) during the second intervention study shown as a Venn diagram.

The kinetic behavior of the most abundant compounds in coffee and chocolate extract was then investigated and is discussed in the following section. Therefore, six individuals were separated into three groups, each composed of a male and a female volunteer. Individuals of the first group drank a cup of coffee, individuals of the second group consumed half a bar of dark chocolate (50 g, min. 70% cocoa), while the third group avoided CF or TB rich foods and drinks and represented the control group. Blood- and sweat were sampled under initial conditions, 20 min, 40 min, 60 min, 90 min, 120 min and 180 min after starting the experiment. Only individual A skipped the sampling process for the last data point of the time course.

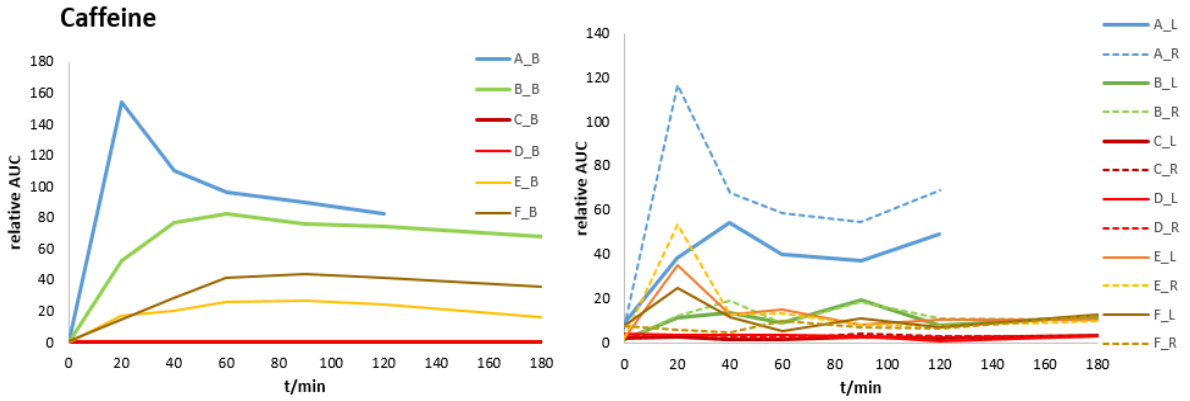

Figure 29: Kinetic profiles of CF in blood-(left) and sweat samples (right) analyzed during intervention study 2. Individuals A and B consumed coffee, individuals E and F consumed chocolate, while individuals C and D represented the control group.

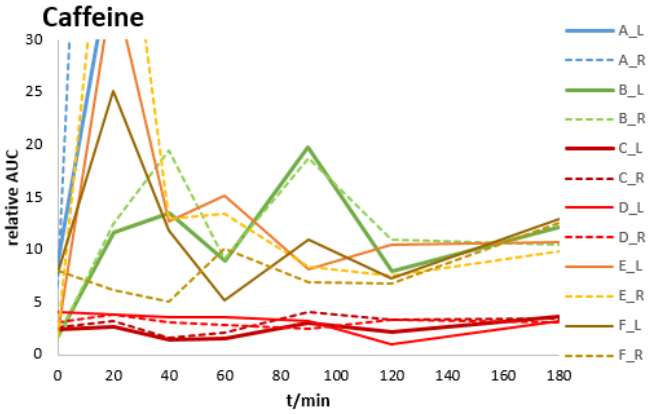

Figure 30: Kinetic profiles of CF in sweat samples analyzed during intervention study 2 (zoomed in). Individuals A and B consumed coffee, individuals E and F consumed chocolate, while individuals C and D represented the control group.

The kinetic profile of CF in blood and sweat can be reviewed in Figure 29 and Figure 30. Donors A and B ingested coffee, donors E and F consumed chocolate, while donors C and D were representing the control group. CF levels in blood increased in the group of coffee consumers, as well as in the group ingesting chocolate, while no significant increase was observable within the control group. The most intense CF peak was observed in blood sampled from individual A 20 min after coffee consumption, while the second participant consuming coffee (individual B) showed slightly different kinetics. Herein, we observed a CF maximum in blood approximately 60 min after coffee intake followed by a linear decrease during the rest of the investigated period of time. CF levels increased as well in the group of chocolate consumers, but maxima occurred not before 90 min after intake. Maximal CF levels found in blood after coffee intake were approximately 3.5 times higher than CF maxima found after chocolate intake. CF levels in blood showed an interindividual variability of 70% 20 min after coffee intake which decreased to approximately 7% after two hours. Due to the missing samples from individual A three hours after coffee ingestion, interindividual variability within the coffee consuming group could not be determined for the last time point of the experiment. After chocolate consumption, the rAUCs of CF in blood sampled from individual E showed a lower maximum level and faster decline when compared to CF levels in blood of individual F, indicating differences in resorption and metabolism. Levels observed in blood sampled from participant E three hours after chocolate intake were 39% lower than the maximum found after 90 min, while the relative

decrease observed within the same period of time was only 19% in blood samples of individual F. Interindividual variability within the chocolate consuming group was 9% in blood sampled 20 min after starting the experiment and increased stepwise to 52% during the investigated period. Sweat CF levels peaked 20 min after ingestion of coffee in samples obtained from individual A, while the CF peak in sweat samples from individual B was observed after 90 min.

Because CF peaks in sweat sampled from the left- and right hand were shifted by 20 min, intraindividual variability of CF levels was exceptional high in sweat sampled from individual A 20 min after coffee ingestion and exceeded 70%, while it varied between 15% and 27% at all other investigated time points. In general, samples obtained from the fingertips of the right hand showed higher CF levels in individual A, while CF levels found in sweat sampled from the left- and right hand of individual B were very similar within the whole experiment leading to a low intraindividual variabilities with CVs between 1% and 26%. A sharp CF peak was observed in finger sweat sampled from individual E and in sweat obtained from the left hand of individual F 20 min after ingestion of chocolate, followed by a sharp drop and a less pronounced, but continuous increase within the rest of the time course. However, due to inconsistent behavior observed in sweat sampled from the left and the right hands of chocolate consumers in combination with similar behavior of TB and catechin/epicatechin (discussed in the sections below; time courses are given in Figure 31 and Figure 43), two compounds highly abundant in chocolate, this unexpected and unusual kinetic behavior might be related to chocolate contaminations from chocolate consumption not completely removed from the pores and ridges of the fingertips.

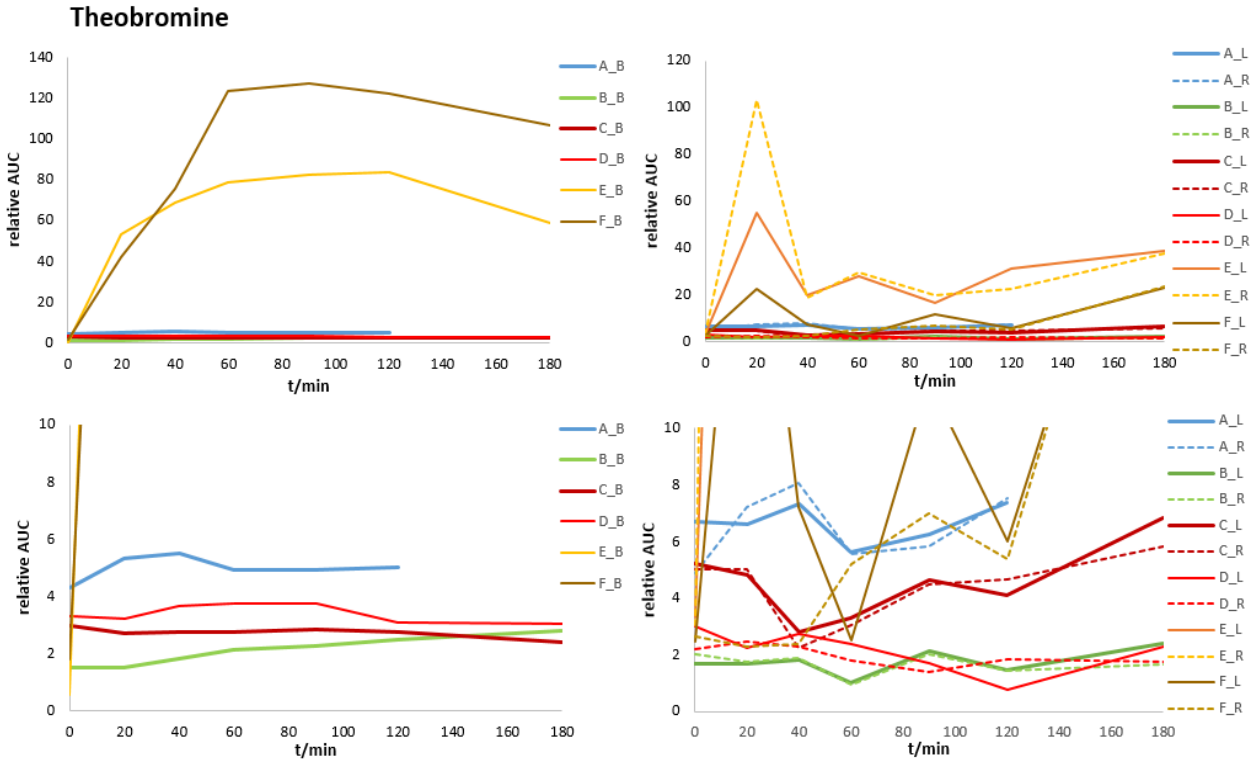

Figure 31: Top figures show the kinetic profiles of TB in blood-(left) and sweat samples (right) analyzed during intervention study 2, while bottom figures are magnifications focused onto samples with lower analyte abundances. Individuals A and B consumed coffee, individuals E and F consumed chocolate, while individuals C and D represented the control group.

Figure 31 shows the kinetic profiles of TB in blood- and sweat after coffee- or chocolate consumption, as well as under control conditions. TB levels in blood samples obtained from individuals E and F peaked 120 min and 90 min, respectively, after chocolate intake and subsequently decreased by 30% and 16%, whereas strong interindividual differences were observed. In similarity to the time courses determined for CF in blood after chocolate intake, the maximum TB level in samples of individual F was 52% higher than the TB maximum in blood samples from individual E. Although TB tended to increase slightly in participants after coffee ingestion, TB levels were similar to the levels in blood of the control group within the investigated period. TB levels in sweat derived from the fingertips showed similar behavior as CF after ingestion of chocolate. Sharp peaks in samples of individual E as well as in sweat sampled from the left hand of individual F were detected 20 min after ingestion of chocolate, followed by a sharp drop and, again, a continuous, but less pronounced increase of TB levels. However, TB levels in blood and sweat clearly exceeded CF levels after chocolate consumption. Due to inconsistent behavior within sweat sampled from the fingertips of the left- and the right hand of volunteer F combined with similar behavior of catechin/epicatechin and CF, two other abundant bioactives identified in chocolate extracts, contaminations from chocolate consumption were seen as a possible origin of this first sharp peak event. Surprisingly, TB levels in blood of individual E were lower than levels found in blood of individual F, while TB levels were distributed the other way around in sweat samples of both volunteers.

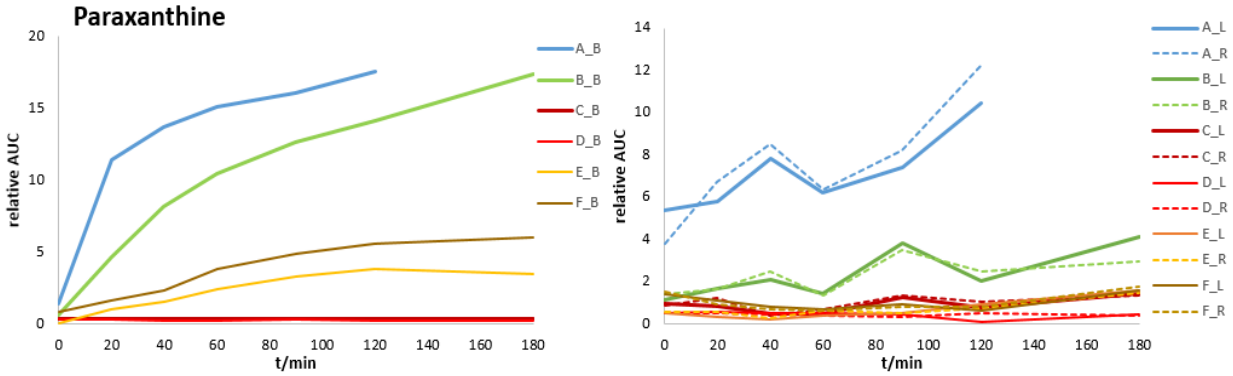

Figure 32: Kinetic profiles of PX in blood-(left) and sweat samples (right) analyzed during intervention study 2. Individuals A and B consumed coffee, individuals E and F consumed chocolate, while individuals C and D represented the control group.

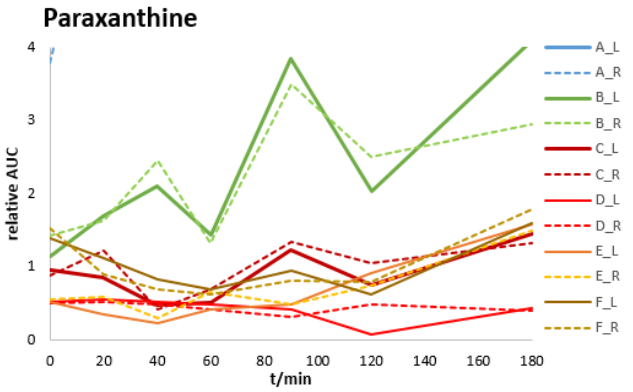

Figure 33: Kinetic profiles of PX in sweat samples analyzed during intervention study 2 (zoomed in). Individuals A and B consumed coffee, individuals E and F consumed chocolate, while individuals C and D represented the control group.

Figure 32 and Figure 33 are showing the time courses of PX in blood and sweat. Because PX is the mayor primary metabolite of CF in human beings, its levels in blood samples increased after coffee-, as well as chocolate consumption and represent the metabolism of CF by the CYP in the liver. PX levels sharply increased within the first 20 min after coffee intake. Then, a phase of linear, but less rapid increase was observed in blood of individuals A and B until the last time points investigated. Maximum PX levels in blood were detected 120 min after chocolate consumption in individual E, while PX levels in blood sampled from individual F increased until the end of the investigated period. Maximal PX levels were more than three times elevated after coffee intake in comparison to PX maxima found after chocolate ingestion, which is consistent with the corresponding data for its precursor molecule CF. Generally, PX levels in blood- and sweat samples from individual A exceeded levels samples obtained from individual B. Although PX levels in sweat sampled after ingestion of chocolate tended to increase during the last 60 min of the experiment, it was not possible to distinguish the chocolate consuming group from the control group unambiguously solely based on PX levels in sweat samples. Under starting conditions, the interindividual variability was 50% in blood sampled from the group of coffee consumers, but decreased to 15% calculated for blood sampled 120 min after coffee intake. Interindividual variability in sweat samples was higher and varied between 42% and 78%, while the intraindividual variability in sweat didn't exceed 25% after coffee intake. After consumption of chocolate, interindividual variability of PX levels in blood varied between 27% and 38%, while levels in sweat samples showed interindividual variabilities ranging from 7% to 57%. The intraindividual variability in sweat didn't exceed 37% after ingestion of chocolate.

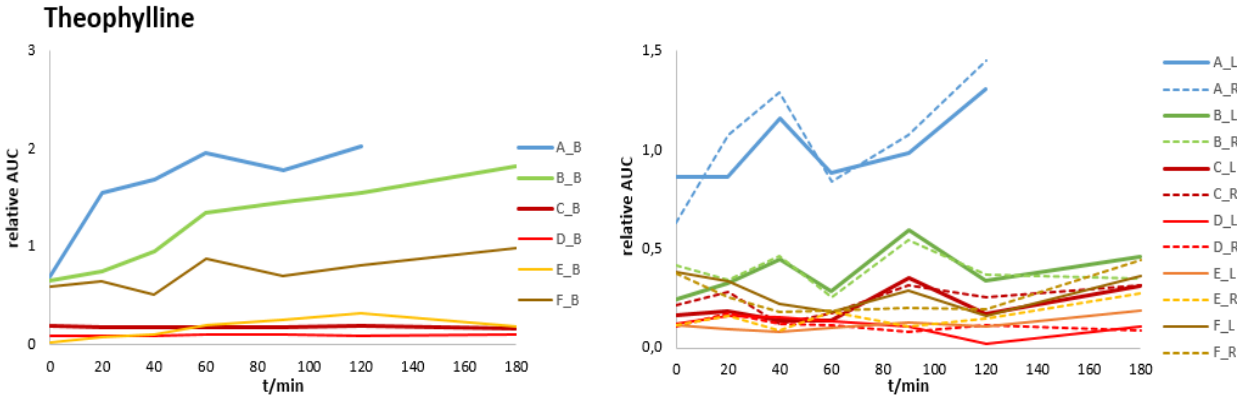

Figure 34: Kinetic profiles of TP in blood- (left) and sweat samples (right) analyzed during intervention study 2. Individuals A and B consumed coffee, individuals E and F consumed chocolate, while individuals C and D represented the control group.

Kinetic profiles of TP in blood and sweat are given in Figure 34 and Figure 35. Levels in blood- and sweat samples increased after the consumption of coffee, while TP levels increased in a less pronounced fashion in blood samples obtained after consumption of chocolate. After coffee intake, the blood levels of TP in samples of individuals A and B increased until the end of the observed period. Sweat levels increased in samples of individual A with a local maximum 40 min- and a global maximum 120 min after coffee consumption, while levels in sweat of individual B showed a local maximum 40 min after intake and a global maximum 90 min after intake. However, data indicates further increase of blood- and sweat levels outlasting the observed period, although experiments with an extended sampling period would be necessary to obtain deeper insights. TP content in sweat samples of individual A unambiguously exceeded the levels present in any other investigated individual, which might be related to the consumer's behavior of the participants of this study. The TP levels peaked in blood sampled from individual E 120 min after chocolate intake, while levels increased until the end of the experiment in blood samples of individual F. TP levels in sweat samples of individuals E and F could not be distinguished from levels found in the control group.

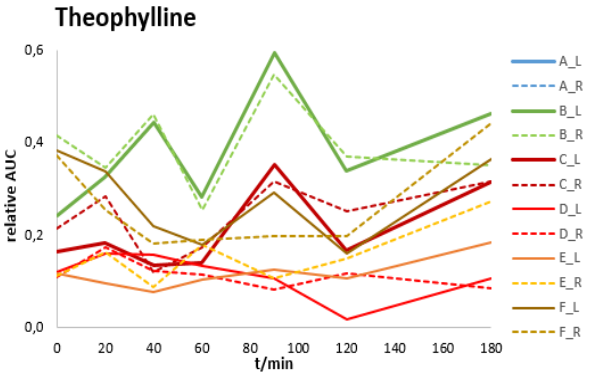

Figure 35: Kinetic profiles of TP in sweat samples analyzed during intervention study 2 (zoomed in). Individuals A and B consumed coffee, individuals E and F consumed chocolate, while individuals C and D represented the control group.

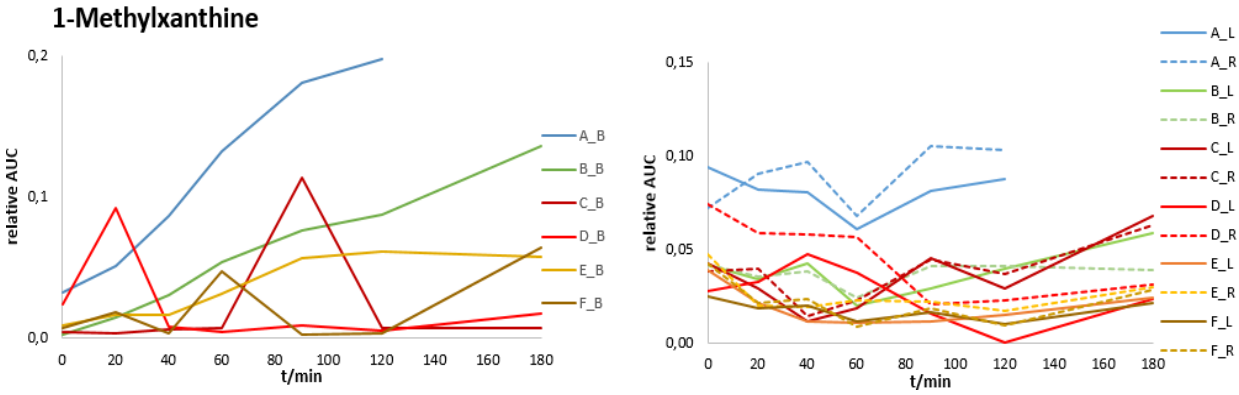

Figure 36: Kinetic profiles of 1-MX in blood- (left) and sweat samples (right) analyzed during intervention study 2. Individuals A and B consumed coffee, individuals E and F consumed chocolate, while individuals C and D represented the control group.

Figure 36 shows blood and sweat levels of 1-MX determined during this intervention study. Although 1-MX was only present at trace amounts, increasing 1-MX levels were observed in blood samples of individuals A, B and E after the consumption of coffee or chocolate, respectively. 1-MX in samples of the control group, as well as in blood samples obtained from volunteer F were oscillating and showed no clear trend. However, this might be explained by the general low levels of 1-MX close to its detection limit. Blood levels in samples of individuals A and B increased during the whole investigated period of time. After chocolate consumption, 1-MX increased in blood of individual E and showed a maximum in blood sampled after 120 min. In contrast to individuals A, B and E, no trend could be determined for the kinetic curve of 1-MX in blood samples obtained from individual F. As already observed for PX and TP, the primary metabolites of CF, highest 1-MX levels under starting conditions were found in sweat- and blood sampled from individual A. Except for individual A, 1-MX levels in sweat didn't vary substantially between the control group and coffee- or chocolate consumers.

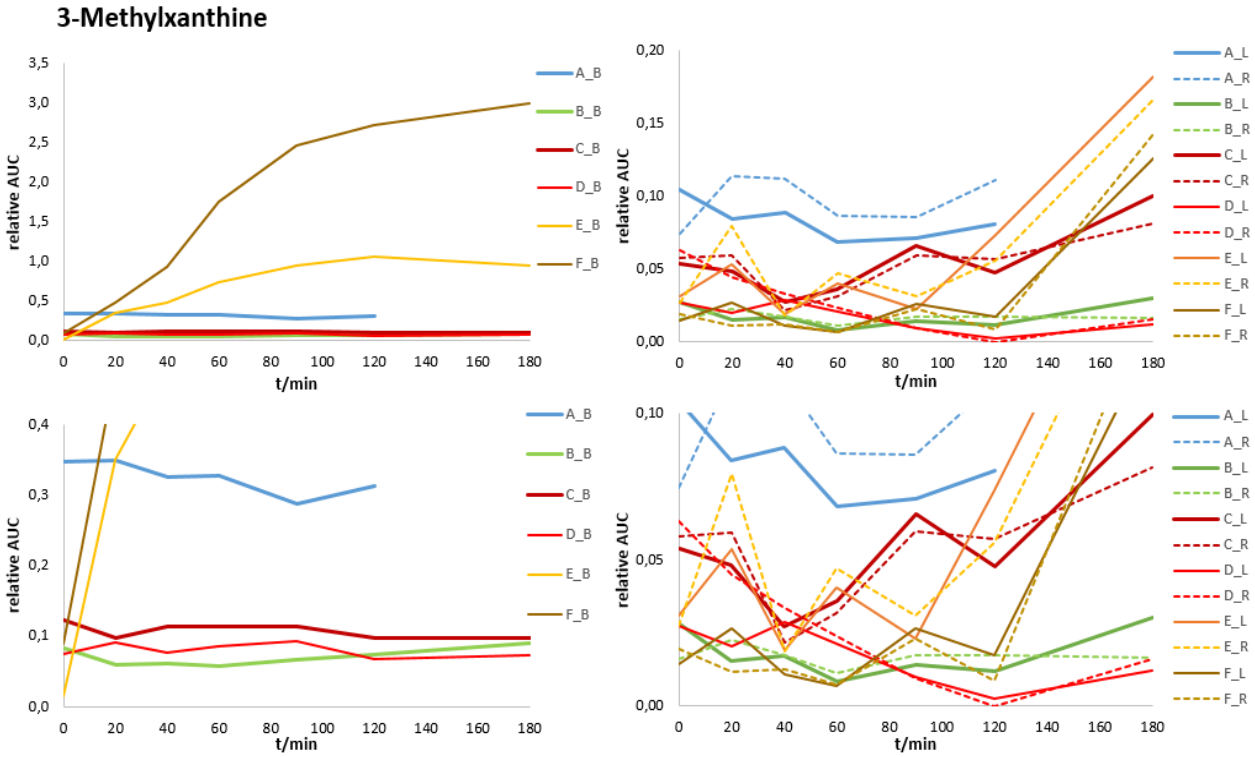

Figure 37: Top figures show the kinetic profiles of 3-MX in blood- (left) and sweat samples (right) analyzed during intervention study 1, while bottom figures are magnifications focused onto samples with lower analyte abundances. Individuals A and B consumed coffee, individuals E and F consumed chocolate, while individuals C and D represented the control group.

Figure 37 shows the kinetic profiles determined for 3-MX in blood- and sweat samples. 3-MX levels in blood increased after the consumption of chocolate, while no variations of 3-MX levels were observed upon the consumption of coffee. The levels varied a lot between subjects E and F, indicating high interindividual variability of TB metabolism. The 3-MX levels found in sweat of individual E were exceeding levels determined in sweat of individual F, while levels in blood samples showed a different picture, with lower levels found in blood of individual E. A similar behaviour was already observed for TB levels after chocolate consumption. The blood levels peaked 120 min and 180 min after ingestion of chocolate in individuals E and F, respectively. The 3-MX maximum in blood of individual F was approximately three times higher than maximum levels observed in samples obtained from individual E. 3-MX levels showed no substantial increase after the ingestion of coffee, while they increased in sweat obtained from individual C, member of the control group. Nevertheless, this increase showed no correlation with blood levels and was most likely related to the low amounts of 3-MX detected in sweat. 3-MX in sweat samples of individuals E and F increased 90 min and 120 min after chocolate intake, respectively. To investigate kinetic behaviour of 3-MX in sweat after chocolate consumption in more detail, further experiments with an extended sampling period would be necessary.

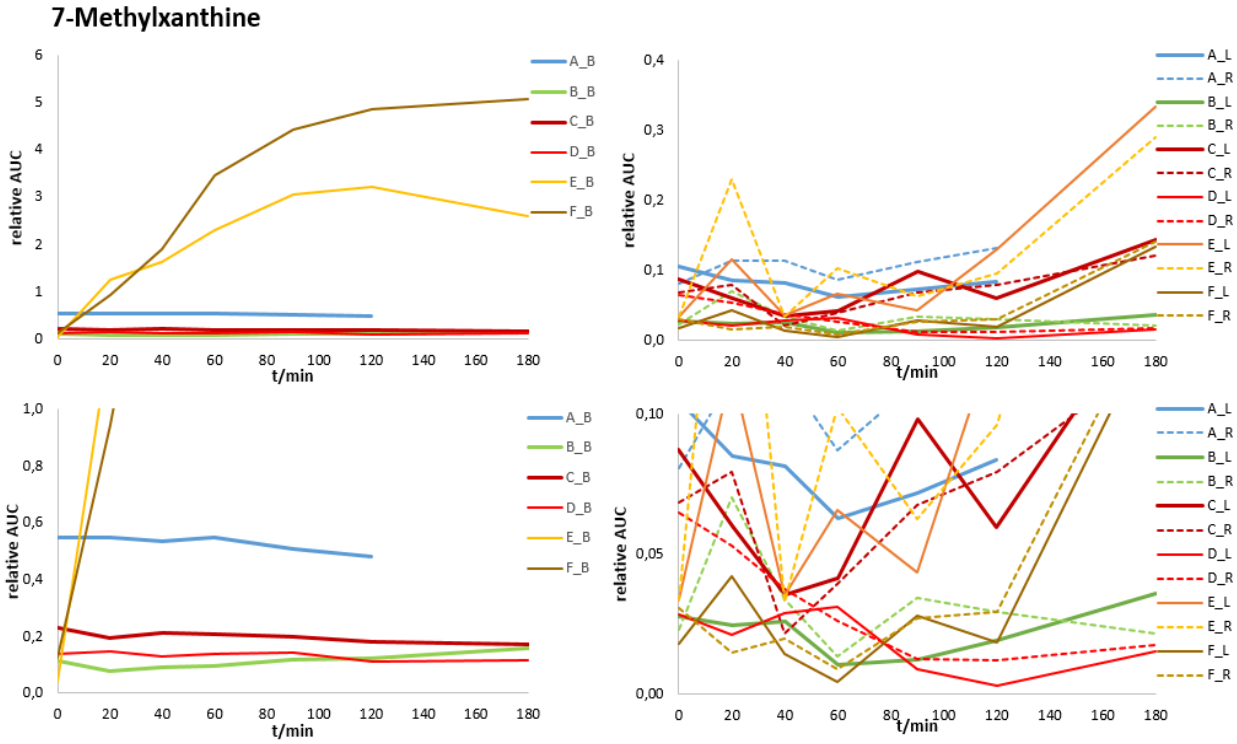

Figure 38: Top figures show the kinetic profiles of 7-MX in blood-(left) and sweat samples (right) analyzed during intervention study 1, while bottom figures are magnifications focused onto samples with lower analyte abundances. Individuals A and B consumed coffee, individuals E and F consumed chocolate, while individuals C and D represented the control group.

Kinetic curves determined for 7-MX were similar to curves obtained for 3-MX discussed in the section above. While 7-MX peaked 120 min after chocolate consumption followed by a slight decrease in blood samples of individual E, its levels increased in blood samples of individual F until the end of the investigated period. As observed for 3-MX and TB, blood levels of coffee consumers and the control group stayed rather constant, whereas under initial conditions 7-MX levels in samples of individual A were higher than levels in samples of the other volunteers. Random variations in sweat sampled from the fingertips of non-consumers of chocolate were observed. A phase of rapid linear increase of 7-MX starting 90 min after chocolate intake was observed in sweat sampled from individual E and after 120 min in sweat sampled from individual F. Hence, as already mentioned in the discussion of 3-MX levels in the previous section, these results can be seen as hint for delayed secretion of 7-MX in sweat which might be worth investigating in further experiments using elongated sampling periods.

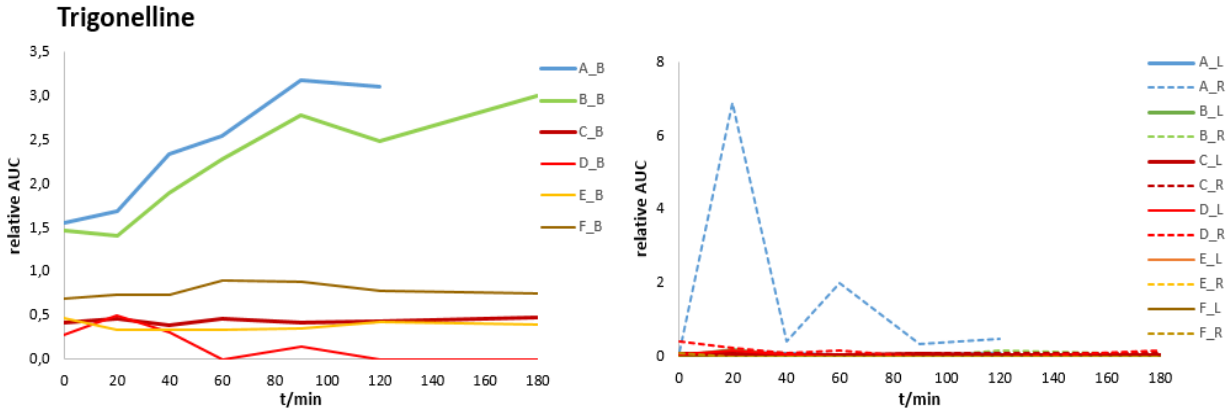

Figure 39: Kinetic profiles of Trigonelline in blood- (left) and sweat samples (right) analyzed during intervention study 2. Individuals A and B consumed coffee, individuals E and F consumed chocolate, while individuals C and D represented the control group.

The kinetic profiles of trigonelline in blood and sweat are given in Figure 39 and Figure 40. Trigonelline levels in blood increased in individuals A and B after ingestion of coffee, respectively. Similarity between blood kinetics of trigonelline within both investigated individuals was striking, which can be underlined by the low interindividual variability not exceeding 16% during the whole experiment. Peak levels were detected 90 min after the experiment started in individual A, while levels in blood of individual B increased until the end of the investigated period. However, because samples of subject A corresponding to the last time point are missing, further increase of trigonelline levels in blood can't be excluded based on our data. Low and stable trigonelline levels were observed in the blood samples obtained from the chocolate consuming- and the control group. Trace amounts of trigonelline were observed in some sweat samples, yet variations appeared in a rather random fashion. A trigonelline peak was observed 20 min after coffee intake in sweat sampled from the right hand's fingertips of individual A and subsequently decreased rapidly. A second local maximum occurred 60 min after intake of coffee. The kinetics of trigonelline in sweat samples of the right hand of individual A could neither be related to the levels found in the sweat sample obtained from the left hand, nor to the corresponding blood levels of trigonelline.

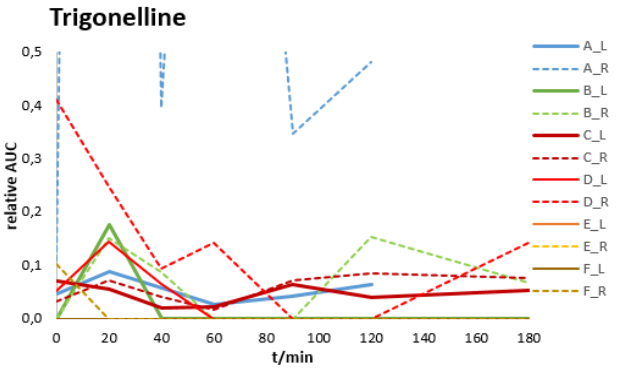

Figure 40: Kinetic profiles of trigonelline in sweat samples analyzed during intervention study 2 (zoomed in). Individuals A and B consumed coffee, individuals E and F consumed chocolate, while individuals C and D represented the control group.

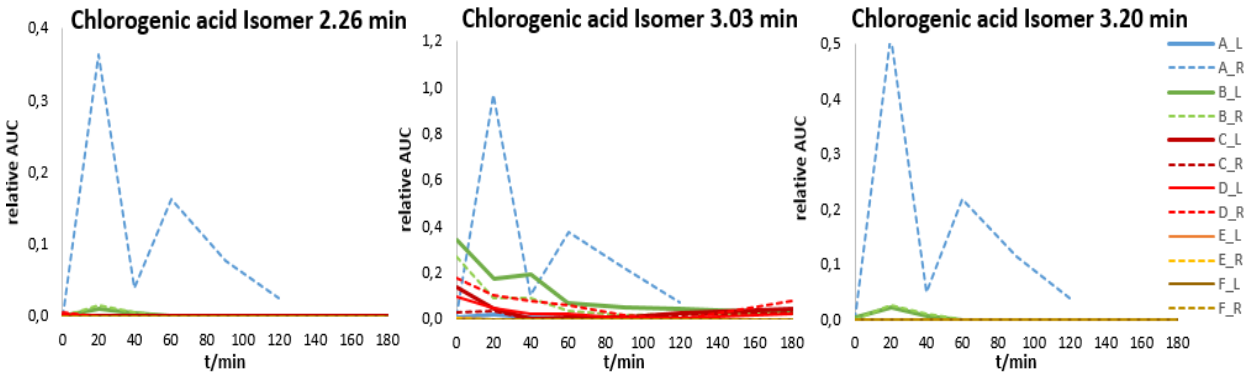

Figure 41: Kinetic profiles of CGA isomers in sweat analyzed during intervention study 2. Individuals A and B consumed coffee, individuals E and F consumed chocolate, while individuals C and D represented the control group.

CGA isomers were observed in sweat samples of several individuals, while no CGA isomers were detected in blood extracts. However, intense CGA peaks were only detected in sweat derived from the right hand's fingertips of individual A. A similar behavior was observed for trigonelline and quinic acid, a possible product of CGA metabolism and one of the major bioactives present in coffee. The migration of charged substances, as trigonelline, and acidic components, as CGAs, into sweat is mechanistically inhibited according to literature (described in more detail in the indtroductory section). Additionally, unconjugated CGA components in blood were neither detected in our experiments, nor by several other authors. Therefore, the unusual kinetics of trigonelline and CGA isomers in sweat derived from the fingertips reported here should be an objective of further investigations.

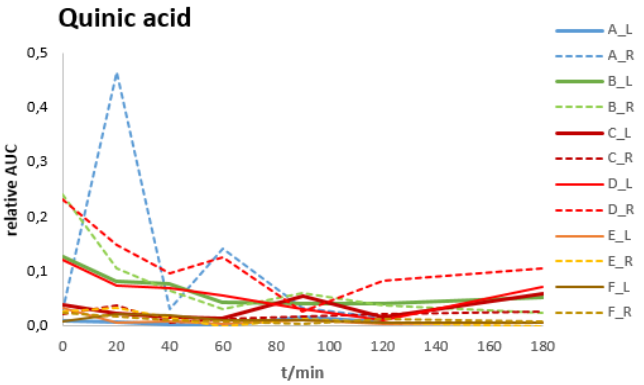

Figure 42: Kinetic profiles of quinic acid in sweat analyzed during intervention study 2. Individuals A and B consumed coffee, individuals E and F consumed chocolate, while individuals C and D represented the control group.

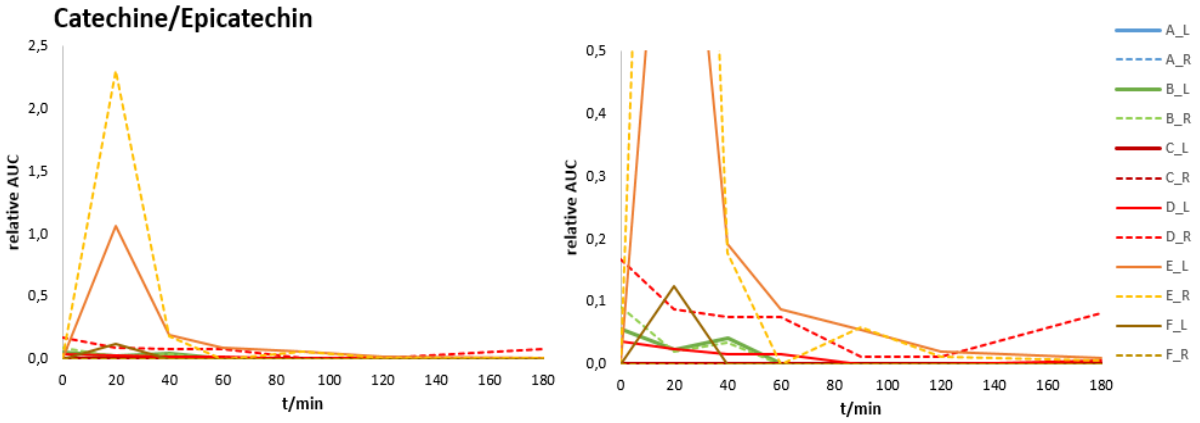

Figure 43: Kinetic profiles of catechin/epicatechin in sweat analyzed during intervention study 2. Individuals A and B consumed coffee, individuals E and F consumed chocolate, while individuals C and D represented the control group.

Catechin/epicatechin was not detected in any blood sample peaks were observed in sweat sampled 20 min after the ingestion of chocolate. Maximum catechin/epicatechin levels were observed in sweat sampled from individual E 20 min after chocolate intake, while only a small peak in sweat sampled from the fingertips of the left hand of individual F was observed. Similar kinetic behavior was already discussed for TB in sweat sampled from the fingertips after chocolate consumption. Again, further investigation of the kinetic behavior of catechin/epicatechin would be necessary to determine, whether TB, CF and epicatechin/catechin peaks occurring 20 min after chocolate consumption were related to unexpected individual kinetic profiles of the compounds in sweat, or might arise from remaining contaminations found in the ridges and pores of the fingertips originating from the consumption of chocolate.

Concluding, the kinetic profiles of CF and its primary metabolites PX, TP and TB in sweat sampled from the fingertips showed clear differences after the consumption of coffee and chocolate. High CF and PX levels indicated intake of CF-containing foods or drinks, as coffee or chocolate, while TB levels substantially increased after the ingestion of chocolate.

Development and validation of an UPLC-MS method for the quantitation of caffeine and its primary metabolites in sweat derived from the fingertips:

Based on the method used for the qualitative analysis of sweat sampled from the fingertips and blood samples, a shorter chromatographic method for the separation of CF and its primary metabolites TB, PX and TP was developed to ease high throughput experiments. Figure 44 shows example chromatograms of CF, d9-CF as well as the dimethylxanthine isomers TB, PX and TP in sweat and demonstrates sufficient analyte separation.

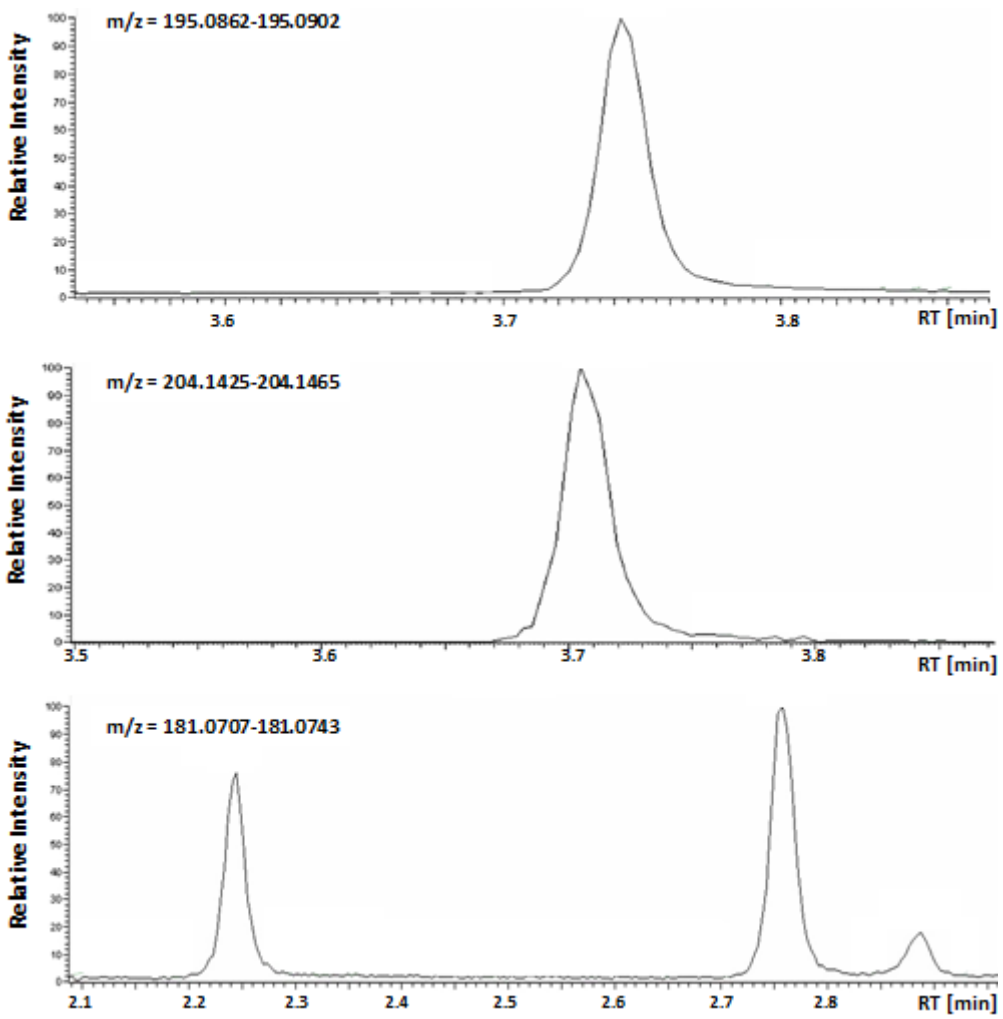

Figure 44: Top down: example chromatograms of CF, d9-CF and the isomers TB, PX and TP (from left to right) in a sweat sample.

Standard calibration curves were obtained by fitting linear functions to the rAUCs of CF, TB, PX and TP plotted against the corresponding concentrations of the calibration standards. The concentrations used to construct the calibration curve were 0.5 pg/µL, 1 pg/µL, 10 pg/µL, 50 pg/µL, 100 pg/µL and 200 pg/µL. All data points used for the generation of the calibration curves were measured as duplicates. The coefficients of determination (R^2) were determined and exceeded 0.99 for all four calibration curves (Figure 45). The CVs of the technical replicates didn't exceed 6.5%, 8.6%, 8.4% and 7.5% in the case of CF, TB, PX and TP, respectively.

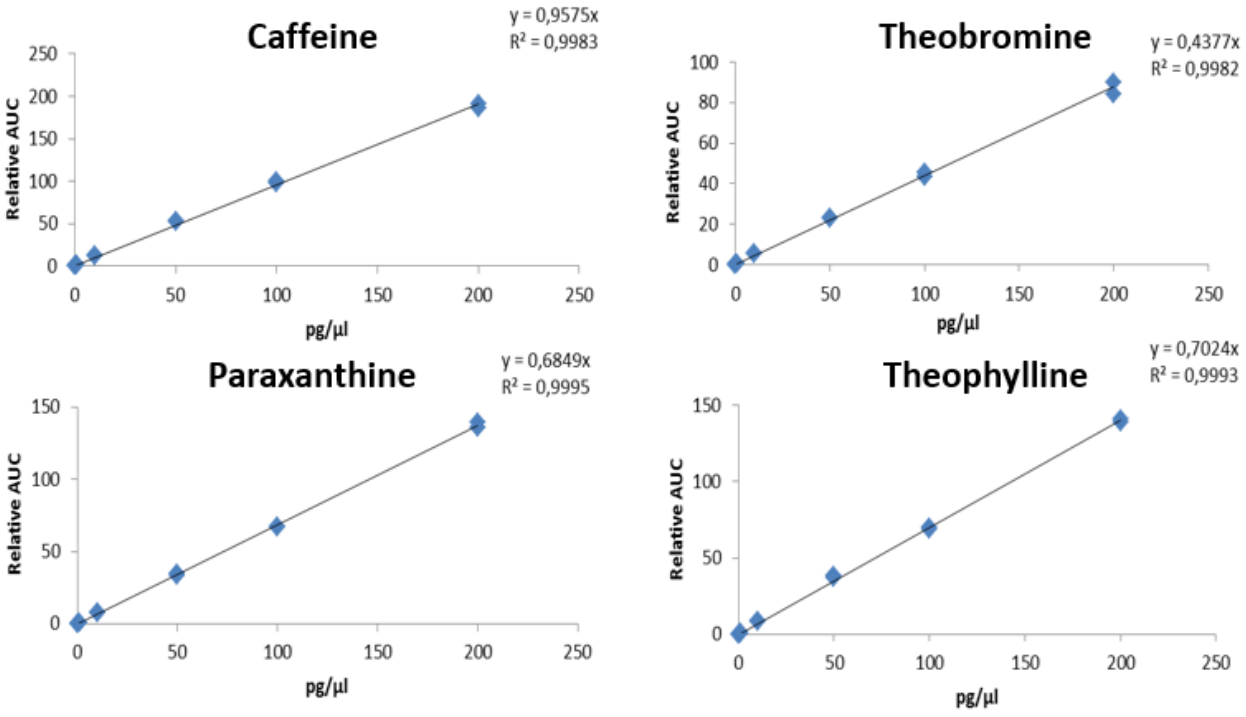

Figure 45: Calibration models developed for CF and its primary metabolites TB, PX and TP.

The LOD was calculated as the target analyte's mean concentration in the blank plus three times its standard deviation. The limit of quantification (LOQ) was determined as the mean concentration of the target analyte in the blank plus ten times its standard deviation. The LODs ranged from 47 fg/µL in the case of TP to 329 fg/µL for CF, while the LOQs were ranging from 112 fg/µL (TP) to 783 fg/µL (CF) and are represented in detail in Table 3.

[fg/µL]	TB	PX	TP	CF
LOD	83	73	47	329
LOQ	156	186	113	783

Table 3: Limits of detection (LODs) and limits of quantitation (LOQs) of the four analytes TB, PX, TP and CF.

The extraction efficiency was determined by analyzing extracts of filter papers spiked with 1 µL of a multi-standard solution containing 1 or 10 ng of all analytes. Analyte concentrations in extracts and in standard solutions were then compared (Figure 46). Three individual extractions were used to determine the average efficiency, its standard deviation as well as the corresponding CVs. The average extraction efficiencies were similar for all four analytes and varied between 84.1% and 75.4%. CVs of the triplicated extraction procedures varied between 15.1% and 28.1% depending on the investigated analyte and its concentration. The extraction variability was <20% for all analytes in extracts of filters spiked with 10 ng of all analytes, while it exceeded 20% in the case of 1 ng spikes of TB, PX and TP. More detailed information can be obtained from Table 4.

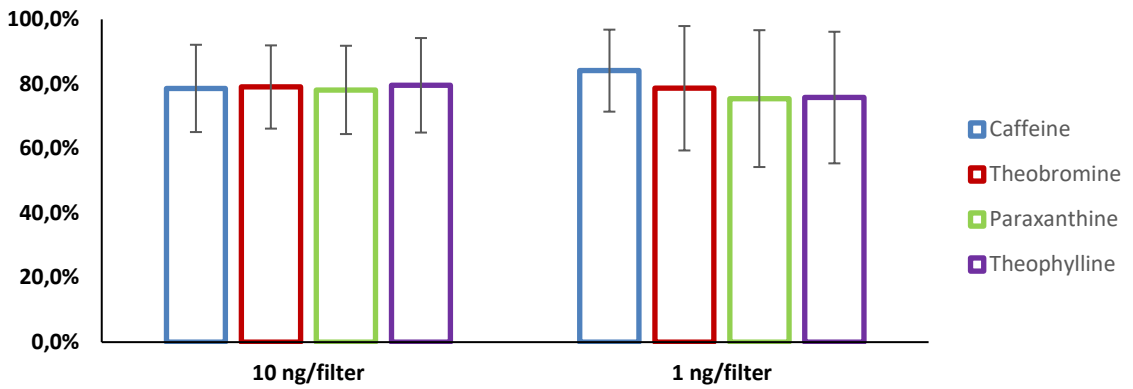

Figure 46: Extraction efficiencies of CF, TB, PX and TP determined by spiking three filters with 1µL of a multi-standard solution containing 1 or 10 ng of all analytes. Extraction procedure as well as analysis of the extracts was triplicated. Error bars are showing the extraction variability.

Extraction efficiency				
	CF	TB	PX	TP
10 ng/filter	78,6%	79,0%	78,1%	79,6%
1 ng/filter	84,1%	78,7%	75,4%	75,8%

Extraction variability				
CV%	CF	TB	PX	TP
10 ng/filter	17,2%	16,3%	17,5%	18,4%
1 ng/filter	15,1%	24,5%	28,1%	26,9%

Table 4: Extraction efficiency and extraction reproducibility for CF, TB, PX and TP determined after extraction of filter papers spiked with 1 µL of a multistandard containing 1 ng or 10 ng of all four analytes.

Interindividual sampling stability was tested by sampling left and right index finger and thumb of the a single individual three times three hours after the ingestion of coffee. The results can be reviewed in Figure 47, whereas the three replicates of the overall sampling procedure were labeled R1, R2 & R3. Measurements were triplicated and the variations of the sampled analytes were evaluated. To investigate the interindividual variation depending on the investigated side, samples were grouped based on their origin (left or right hand). Additionally, the overall repeatability of the sampling process was determined. Average rAUCs, standard deviations and CVs were calculated and a two-tailed, unpaired t-test was used to evaluate the significance of the differences between the sample groups. The overall CV of the six samples (left- and right hand, three repetitions) was 25.3% for CF, 22.8% for TB, 24.2% for PX and 18.9% in the case of TP. No significant difference between the left and the right side was observed with p-values exceeding 0.247 for all four analytes. However, a significant increase between the first and the second repetition of the sampling procedure (R1 and R2) was observed in the case of CF with a corresponding p-value of 0.012. CF, TB and PX levels increased significantly from R1 to R3 with p-values of 0.008, 0.003 and 0.002, respectively. This effect might originate from elevated sweat

rates caused by thermal sweating induced by repeated washing of the hands with warm water during the experiment.

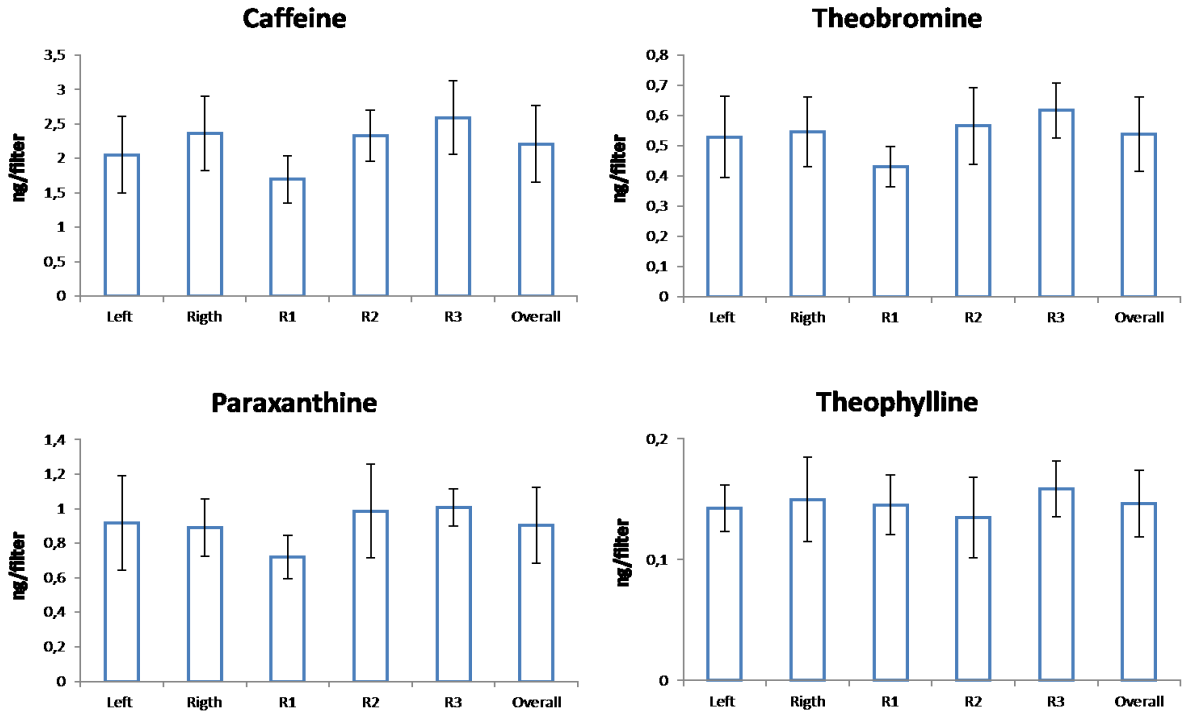

Figure 47: Evaluation of the extraction reproducibility of CF, TB, PX and TP: sweat samples were collected from the left and right hand of a male individual three hours after the consumption of a cup of coffee.

Technical reproducibility (Table 5) was evaluated by calculating CVs for technical triplicates of aqueous multi-standards, extracts of spiked filter paper and sweat samples used for the evaluation of the sampling reproducibility. The technical reproducibility was below 10% for all sample matrices investigated.

Technical reproducibility				
	CF	TB	PX	TP
Standards (aq.)	<4,3%	<4,9%	<5,2%	<2,1%
Extracted from filter	<7,5%	<8,6%	<8,1%	<6,9%
Extracted from sweat	<3,3%	<9,5%	<2,3%	<7,3%

Table 5: Technical reproducibility of the developed UPLC-MS method for the quantitation of CF, TB, PX and TP. CVs of triplicated measurements were calculated for aqueous standard solutions, extracts of spiked filter paper and sweat extracts of an individual three hours after coffee intake.

Matrix effects were evaluated by spiking sweat extracts sampled from an individual not having consumed any methylxanthine rich food or beverage within the last 24 hours with multi-standard solutions (1.2 ng, 12 ng and 24 ng of CF, TB, PX and TP). Relative AUCs of the analytes in the spiked extracts were compared to the corresponding standard solutions. Despite application of dietary restrictions, some background concentration of the target analytes, especially TB, was detected in sweat extracts.

Hence, rAUCs of non-spiked sweat extracts were used to perform a blank subtraction prior to calculating the matrix effects. CF levels were suppressed to 78% in the sample spiked with 1.2 ng, while rAUCs in spiked sweat samples corresponded to 101% and 96% the rAUCs detected in spiked extracts containing 12 ng and 24 ng, respectively. The rAUC of TB in the sweat extract spiked with 1.2 ng corresponded to only 70% of the level determined in the standard solution, while it was elevated by 33% in the extract spiked with 12 ng TB. In all three samples rAUCs of PX and TP were between 94% and 113% of the rAUCs determined in the corresponding standard solution. Figure 48 shows the matrix effects of sweat onto relative AUCs of CF, TB, PX and TP for all three concentrations. Optimally, matrix effects should not exceed ±20%, which is indicated by red dotted lines in Figure 48.

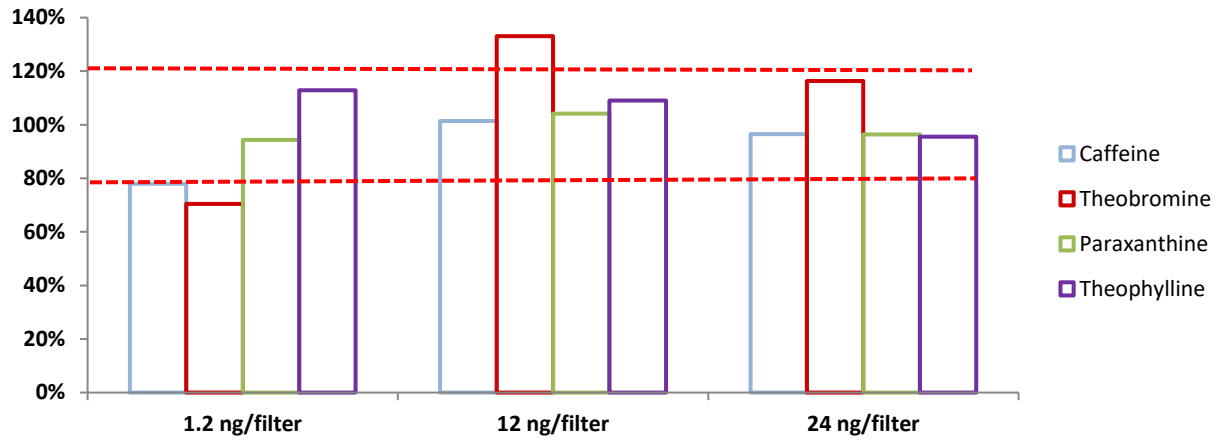

Figure 48: Matrix effects of sweat sampled from the fingertips were determined by spiking sweat extracts obtained from the fingertips with multi-standard solutions containing 1.2 ng, 12 ng and 24 ng of CF, TB, PX and TP.

Quantitation of caffeine, theobromine and paraxanthine in sweat derived from the fingertips during a double-blind study:

Then, the method was used to control the compliance of participants taking part in a three-phase double-blind study concerning the intake of CF. During the double-blind study it was possible to distinguish between its three phases based on quantitative analysis of CF and its metabolites in sweat sampled from the fingertips, whereas external partners used the in-house developed filter paper devices during the sampling procedure. This study aimed to demonstrate the potential and applicability of the developed method for large scale routine testing. Sampling devices were prepared in our laboratory in Vienna, sent to the partner group in Basel, where the double-blind study took place. The design of the study contained three phases: Subjects ingested either three doses of CF or -placebo on a daily basis or underwent a withdrawal phase. Every individual took part in all three phases of the study, which were all composed of two ambulatory phases separated by a two-day phase that took place in the sleeping laboratory at the UPK Basel. Within the laboratory part, sweat was sampled by our partners in two-hour-intervals following the ingestion of the first dose of CF. During the ambulatory phases subjects sampled themselves at home before bedtime. Then, samples were sent back to Vienna, where analyte extraction and quantitation was carried out in our laboratory. A detailed overview on the workflow used during the study is given in the experimental section. From the time courseses of CF and its metabolites PX and TB in sweat samples, we deduced the corresponding phases of the study. Samples were encoded systematically, whereas the sample name included the identity of the subject, the phase of the study, as well as a sequential number. For example, sample A1 21 would correspond to the 21st sweat sample obtained from individual A during study phase one. Table 6 shows the results of the double-blind study. The three phases of the study, namely CF ingestion (C), placebo donation (P) and the withdrawal phase (W), were related to the sample sets obtained from 7 individuals based on the time courses of CF and its primary metabolites TB and PX. The results were confirmed by the partner group by the end of the study. In the following section data interpretation will be discussed exemplarily based on the dataset of individual E. All time courses obtained from samples of the other individuals and the related data interpretation can be reviewed in more detail in the appendix.

Phase / Sub.	1	2	3
A	P	C	W
B	P	C	W
C	C	P	W
D	W	C	P
E	W	P	C
F	P	C	W
G	C	P	W

Table 6: Sample sets of participants A-G undergoing phases 1-3 of the double blind study were related to placebo- (P) or caffeine intake (C) or a withdrawal phase (W).

Figure 49 shows the time courses of CF in sweat sampled during phases 1-3 from individual E. Here, we could observe high amounts of CF during the first half of phase one and during complete phase two with maximum CF levels exceeding 30 ng per filter, while low amounts of CF in the low- and sub ng range per filter were observed in late phase one as well as in phase three. Based on the data, we suggested that E1 corresponded to the withdrawal phase, E2 corresponded to the placebo phase, while phase E3 corresponded to continuous CF intake.

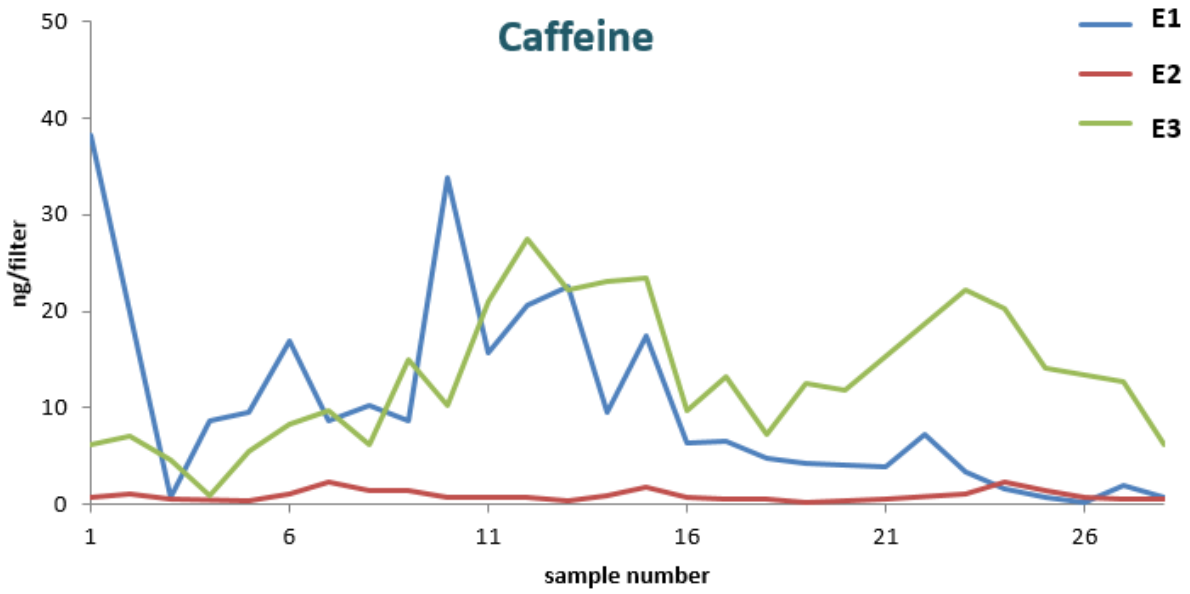

Figure 49: Time course of the amount of CF quantified in sweat samples of subject E during the three phases of the double-blind study.

Figure 50 to Figure 52 are showing time courses of CF, TB and PX for sample groups E1, E2 and E3, respectively. The time courses of all three analytes in sample group E1 were similar. After a high CF level in sweat sampled on the first day and low levels of all analytes in sweat sampled the next day, possibly related to deficient sampling- or sample extraction, CF levels were oscillating around 10 ng per filter until sample number nine. Then, levels increased, with a CF maximum exceeding 30 ng per filter, followed by a gradual decrease of the CF amount per filter PX levels exceeded CF levels in samples corresponding to the stationary part of the study indicating intense CF metabolism. Following the PX maximum of 50.4 ng in sample number 15, PX levels decreased rapidly.

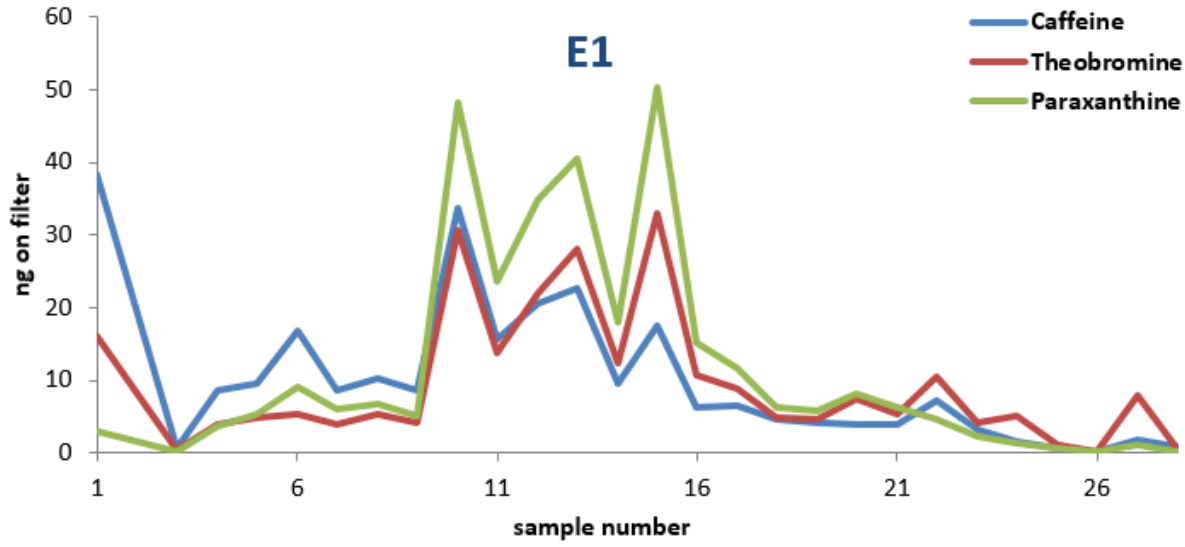

Figure 50: Time course of CF (blue) and its primary metabolites TB (red) and PX (green) quantified in sweat samples of subject E during phase 1 of the double-blind study.

Sample group E2 is characterized by low amounts of CF and PX, not exceeding 2.4 ng per filter and 2.1 ng per filter, respectively. CF peaks were of low intensity and associated with increased TB levels indicating chocolate consumption as a potential source of CF and TB.

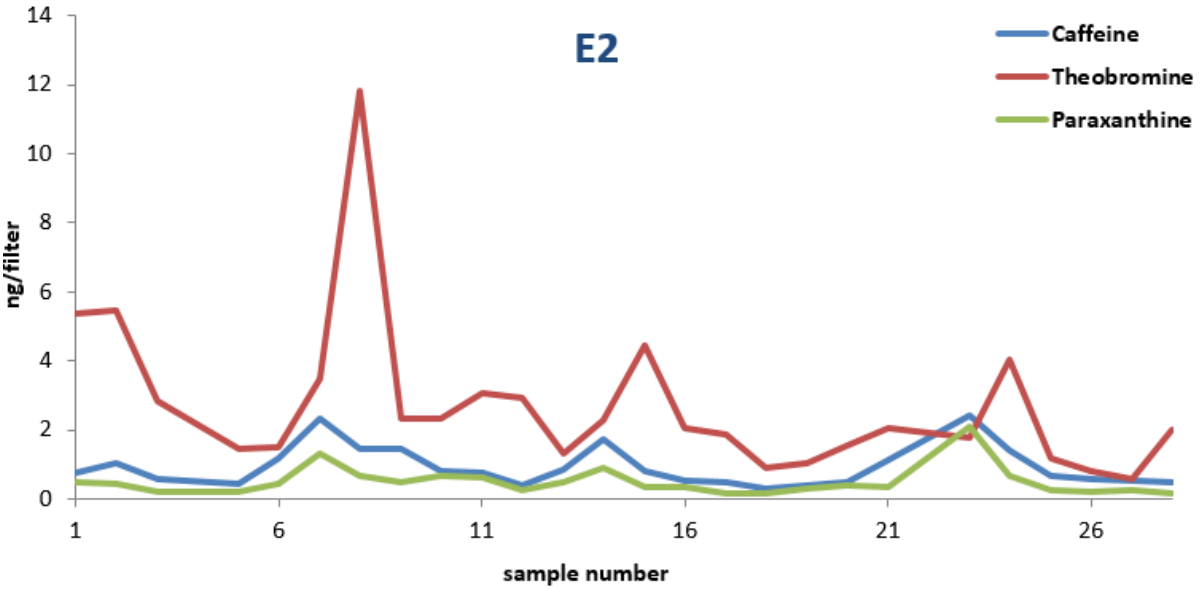

Figure 51: Time course of CF (blue) and its primary metabolites TB (red) and PX (green) quantified in sweat samples of subject E during phase 2 of the double-blind study.

Within the sample group E3 we observed CF amounts varying between 5 ng and 10 ng per filter within the first eight samples, whereas sample number four was characterized by very low levels of all three analytes which, again, might originate from defective sampling- or sample extraction. Then, CF content increased reaching a maximum amount of 27.5 ng per filter in sample 12 and stayed high with amounts

varying between 6.2 ng in sample number 28 and 23.4 ng in sample number 15. The time course of PX was parallel to the CF curve with slightly lower levels not exceeding 24.4 ng. TB behaved similar to the other analytes during the first two thirds of experiment E3 and increased during the last couple of days with peak levels of 32.6 ng per filter found in sample number 24 and 45.1 ng TB found in the last sample. Therefore, we suppose that subject E most likely consumed chocolate during study phases E2 and E3.

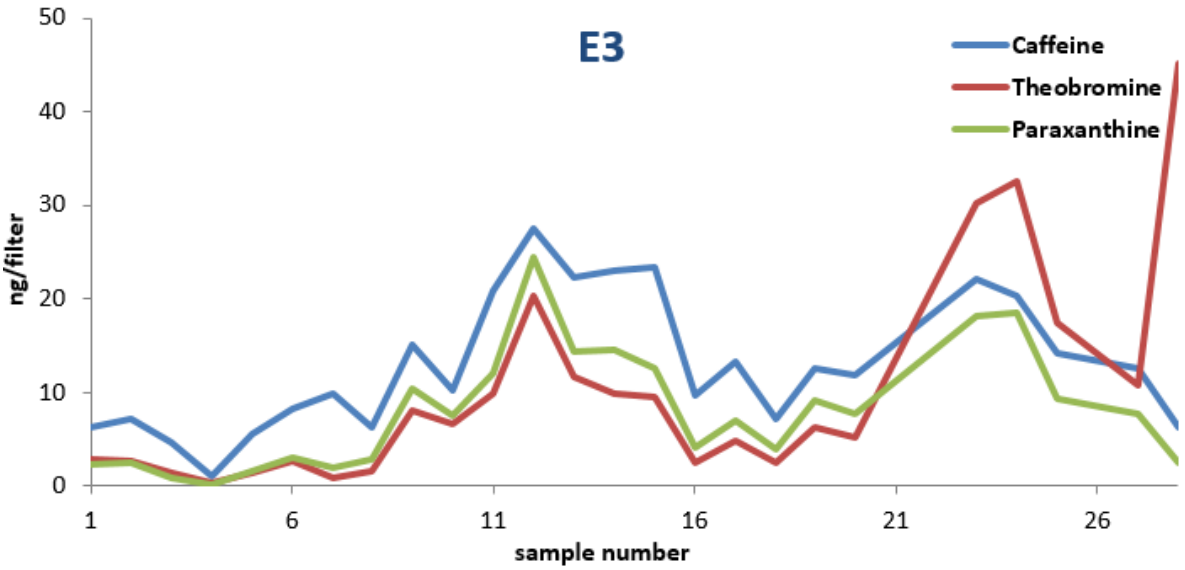

Figure 52: Time course of CF (blue) and its primary metabolites TB (red) and PX (green) quantified in sweat samples of subject E during phase 3 of the double-blind study.

Because the samples analyzed within the double-blind study were analyzed during a period of time exceeding four months, comparability of the results of the individual analytical runs was ensured by monitoring the mean AUCs of the IS in blank samples. The top graph of Figure 53 shows the CVs determined in the blank samples. CVs didn't exceed 6.4% within any of the analytical runs, while the overall CV of all blanks analyzed within this study was determined to be 12.8%. This indicates a high comparability of the results of the single analytical runs. Not all samples within this study were measured as technical triplicates due to restricted availability of the instrument form used for the analysis. To ensure correctness of the results, 38.8% of all samples within this dataset were technically replicated, while 31.2% of the samples were measured as triplicates and 7.6% of the measurements were duplicated. The technical reproducibility was estimated as the stability of the IS in the replicated samples. As can be seen in Figure 53, only 5.3% of the duplicated measurements showed CVs exceeding 15%, while CVs stayed below 5% in 86.4% of all duplicated samples (bottom, left). Triplicates showed a higher overall variability, with 4.6% of the samples exceeding CVs of 20% (bottom, right). The vast majority of these imprecise measurements has been generated in a single analytical run whereas a chromatographic column at the end of its lifetime was used, which resulted in broader peaks and decreased chromatographic reproducibility. Nevertheless, data indicates a high technical stability of the

results obtained during this high throughput study and good comparability of the results generated within the different analytical runs.

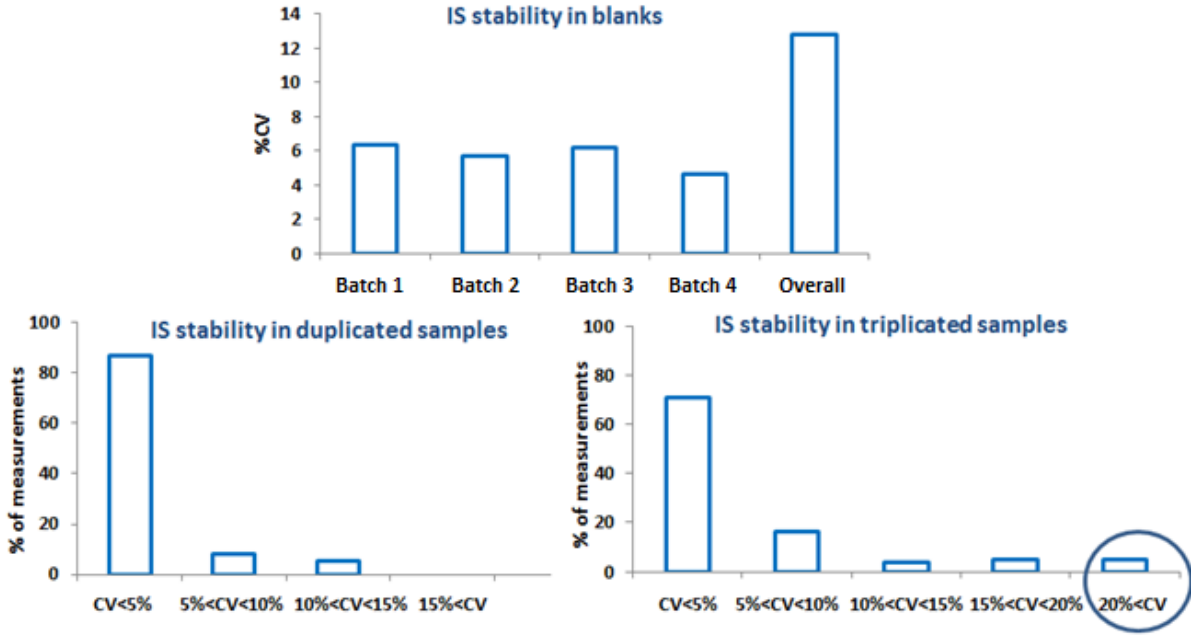

Figure 53: Stability of the AUC of the internal standard (IS) in blanks (top), and in sweat samples measured as duplicates (left) and triplicates (right). The samples were analyzed in four batches, whereas the lag of time between the first- and the fourth batch was 15 weeks.

Discussion and conclusion:

An in house HPLC-MS method developed by Langbauer (1) was adapted and UPLC-full MS- and UPLC-MS^2 methods for the targeted and untargeted analysis of sweat derived from the fingertips were developed. Sampling devices were mass produced from low-linting laboratory wipes using a hollow punch. Together with fast sampling-, sample preparation- and analytical methods, the mass production of the sampling devices allowed high-throughput analysis. An internal compound database containing 95 analyte molecules was generated by MS^2-analysis of diluted coffee, extracted chocolate, as well as sweat- and blood samples. Compounds were identified after automated matching of the fragment spectra to the mzCloud mass spectral database using the compound discoverer software and manual review of likely matches. Identified molecular species should be seen as putatively identified, because most analytes were not verified using standard solutions. Nevertheless, the results of this untargeted approach point out the potential of the developed method. During two intervention studies, the developed compound database was used to determine the kinetic profiles of key bioactives- and their metabolites in sweat- and blood samples after ingestion of coffee or chocolate. CF levels in blood showed similar pharmacokinetics after coffee consumption in most investigated individuals concerning time courses and maxima. Maximal blood concentrations were observed approximately 60 min after coffee intake in most subjects, while blood levels of a single individual peaked 20 min after coffee ingestion. The pharmacokinetic profiles in sweat showed CF maxima occurring between 20 min and 90 min after coffee intake. However, interindividual variability of CF in sweat levels was relatively high, when compared to the similar time courses of CF in blood samples from different subjects. CF levels in blood were lower after chocolate consumption than levels after coffee consumption with maxima occurring 90 min after intake, while CF levels in sweat peaked 20 min after chocolate intake, dropped towards initial levels and increased again. However, the second phase of increasing CF levels started 90 min and 120 min after chocolate ingestion and lasted until the end of the observed period. Especially during the first CF peak 20 min after starting the experiment, sweat levels showed high intraindividual variability, a phenomenon that was observed as well for other abundant metabolites detected in chocolate, as TB and catechin/epicatechin. Although subjects tried to wash their hands properly before the sampling procedure, we can't exclude the possibility that the first CF peak after chocolate intake might originate from contaminations left in the pores and ridges of the fingertips. TB levels in blood were not affected systematically by the consumption of coffee during the investigated period of time, while blood levels drastically increased in the group of chocolate consumers with peak levels observed between 90 min and 120 min after chocolate ingestion. During the first intervention study, increasing TB levels with maxima occurring 60 min to 90 min after coffee intake were observed in sweat sampled from two out of three individuals. However, because no increase in the corresponding blood samples was observed, the increase might be explained by other phenomena, e.g. varying sweat

secretion rates. As already discussed for CF levels in sweat obtained from the fingerprints after chocolate ingestion, peak levels in combination with exceptional high variability of TB levels sampled from the left- and the right hand were observed 20 min after chocolate ingestion followed by a rapid drop of TB content. 90 min and 120 min after chocolate consumption, TB levels showed a second, though less distinct, phase of elevation. Blood levels of PX increased in all subjects after the ingestion of coffee or chocolate. A single individual showed a PX maximum 90 min after coffee intake during the first intervention study, while PX levels in blood samples of all other examined volunteers increased after the ingestion of CF containing foods or drinks until the end of the investigated period. PX levels increased in sweat samples of four out of five subjects after the ingestion of coffee, while no clear increase of PX levels in sweat could be observed after the consumption of chocolate. TP levels were lower in sweat and blood samples, when compared to its isomers TB and PX, but showed a similar kinetic profile as PX. Blood levels increased in all individuals after the ingestion of coffee or chocolate, whereas levels were lower in the chocolate consuming group, when compared to coffee consumers. Peak levels were observed in blood sampled from a single individual 90 min after coffee consumption and in blood of another individual 120 min after chocolate intake, while TP levels increased until the end of the experiment in blood of all other subjects after chocolate or coffee consumption. TP levels in sweat sampled after coffee intake increased in four out of five investigated individuals, while TP levels in samples of one individual showed rather random fluctuations.

1-MX levels increased in blood samples of two out of five individuals after coffee ingestion and in a single individual after consumption of dark chocolate. In general, abundances of 1-MX were low which might be a reason for the ambiguity in the kinetic data for 1-MX in both studies. No increase was observed in sweat samples after the intake of chocolate or coffee. 3-MX and 7-MX levels rapidly increased in blood samples within the first 90 min after the consumption of chocolate. Maximal levels were observed after 120 min in blood samples of one volunteer, while they increased until the end of the investigated period in blood sampled from the second individual. Pharmacokinetics and overall amounts of the monomethylxanthine isomers in blood varied between the investigated subjects, indicating individual variations of metabolism and partitioning of the metabolites. Meanwhile, increasing levels were observed in sweat samples 90 min and 120 min after chocolate consumption, but further experiments using elongated sampling periods would be necessary to permit any reliable statement onto the pharmacokinetics of the monomethyl xanthine isomers in sweat. Although sweat levels of 3-MX and 7-MX seemed to increase in two out of three individuals after coffee intake during the first intervention study, increase in sweat was low, showed no correlation to the blood levels and might be explainable by variations of the sweat rates. Concluding, blood- or sweat levels of 3-MX and 7-MX didn't increase systematically after the ingestion of coffee. In general, high levels of CF metabolites PX, TB, TP, 1-MX, 3-MX and 7-MX in blood sampled under initial conditions was associated with high levels

present in sweat samples. This indicates a correlation between consumer's behaviour and analyte levels in sweat even 24 h and 32 h after the last time CF or TB containing foods or drinks were ingested.

Trigonelline levels in blood increased in all individuals after consuming trigonelline rich coffee, but were not affected by the ingestion of chocolate. However, unexpected pharmacokinetics of trigonelline were observed in sweat samples after coffee consumption. An intense peak of trigonelline levels was observed 60 min after coffee consumption in sweat sampled from one individual during the first intervention study, while another individual showed a less intense trigonelline maximum 90 min after coffee consumption. During the second intervention study, two peaks 20 min and 60 min after coffee ingestion were observed in sweat sampled form the right hand of one volunteer. Meanwhile, trigonelline levels in sweat samples from other volunteers were not affected by the consumption of coffee and no relation to the pharmacokinetic profile of trigonelline in blood was observed. Levels of quinic acid and CGA isomers, which were not detected in any blood sample, showed a similar pattern as trigonelline in sweat samples. According to literature, CGAs undergo heavy metabolism after ingestion and are mainly found in blood as conjugates, for example glucuronides (32). Additionally, partitioning of trigonelline, CGA isomers and quinic acid into sweat should be inhibited mechanistically due to the positive charge of trigonelline, and the acidic nature of the CGAs and their metabolite quinic acid. If unexpected pharmacokinetics of CGAs in sweat were due to variations caused by individual differences in skin permeability, skin pH or enzymatic activity was not investigated during the experiments reported here. Additionally, catechin/epicatechin showed unusual pharmacokinetic behaviour in sweat after the ingestion of chocolate. Maximal levels in sweat sampled from the fingertips of both hands of one individual occurred 20 min after chocolate consumption, while a peak level in sweat sampled from the left hand of the second individual was observed 20 min after chocolate consumption; a similar pattern as was already observed for TB and CF after the intake of chocolate. Epicatechin/Catechin was not detected in any blood sample during the experiments reported here. Therefore, we have to consider the possibility that peak levels found early after chocolate consumption might originate from contaminations found in the ridges and pores of the fingertips' surfaces.

For another study a quicker UPLC-MS method for the quantitation of CF and its primary metabolites TB, PX and TP in sweat derived from the fingertips was developed and validated. The method was regarded as suitable for our purpose, namely distinguishing between the consumption of CF- and a placebo, based on semi-quantitative data of CF and its primary metabolites PX and TB in sweat sampled from the fingertips. In a three-phase trial, sample sets obtained from seven individuals were successfully related to CF- or placebo intake, or a withdrawal phase and the compliance of the volunteers was examined. Sweat sampling as well as CF- and/or placebo administration was guided by members of

our partner group in Basel. Subjects took three doses of CF or placebo every day and sampled themselves during ambulatory phases once a day before bedtime, while sweat was sampled by our partners in two-hour intervals during the daytime in the stationary part of the study. The ambulatory phases of the study lasted eight days and were separated in time by the stationary phase. Although sampling, sample extraction and analysis were successful in most cases, several problems occurred during this study. For example, samples corresponding to the second ambulatory part of one individual (individual A1; samples 21-28) were lacking, because the subject forgot to take the samples. Additionally, “cloud” formation was observed in a few samples during the extraction and foam formation occurred in a single sample (Figure 54). To prevent the chromatographic system from damage caused by detergents and similar chemicals, the corresponding samples were excluded from analysis. Although the contaminants were not analyzed during this work, cloud formation was probably related to greasy residues on the fingertips, for example cosmetics or sebaceous contaminations from other parts of the body that were not removed during the washing process of the hands, while foam formation most likely occurred in cases, where sweat was sampled after insufficient removal of soap during the washing procedure. However, these phenomena were only observable in a few samples and stopped after the subjects were reminded to wash their hands carefully and ensure complete removal of soapy residues from the palms. The successful discrimination between CF- and placebo ingestion, as well as the withdrawal phase shows the potential and utility of the developed technique and of sweat obtained from the fingertips as an alternative specimen for routine testing.

Figure 54: Foam formation (left) and cloudiness (right) occurred in some samples during the extraction procedure

Outlook:

Successful untargeted- and targeted metabolomics analysis of sweat sampled from the fingerprints after the ingestion of coffee or chocolate could point out the potential and applicability of this and similar methods. Although an internal compound database containing 95 analytes was established, most compounds within the database have to be seen as putatively identified. Therefore, verification of the results using standard solutions would be the next step to expand the method to quantitative analysis of xenobiotics different to CF and its metabolites in sweat sampled from the fingertips, which is already planned and executed within this group. The successful discrimination of the three phases of a double-blind study, namely CF- or placebo intake and a withdrawal phase, and investigation of the volunteers' compliance based on the levels of CF and its primary metabolites TB and PX demonstrated the suitability of methods based on our sampling procedure in combination with HPLC-MS for routine testing. However, several questions stayed unanswered during this work. For instance, issues concerning the normalization of the sampled amount of sweat would be an interesting topic for future research. In a subsequent master thesis, Julia Brunmair investigated the kinetics of methylxanthines, CGAs, as well as the flavanols catechin and epicatechin in blood and sweat after the ingestion of chocolate and/or coffee in more detail. Additionally, she developed an untargeted metabolomics method using the negative ionization mode for UPLC-MS^2 experiments to extend the range of potential analytes.

Abstract:

Within the scope of this work, an untargeted metabolomics method for the investigation of blood and sweat sampled from the fingerprints was developed using an UPLC-MS (Ultra Performance Liquid Chromatography- Mass spectrometry) platform. An internal compound database containing 95 small molecules was developed by tandem mass spectrometric (MS^2) analysis of diluted coffee, extracted chocolate, as well as sweat samples and blood extracts obtained from seven individuals, before- and after the consumption of coffee or chocolate. During two intervention studies the pharmacokinetic profiles of the most abundant xenobiotics present in coffee and chocolate, as well as the primary- and secondary metabolites of caffeine (CF), were investigated in sweat and blood. Based on the kinetic data, the distinction of coffee and chocolate consumption was possible using CF-, theobromine (TB)- and paraxanthine (PX) levels in sweat as marker substances. The chromatographic method was optimized and a method for the quantitation of CF and its primary metabolites in sweat was established and validated. During a field study the developed method was used to control the compliance of volunteers participating in a double-blind study at the Centre of Chronobiology of the Psychiatric Hospital of the University of Basel (UPK Basel). Every volunteer took part in three phases of the study either ingesting CF or a placebo or underwent a withdrawal phase. Phases were composed of two ambulatory parts separated by a stationary part. Sampling devices were prepared at the Department of Analytical Chemistry of the University of Vienna and were sent to the UPK Basel prior to sampling, where sampling itself was carried out by our partners during the stationary part of the study, while subjects sampled themselves during the ambulatory part. Sweat samples were sent back to Vienna, where CF and its metabolites were extracted and quantified. Based on the CF-, TB- and PX content in sweat, we were able to successfully correlate sets of samples to the corresponding phases of the trial. This work demonstrates the applicability of the developed method for routine testing and high throughput analysis.

Keywords: *caffeine, sweat, fingerprints, metabolomics, double-blind study, intervention study, pharmacokinetics, HPLC-MS*

Zusammenfassung:

Im Zuge dieser Arbeit wurde eine Methode zur ungezielten Analyse des Metaboloms von Blut und Schweiß aus dem Fingerabdruck entwickelt, wobei für die Analyse eine Ultra Performance Liquid Chromatography (UPLC) Plattform in Kombination mit Massenspektrometrie (MS) verwendet wurde. Basierend auf tandem-massenspektrometrischer (MS^2) Untersuchung von Blut- und Schweißproben von sieben Probanden, wobei die Probennahme vor- oder nach Einnahme von Kaffee oder Schokolade durchgeführt wurde, sowie verdünntem Kaffee und Schokoladenextrakt, wurde eine interne Datenbank entwickelt, in der 95 Metabolite enthalten waren. Im Rahmen zweier Interventionsstudien wurde das pharmakokinetische Verhalten der abundantesten xenobiotischen Verbindungen in Kaffee und Schokolade, sowie der primären und sekundären Metabolite von Koffein, nach Einnahme von Kaffee und Schokolade untersucht. Basierend auf den kinetischen Daten in Schweiß war es möglich zwischen dem Konsum von Kaffee und Schokolade zu unterscheiden, wobei der Koffein-, Paraxanthin- und Theobromingehalt in Schweißproben als Marker herangezogen wurde. Die chromatographische Methode wurde optimiert und ein Modell zur Quantifizierung von Koffein und seiner Primärmetabolite in Schweiß entwickelt und validiert. Im Rahmen einer Feldstudie wurde die Compliance teilnehmender Probanden bezogen auf den Konsum koffeinhaltiger Lebensmittel überprüft. Während der Doppelblindstudie im Zentrum für Chronobiologie an den Universitären psychiatrischen Kliniken in Basel (UPK Basel) nahmen Probanden an drei Phasen der Studie teil, wobei entweder Koffein, oder ein Placebo eingenommen-, oder eine Entzugsphase durchlaufen wurde. Auf Filterpapier basierende Probennehmer wurden am Institut für Analytische Chemie der Universität Wien hergestellt und an die Partnergruppe geschickt. Die Schweißproben wurden im stationären Teil der Studie von unseren Partnern am UKP Basel gesammelt, während die Probanden im ambulanten Teil selbst die Probennahme durchführten. Die Proben wurden anschließend nach Wien zurückgesandt, wo Probenextraktion und Quantifizierung von Koffein und seiner Primärmetabolite durchgeführt wurden. Der Koffein-, Paraxanthin- und Theobromingehalt in extrahierten Schweißproben wurde erfolgreich zur Zuordnung der verblindeten Probenkohorten zu den jeweiligen Teilen der Doppelblindstudie und zur Überprüfung der Compliance der Probanden während der Studie herangezogen. Durch diese Arbeit konnte die Anwendbarkeit dieser und ähnlicher Methoden für Routineanalytik und Hochdurchsatzexperimente erfolgreich demonstriert werden.

Appendix:

Internal compound database:

No.	Name	M(mono.)	Δm[ppm]	RT[min]
1	1-Aminocyclohexanecarboxylic acid	143.0946	0.4	0.57
2	1-Dodecyl-2-pyrrolidone	253.2406	-1.5	6.42
3	1-Methylxanthine	166.0491	0.5	1.67
4	2-Aminonicotinic acid	138.0429	1.0	0.69
5	3,5-di-tert-Butyl-4-hydroxybenzaldehyde	234.1620	1.5	5.93
6	3-Hydroxypicolinic acid	139.0269	0.8	0.75
7	3-Methylxanthine	166.0491	0.5	1.56
8	4-Indolecarbaldehyde	145.0528	1.3	4.33
9	5'-S-Methyl-5'-thioadenosine	297.0890	-0.1	2.34
10	7-Methylxanthine	166.0491	1.1	1.41
11	Acetylcholine	146.1176	-1.1	0.39
12	Acetyl-L-carnitine	204.1230	-0.6	0.51
13	Acetyl-β-methylcholine	160.1332	0.5	0.49
14	Adenosine	267.0968	0.5	1.02
15	Arginine	174.1117	1.8	0.35
16	Aspartic acid	133.0375	-0.5	0.39
17	Betaine	118.0863	0.3	0.40
18	Caffeine	194.0804	1.1	3.26
19	Caprolactam	113.0841	1.0	2.64
20	Carnitine	162.1125	0.5	0.37
21	Catechin/Epicatechin	290.0790	-1.0	3.51
22	Chlorogenic acid Isomer 2.26 min	354.0951	2.3	2.26
23	Chlorogenic acid Isomer 2.78 min	354.0951	0.7	2.78
24	Chlorogenic acid Isomer 3.03 min	354.0951	2.1	3.03
25	Chlorogenic acid Isomer 3.20 min	354.0951	2.0	3.20
26	Choline	104.1070	0.4	0.36
27	Citrulline	175.0957	0.2	0.39
28	Creatine	131.0695	1.5	0.41
29	Creatinine	113.0589	0.7	0.39
30	Decanamide	171.1623	0.8	5.70
31	Decanoylcarnitine	316.2482	-0.2	5.36
32	Dibutyl phosphate	210.1021	0.6	6.07
33	Didecyldimethylammonium	326.3781	-1.7	5.59
34	Diethyl phthalate	222.0892	-2.2	5.50
35	Diphenhydramine	255.1623	-0.2	5.11
36	Dodecyltrimethylammonium	228.2686	1.5	5.38
37	Ergothioneine	230.0958	1.2	0.48
38	Erucamide	337.3345	0.3	5.78
39	Ethylenediaminetetraacetic acid (EDTA)	292.0907	-0.3	0.55

No.	Name	M(mono.)	Δm[ppm]	RT[min]
40	Glutamic acid	147.0532	0.7	0.39
41	Hippuric acid	179.0582	-0.2	2.87
42	Histamine	111.0797	-0.5	0.33
43	Histidine	155.0695	-0.3	0.36
44	Hypoxanthine	163.0385	-0.9	1.28
45	Iditol	182.0790	0.4	0.40
46	Indole-3-acrylic acid/trans-3-Indoleacrylic acid	187.0633	0.5	2.12
47	Inosine	268.0808	-1.7	1.28
48	Isoleucine	131.0946	-0.7	0.85
49	Leucine/Norleucine	131.0946	1.1	0.93
50	Lysine	146.1055	-0.8	0.33
51	Mefenamic acid	241.1103	0.4	6.12
52	Methionine	149.0511	1.1	0.60
53	Methionine sulfoxide	165.0460	-1.0	0.40
54	Minoxidil	209.1277	-0.1	3.18
55	N-Acetyl-Serine	147.0532	0.6	0.55
56	Nicotinamide	122.048	0.1	0.61
57	Nicotinic acid	123.0320	-1.2	0.63
58	N-methylhydantoin	114.0429	-1.3	0.86
59	Oleamide	281.2719	3.7	6.24
60	Ornithine	132.0899	0.5	0.33
61	Oxybenzone	228.0786	1.0	5.78
62	Palmitoylcarnitine	400.3421	1.3	5.87
63	Panthenol	205.1314	-0.2	2.05
64	Paraxanthine	180.0647	1.3	2.50
65	PEG n5	238.1416	-1.9	2.65
66	PEG n6	282.1679	-0.8	3.11
67	PEG n7	326.1941	0.2	3.57
68	PEG n8	370.2197	0.0	3.96
69	Phenylalanine	165.0790	-0.3	1.50
70	Progesterone	314.2246	-0.4	5.93
71	Proline	115.0628	0.1	0.43
72	Prolineamide	114.0793	0.4	0.37
73	Propionylcarnitine	218.1387	-0.7	0.90
74	Pyrogallol	126.0317	1.4	1.59
75	Pyroglutamic acid	129.0426	0.3	0.81
76	Quinic acid	192.0634	-2.6	0.47
77	Serine	105.0426	-0.4	0.38
78	Sorbic acid	112.0524	-1.0	4.65
79	Spermidine	145.1579	1.5	0.32
80	Stachydrine	144.1019	0.9	0.47
81	Theobromine	180.0647	0.6	2.08

No.	Name	M(mono.)	Δm[ppm]	RT[min]
82	Theophylline	180.0647	1.4	2.61
83	Threonine/Homoserine	119.0582	-0.6	0.39
84	Triethanolamine	149.1052	0.9	0.43
85	Triethyl phosphate	182.0708	-0.9	5.23
86	Trigonelline	138.0550	-1.7	0.43
87	Triphenylphosphine oxide	278.0861	-3.6	5.54
88	Tryptophan	204.0899	0.7	2.15
89	Tyrosine	181.0739	0.8	0.86
90	Uracil	112.0273	0.3	0.61
91	Uric acid	168.0283	-0.1	0.70
92	Urocanic acid Isomer 0.533 min	138.0429	1.2	0.53
93	Urocanic acid Isomer 0.678 min	138.0429	0.7	0.68
94	Valine	117.0790	0.2	0.52
95	Xanthine	152.0334	0.9	0.88

Table 7: Internal metabolite database developed from MS^2-data of sweat-, blood-, coffee- and cocoa samples.

Complementary quantitative data of caffeine, theobromine and paraxanthine determined in sweat from the fingertips during a double-blind study:

Amounts of CF quantified in samples obtained from subject A are shown in Figure 55. The data set was sufficient to distinguish between the three phases of the study, although we didn't receive samples A1 21-28 which corresponded to the final ambulatory part of phase one. Samples obtained from A2 were related to the ingestion of CF with high CF levels in the last third of the sample set. CF levels were only slightly elevated in comparison to the placebo phase A1 during the first ten samples of experiment A2. Phase A3 was characterized by high levels during the first half of the experiment with a peak level of 68.9 ng found in sample number two slowly declining to levels in the low ng and sub ng range in samples number 21 to 28.

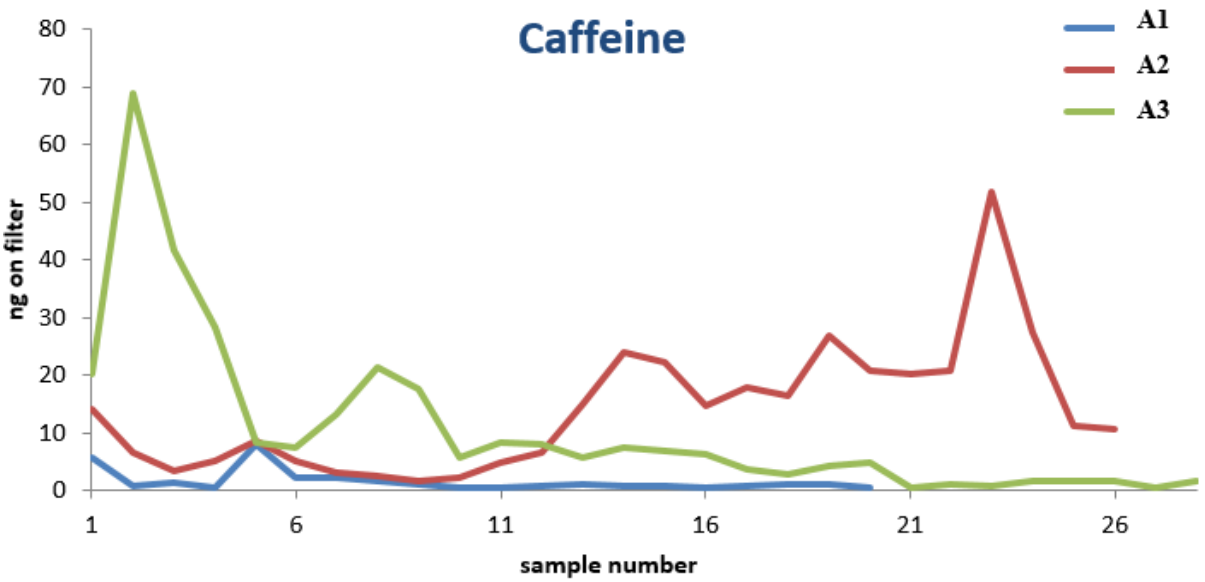

Figure 55: Time course of the amount of CF quantified in sweat samples of subject A during all three phases of the double-blind study.

High levels of TB combined with low levels of CF and PX were observed in sample set A1. Besides a CF peak of 7.9 ng per filter, CF and PX levels stayed in the low- and sub ng per filter range. Hence, A1 was related to the placebo phase. In general TB levels were elevated in A1 indicating possible consumption of cocoa products. Additionally, the CF peak in sample 05 was associated with the peak level of the TB (17.9 ng per filter). As described above, samples 21 to 28 were missing due to problems during the sampling procedure carried out by external partners.

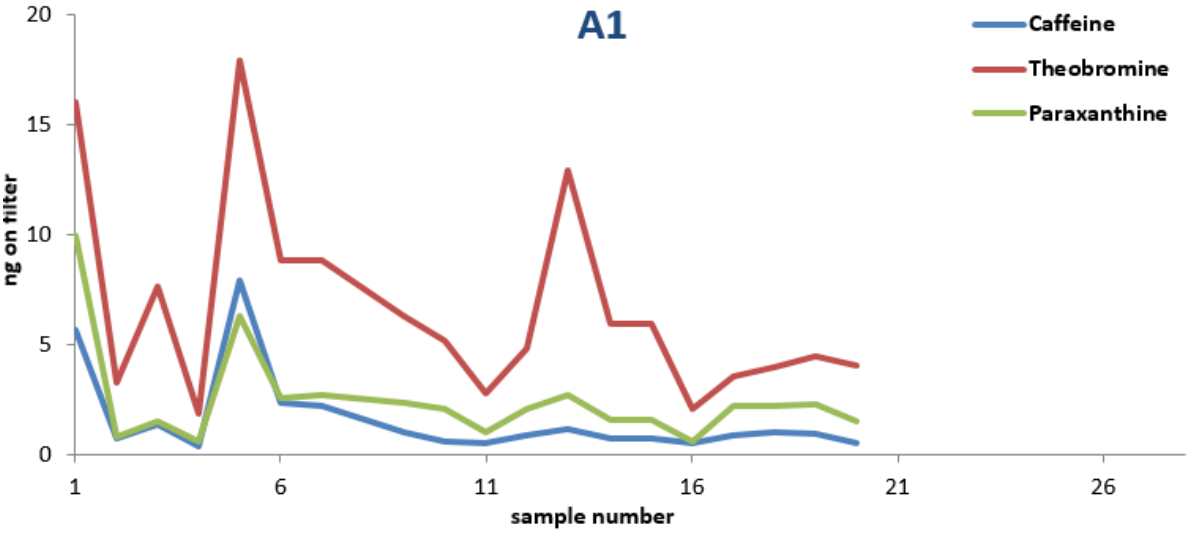

Figure 56: Time course of CF (blue) and its primary metabolites TB (red) and PX (green) quantified in sweat samples of subject A during phase 1 of the double-blind study.

In samples A2 CF levels varied between 2.4 ng per filter and 14.2 and ng per filter, increased during the second half of the sample set and peaked in sample number 23 with a CF maximum of 51.8 ng per

filter. PX levels were similar to amounts of CF and peaked with 59.9 ng PX in sample number 23 indicating intense CF metabolism. TB levels were lower than CF- or PX levels but had a parallel time course.

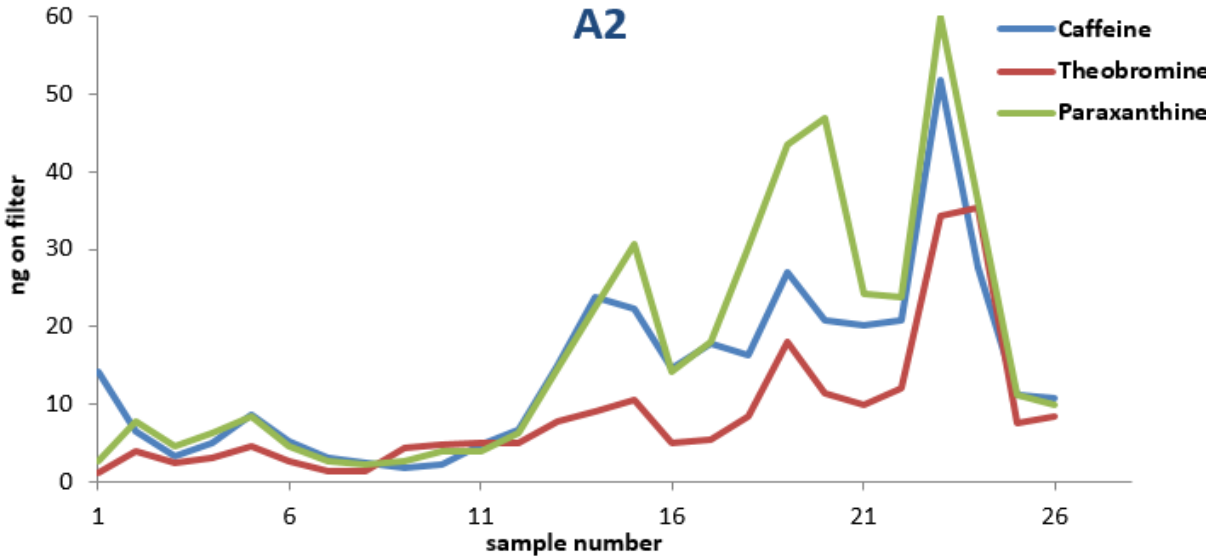

Figure 57: Time course of CF (blue) and its primary metabolites TB (red) and PX (green) quantified in sweat samples of subject A during phase 2 of the double-blind study.

Figure 58 shows the time course of the CF, TB and PX amounts found in sweat sampled from individual A during phase three. The time courses were characterized by exceptional high levels of all three analytes during the first couple of days, with CF reaching 68.9 ng per filter and PX reaching 109 ng per filter in sample number 02, while the peak level TB was 71.6 ng per filter detected in sample 04. Following the maxima, analyte levels started to decline gradually. While CF and PX levels decreased to the low- and sub ng range in samples 21 to 28, a TB peak exceeding 50 ng per filter was observed in sample 27. The set A3 was assumed to correspond to the withdrawal phase of the double-blind study.

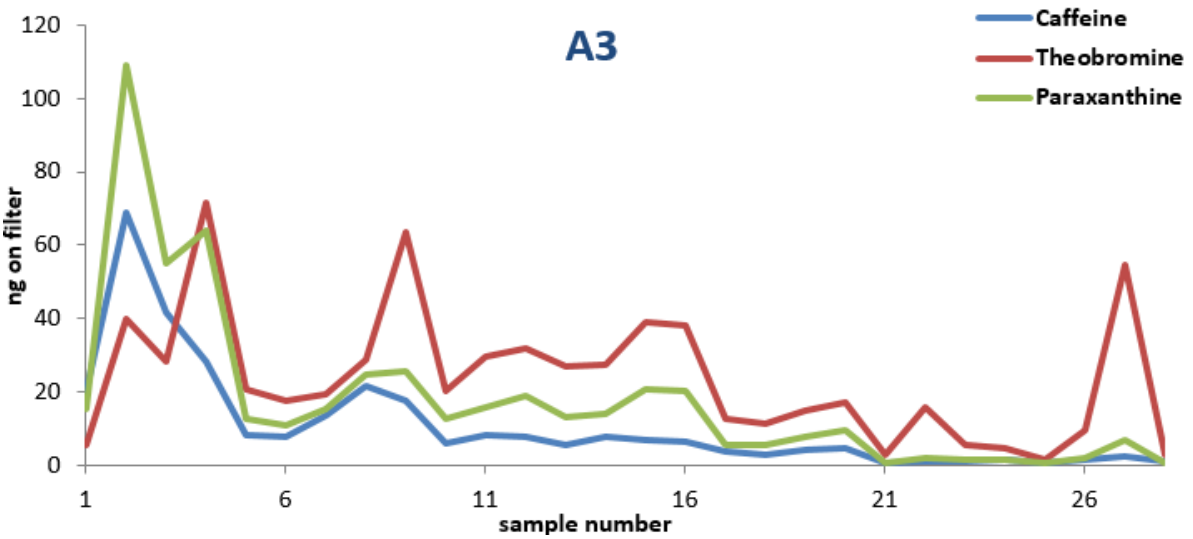

Figure 58 Time course of CF (blue) and its primary metabolites TB (red) and PX (green) quantified in sweat samples of subject A during phase 3 of the double-blind study.

Sample set B1 was characterized by a sharp CF peak found in sample number four, while CF levels were low in most other sweat extracts found within this set of samples. CF levels were high during the first half of B2 with a maximum detected in sample number 9 and decreased following sample 15. Group B3 started with slightly elevated levels of CF which gradually decreased during the time course. Nevertheless, compared to samples obtained from other individuals, only small amounts of CF were found in all sample extracts obtained from subject B. Especially phases B1 and B3 were difficult to interpret with CF not exceeding 5 ng per filter in most samples.

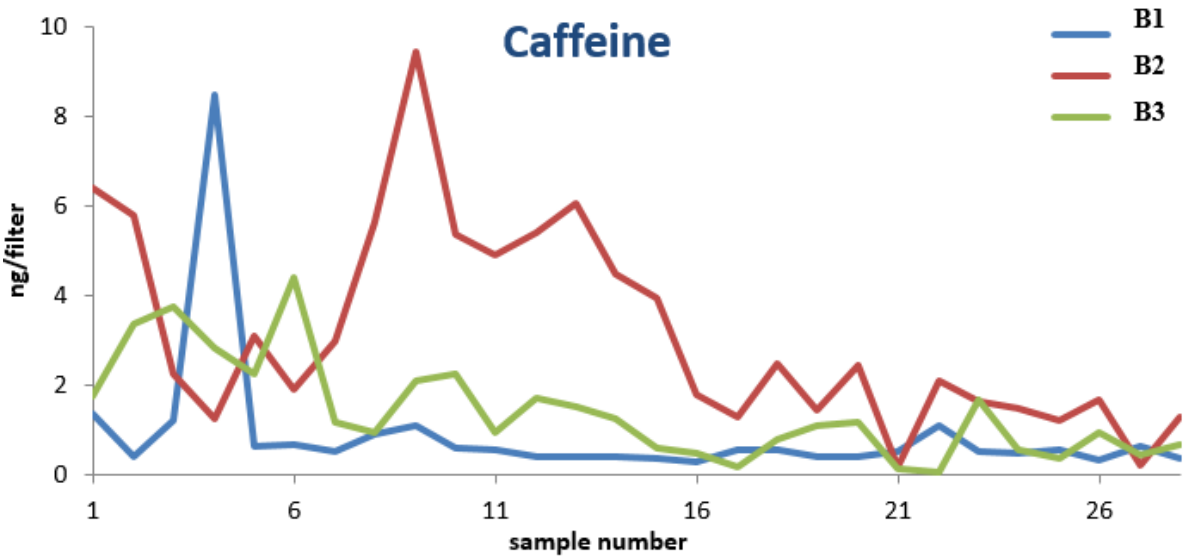

Figure 59: Time course of the amount of CF quantified in sweat samples of subject B during all three phases of the double-blind study.

PX levels stayed below 1.1 ng per filter within the whole sample series B1, while TB levels were clearly elevated with a peak value of 13.1 ng found in sweat sample number 9. Therefore, we assumed that B1 corresponds to the placebo phase of the trial.

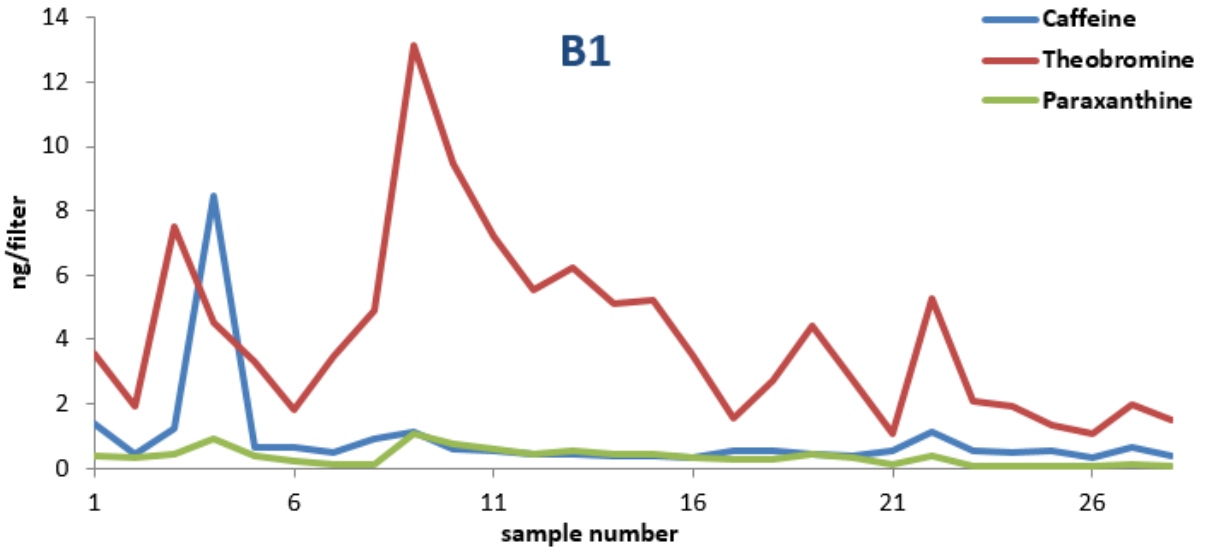

Figure 60: Time course of CF (blue) and its primary metabolites TB (red) and PX (green) quantified in sweat samples of subject B during phase 1 of the double-blind study.

6.4 ng CF, 2.2 ng TB and 1.5 ng PX were detected in sweat sampled at the first day of experimental phase B2. A CF maximum of 9.5 ng was found in sample number 9. TB and PX maxima were found in the sweat sample number 13, which contained 8.8 ng TB and 5.8 ng PX. Amounts of analytes dropped in sample 16 and did not exceed 2.5 ng CF, 2.9 ng TB and 1.7 ng PX during the rest of the time course. PX found within the last couple of days indicated, at least some, consumption of CF. Although data of series B2 was not easy to interpret the series was related to CF intake.

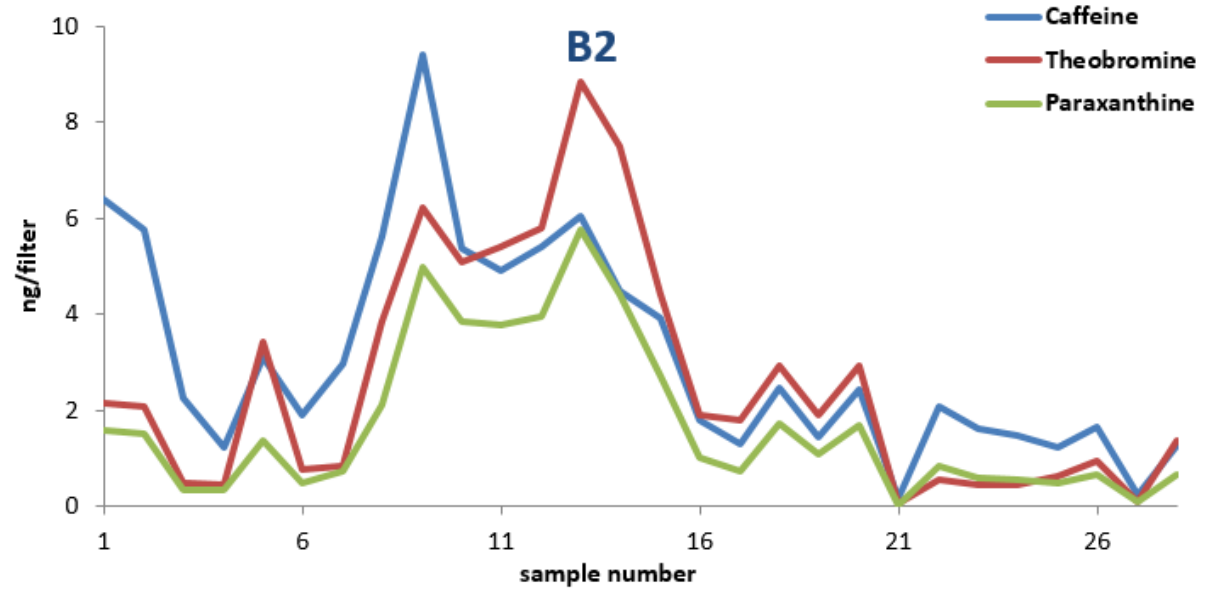

Figure 61: Time course of CF (blue) and its primary metabolites TB (red) and PX (green) quantified in sweat samples of subject B during phase 2 of the double-blind study.

Figure 62 shows the time courses of CF, TB and PX determined in samples B3. All analytes were detected at intermediate and low amounts during the major part of the experiment. CF levels varied

between 4.4 ng per filter and blank levels. The time course started with higher CF levels and decreased during the experiment. TB showed similar behavior with a maximum of 4.7 ng found in sample number 6. PX showed a time course similar to TB with a peak level of 2.9 ng in the same sample, but diminished in samples 21-28. PX levels were merely detectable during the rest of the study. PX levels close to absence during the last eight days of the experiment were regarded as hint indicating that B3 corresponded to the withdrawal phase.

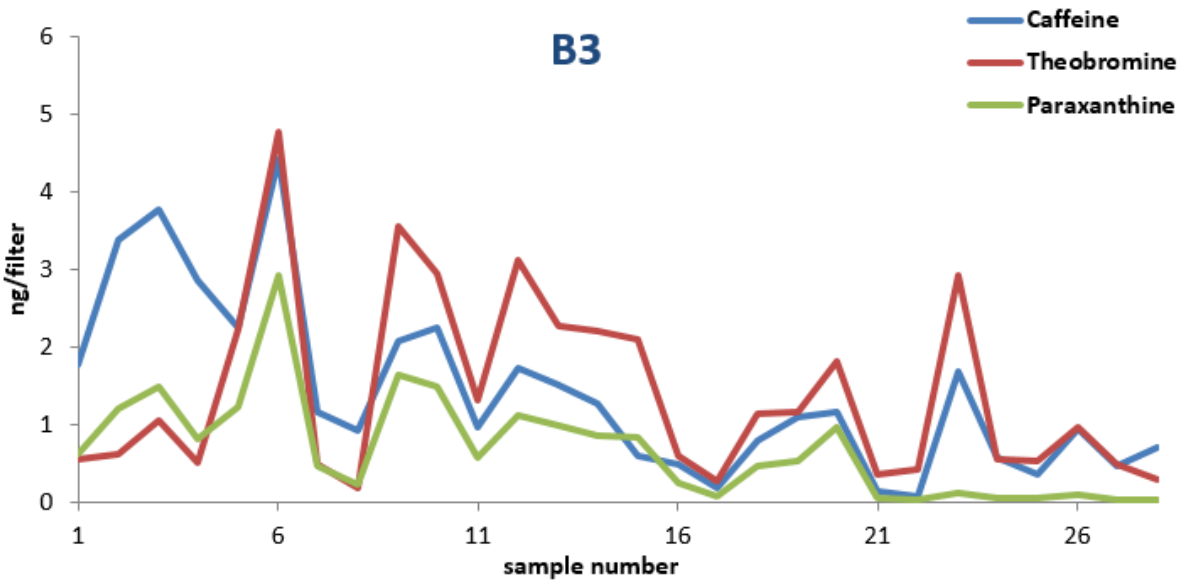

Figure 62: Time course of CF (blue) and its primary metabolites TB (red) and PX (green) quantified in sweat samples of subject B during phase 3 of the double-blind study.

Based on the amounts of CF in the extracted sweat samples sample set C1 was assumed to correspond to a phase of continuous CF intake, whereas decreasing CF levels at the end of series three indicated that C3 corresponded to the withdrawal phase. During the series C2, which was identified as the placebo phase, CF levels were relative high with a maximum of 3.4 ng extracted from sweat sampled on day number 8, when compared to placebo phases of other subjects. Additionally, an increase in CF levels in sample number 24 indicates ingestion of CF containing goods. All curves discussed here are given in Figure 63.

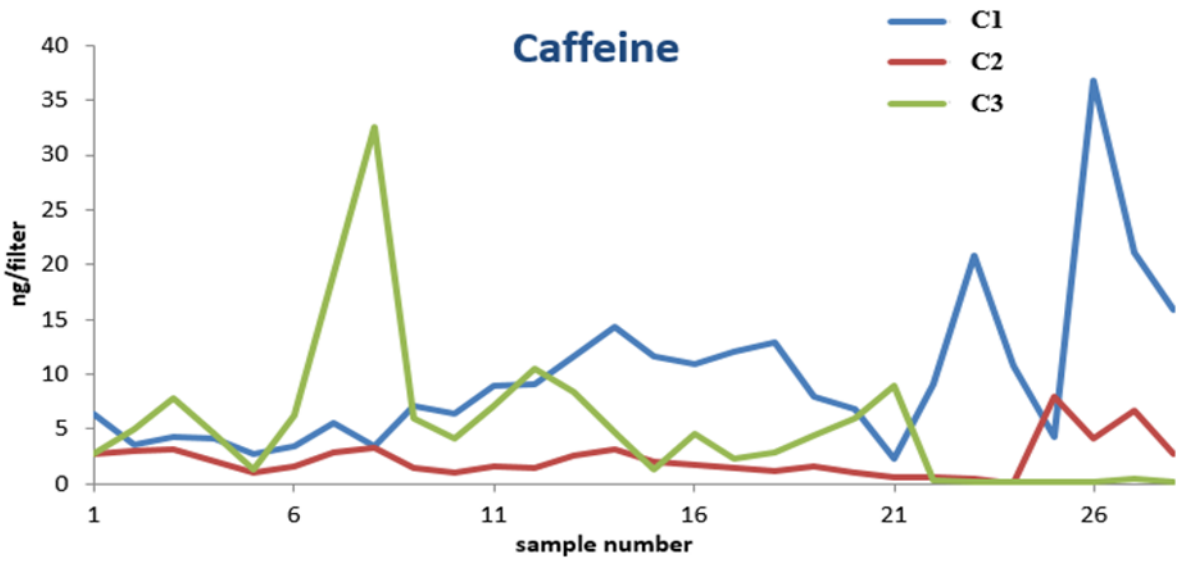

Figure 63: Time course of the amount of CF quantified in sweat samples of subject C during all three phases of the double-blind study.

TB levels were exceptionally high within samples obtained from individual C during any phase of the study, indicating that a TB source, which is likely to contain CF as well, was part of the diet. In series C1 we observed relative low CF levels in the first 8 samples. Then, levels increased and peaked in sample 14 with 14.4 ng CF extracted from the corresponding filter paper. Two sharp and distinct drops of the CF level in samples 21 and 24 were accompanied with CF maxima of 20.9 ng and 36.7 ng found in sweat samples number 23 and 26, respectively. TB and PX levels increased and decreased in parallel to CF, whereas PX was slightly less abundant than CF, while in contrast, TB was remarkably elevated compared to the other analytes. Absolute TB peaks were found in samples 23 and 26 with 60.2 ng and 57.0 ng, respectively.

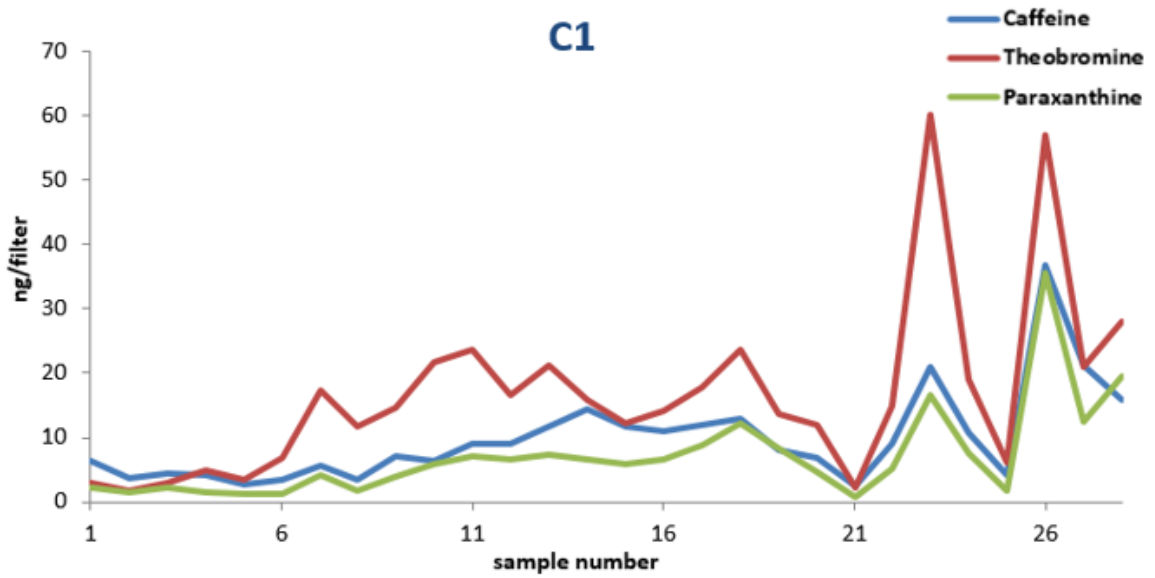

Figure 64: Time course of CF (blue) and its primary metabolites TB (red) and PX (green) quantified in sweat samples of subject C during phase 1 of the double-blind study.

CF amounts stayed in the low- and sub ng per filter range during the major part of the sample series C2, with levels not exceeding 3.4 ng per filter. Nevertheless, an 8 ng per filter CF peak occurred in sample 25. TB levels clearly exceeded CF amounts and varied between 5 ng per filter and 25 ng per filter. PX levels stayed below 2.4 ng per filter during the whole experiment. Therefore, C2 was suggested to correspond to placebo ingestion (Figure 65).

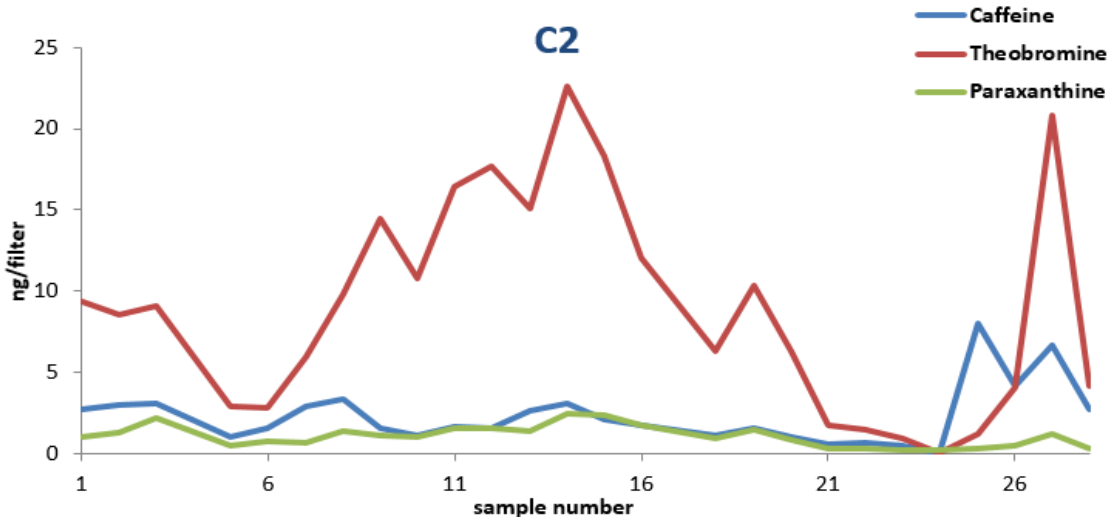

Figure 65: Time course of CF (blue) and its primary metabolites TB (red) and PX (green) quantified in sweat samples of subject C during phase 2 of the double-blind study.

Series C3 (compare Figure 66) was related to the withdrawal phase. Maximum analyte intensities occurred in extracts of sample 7 in case of TB and PX with levels of 25.7 ng per filter and 16.2 ng per filter, respectively, while a maximum CF amount of CF 32.6 ng was determined in sample 8. Analyte levels decreased gradually and dropped towards blank levels in samples corresponding to the last eight days of the series. Interestingly TB was the most abundant metabolite within the mid part of the experiment which was similar in during phases C1 and C2.

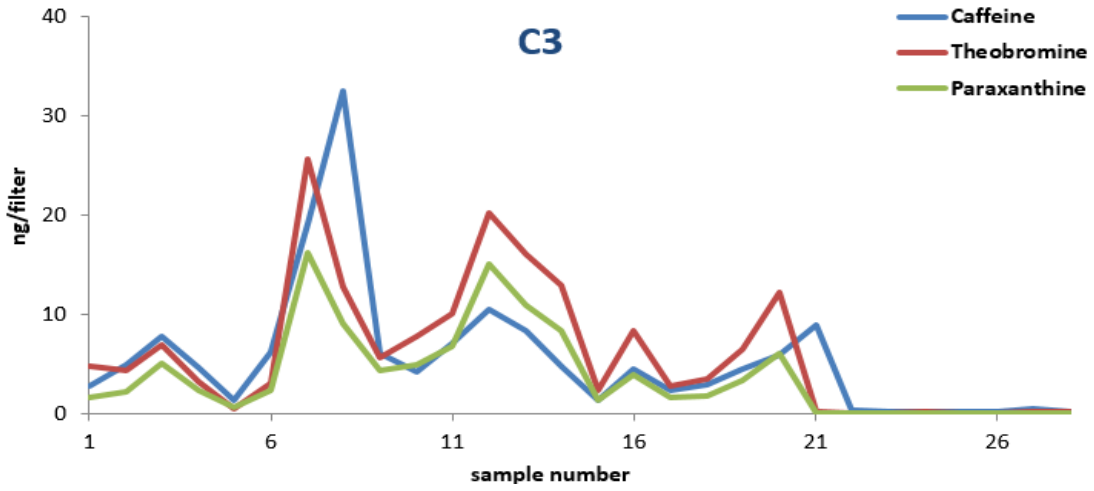

Figure 66: Time course of CF (blue) and its primary metabolites TB (red) and PX (green) quantified in sweat samples of subject C during phase 3 of the double-blind study.

CF amounts quantified in extracts of samples of individual D are given in Figure 67. Sample series D2 corresponded to continuous CF consumption, while datasets D1 and D3 were difficult to interpret. Sample series D3 started with high CF levels peaking with 24.8 ng per filter in sample 2 followed by a rapid decrease of CF and low amounts not exceeding 1 ng, except in samples 21 and 24. Because samples of series D1 showed similar amounts of CF, unambiguous identification of the corresponding phases of the study solely based on CF time courses was not possible.

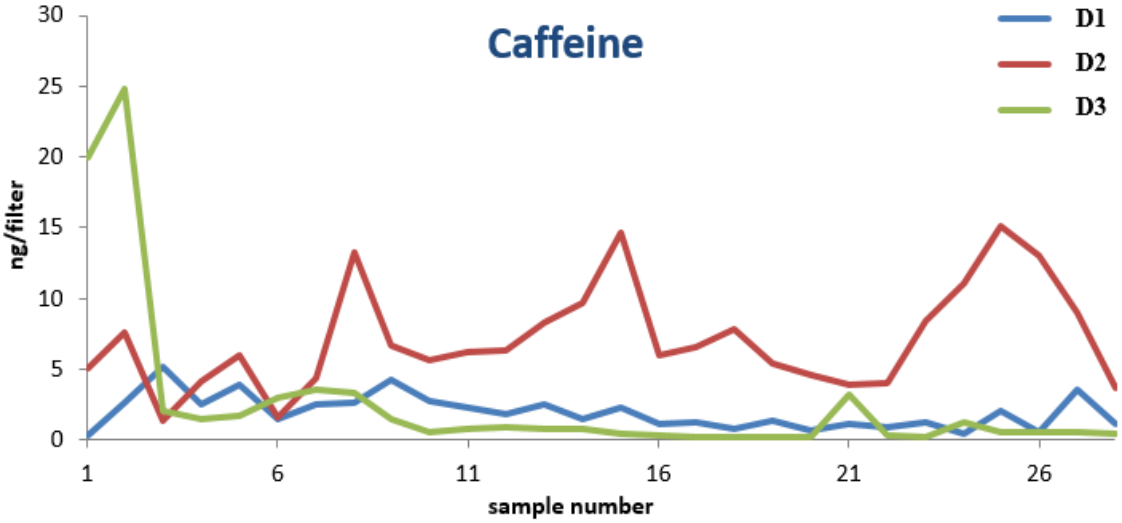

Figure 67: Time course of the amount of CF quantified in sweat samples of subject D during all three phases of the double-blind study.

All investigated analytes started at sub ng levels in the sample D1 01. While CF amounts did not exceed 5.2 ng during the whole sample set, PX levels sharply increased in sample number 9. A PX maximum of 10.2 ng was observed in sample number 15, followed by levels decreasing until the end of the series. TB levels were very similar to PX levels except for a TB maximum of 33.9 ng in sample 27. Especially the time course of PX indicated CF consumption during the first half of the experiment. Therefore, it was assumed that series D1 corresponded to the withdrawal phase.

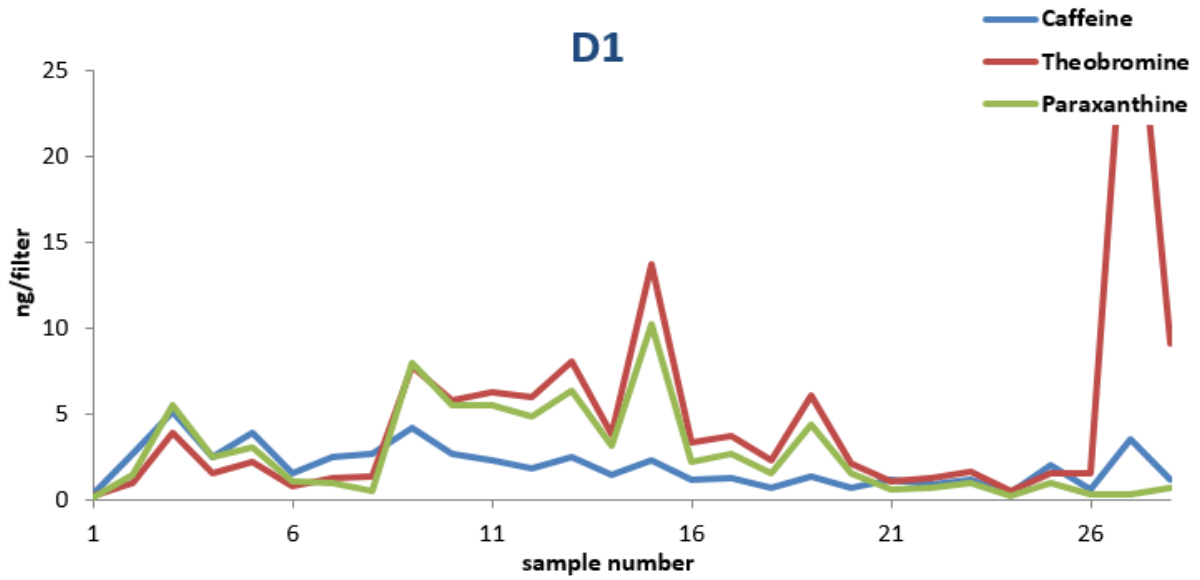

Figure 68: Time course of CF (blue) and its primary metabolites TB (red) and PX (green) quantified in sweat samples of subject D during phase 1 of the double-blind study.

Samples of the series D2 corresponded to regular consumption of CF. All three analytes showed similar levels varying between 5 ng and 20 ng during the major part of the experiment. TB and PX showed maxima of 35.1 ng and 23.7 ng in sample number 26, while a CF maximum of 15.1 ng was determined in sample 25.

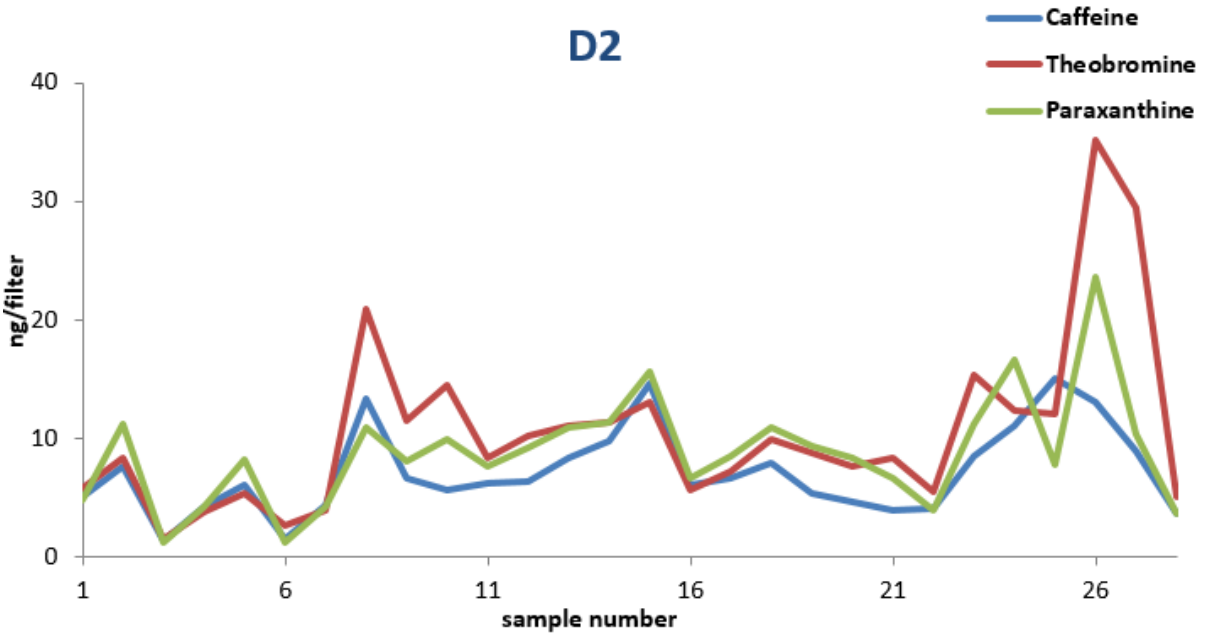

Figure 69: Time course of CF (blue) and its primary metabolites TB (red) and PX (green) quantified in sweat samples of subject D during phase 2 of the double-blind study.

Figure 70 shows the time courses of CF, TB and PX in sweat samples of individual D during the third phase of the study. Peak levels of all metabolites were detected in sample 02, while PX and CF levels

stayed in the low- and sub ng range during the rest of the study. Concluding, sample group D3 was identified as the placebo phase of the study.

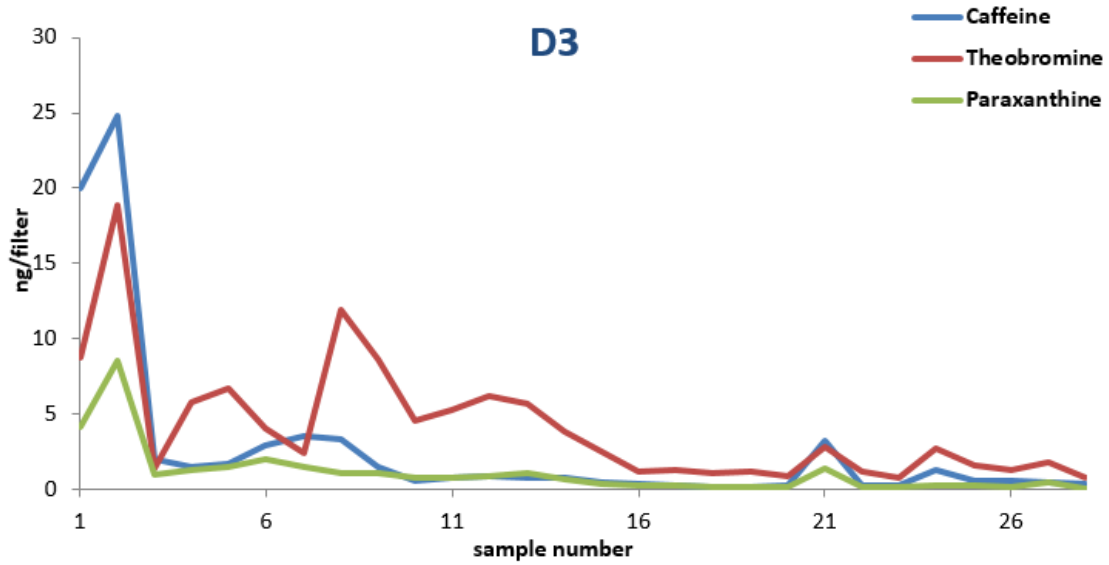

Figure 70: Time course of CF (blue) and its primary metabolites TB (red) and PX (green) quantified in sweat samples of subject D during phase 3 of the double-blind study.

Figure 71 shows CF levels in sweat samples of individual F. CF levels varied between 7 ng and 25 ng during the major part of F2, which was related to the CF ingestion phase of the study, while F1 was easily identified as the placebo phase due to constant low levels of CF within the sample group. F3 was characterized by CF levels varying around 4 ng per filter in extracts of the first four samples followed by a sharp increase in sample 7 and subsequent gradual decrease reaching the sub ng per filter range in samples 22-28. Therefore, sample set F3 was related to the withdrawal phase of the study.

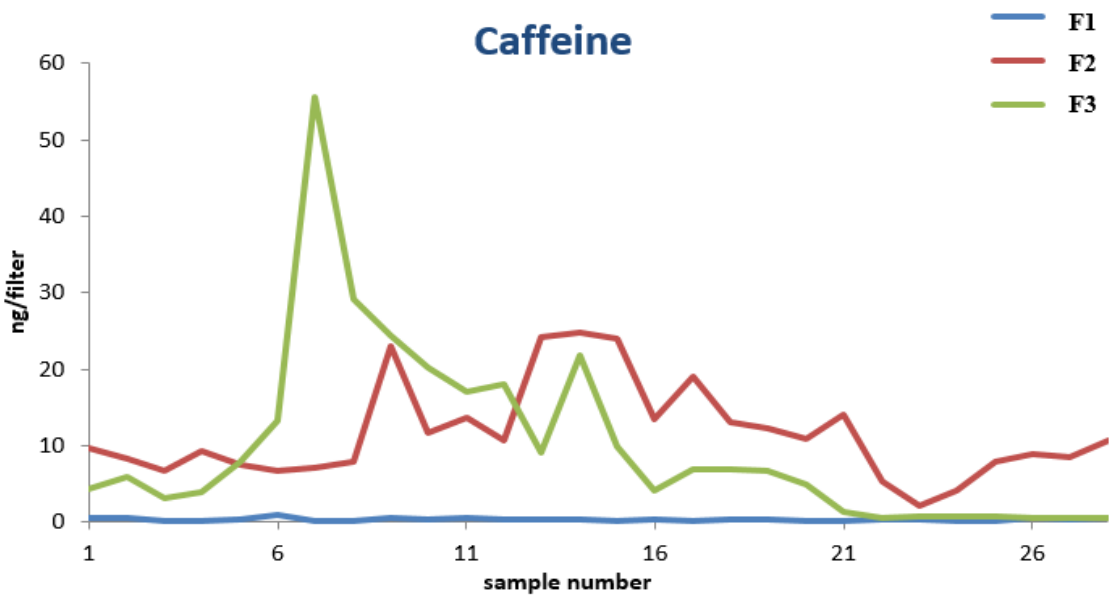

Figure 71: Time course of the amount of CF quantified in sweat samples of subject F during all three phases of the double-blind study.

PX levels in sample set F1 didn't exceed 1.6 ng per filter. TB levels were only elevated in the samples number 6, 9 and 26 to 29.

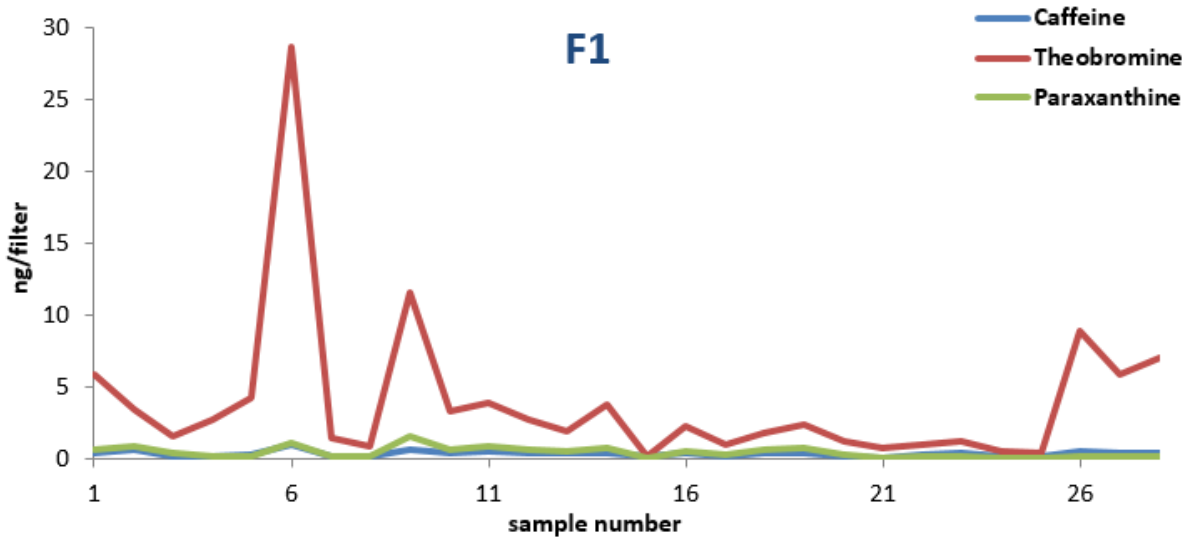

Figure 72: Time course of CF (blue) and its primary metabolites TB (red) and PX (green) quantified in sweat samples of subject F during phase 1 of the double-blind study.

As described above, sweat sampled from subject F during phase two contained relative high levels of CF during the major part of the experiment and was related to continuous ingestion of CF.

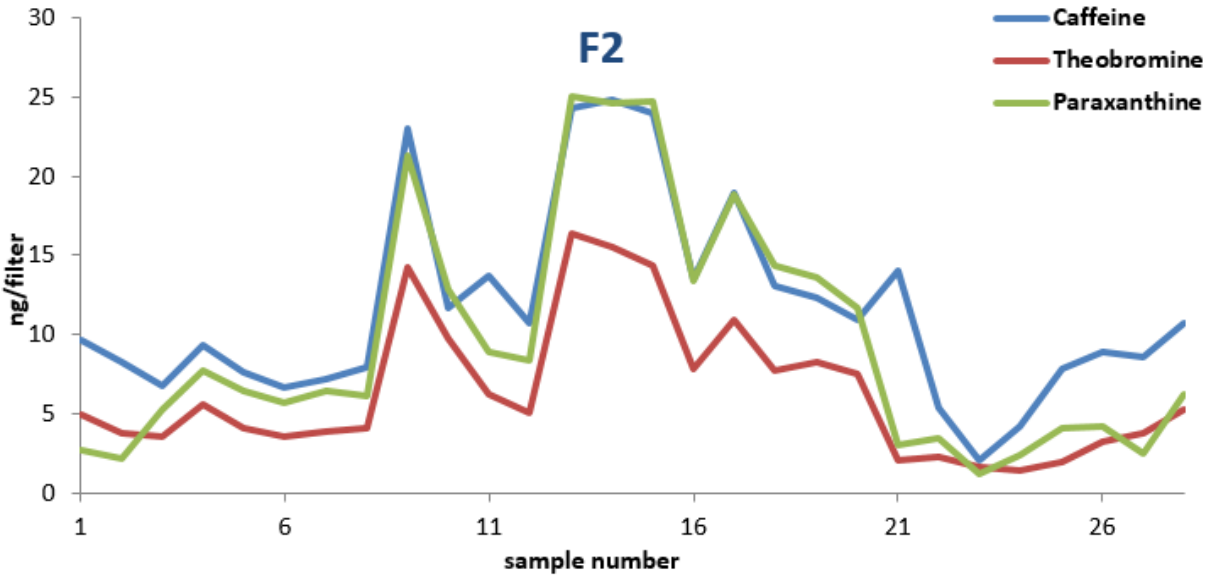

Figure 73: Time course of CF (blue) and its primary metabolites TB (red) and PX (green) quantified in sweat samples of subject F during phase 2 of the double-blind study.

Low levels of all three analytes were observed in the first six samples of F3. After a CF maximum in sample 07, CF levels decreased gradually, while PX and TB levels stayed high in samples 07-14. All

analytes were found in the low- and sub ng range in sample extracts 21 to 28. Therefore, we concluded that subject F underwent CF withdrawal during phase three.

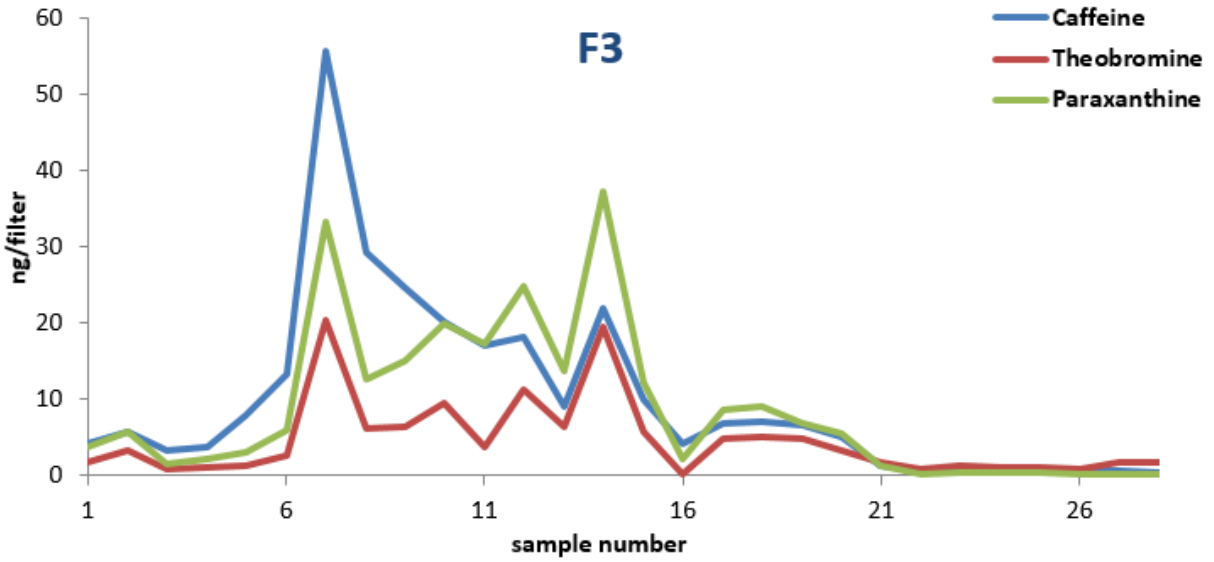

Figure 74: Time course of CF (blue) and its primary metabolites TB (red) and PX (green) quantified in sweat samples of subject F during phase 3 of the double-blind study.

All three phases of the study were unambiguously identified based on the time courses of CF in samples obtained from individual G (Figure 75). G1 was characterized by CF levels varying around 15 ng per filter during the whole batch with a maximum of 37.9 ng found in sample number 15, while CF levels stayed low during entire G2. Sample set G3 corresponded to the withdrawal phase and was characterized by high CF levels in the first third of the sample series followed by declining CF levels.

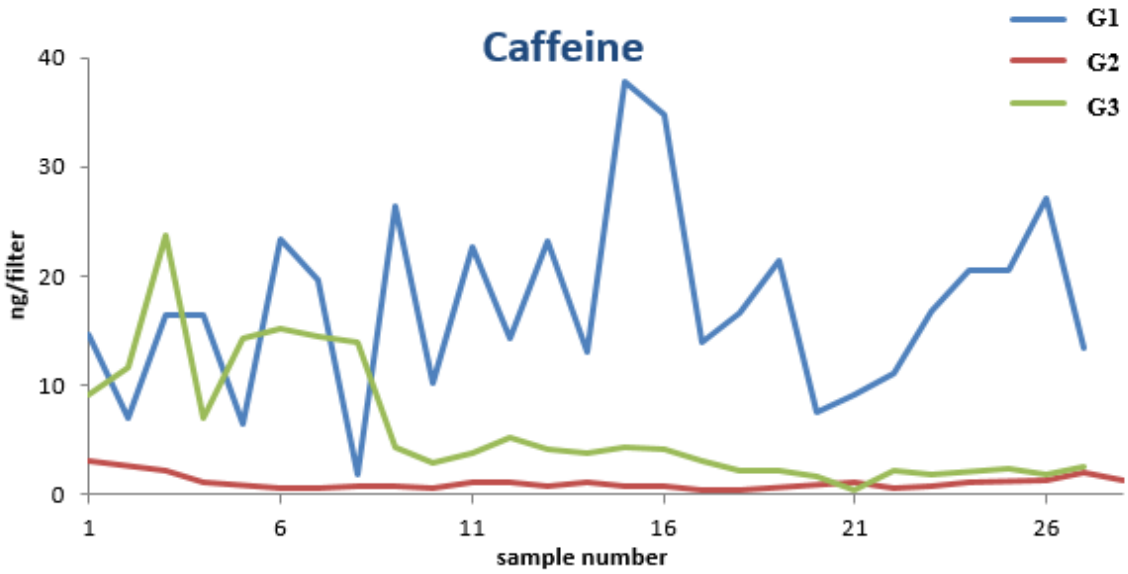

Figure 75: Time course of the amount of CF quantified in sweat samples of subject G during all three phases of the double-blind study.

As described above CF levels varied between 10 ng and 25 ng within the major part of G1. The high PX content within the entire batch is in good consensus with the CF levels and supports the association of the set G1 with continuous CF ingestion. The plots for all three analytes are given in Figure 76.

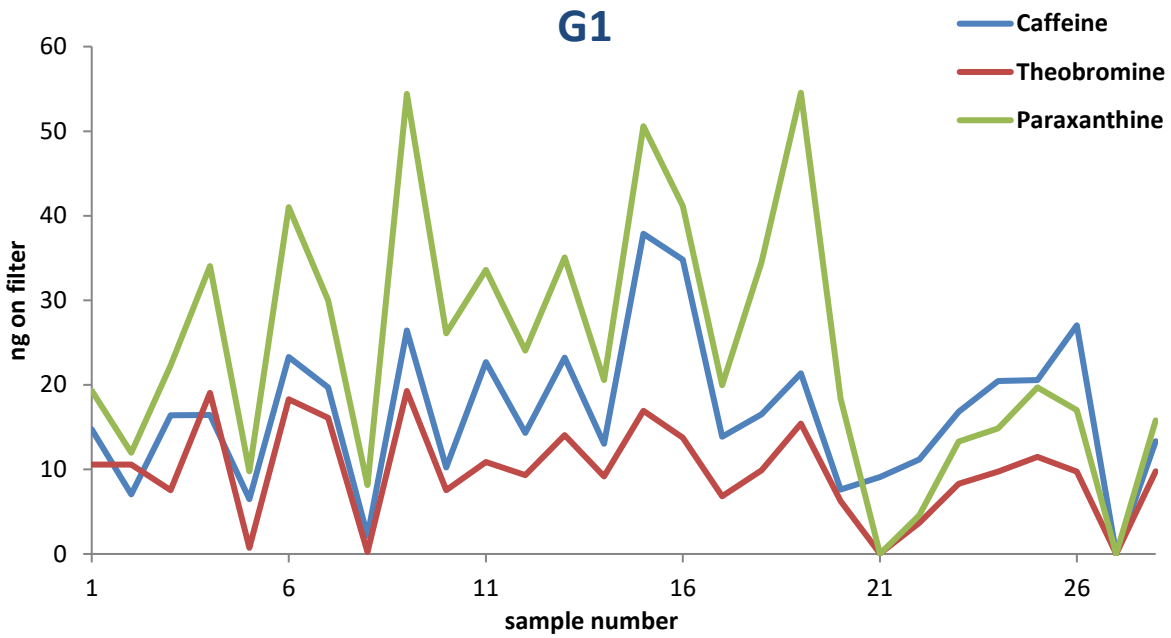

Figure 76: Time course of CF (blue) and its primary metabolites TB (red) and PX (green) quantified in sweat samples of subject G during phase 1 of the double-blind study.

Sample set G2 was characterized by CF and PX levels in the low- and sub ng range for most time points and corresponded to placebo ingestion. Only TB levels were elevated in samples 24 to 28.

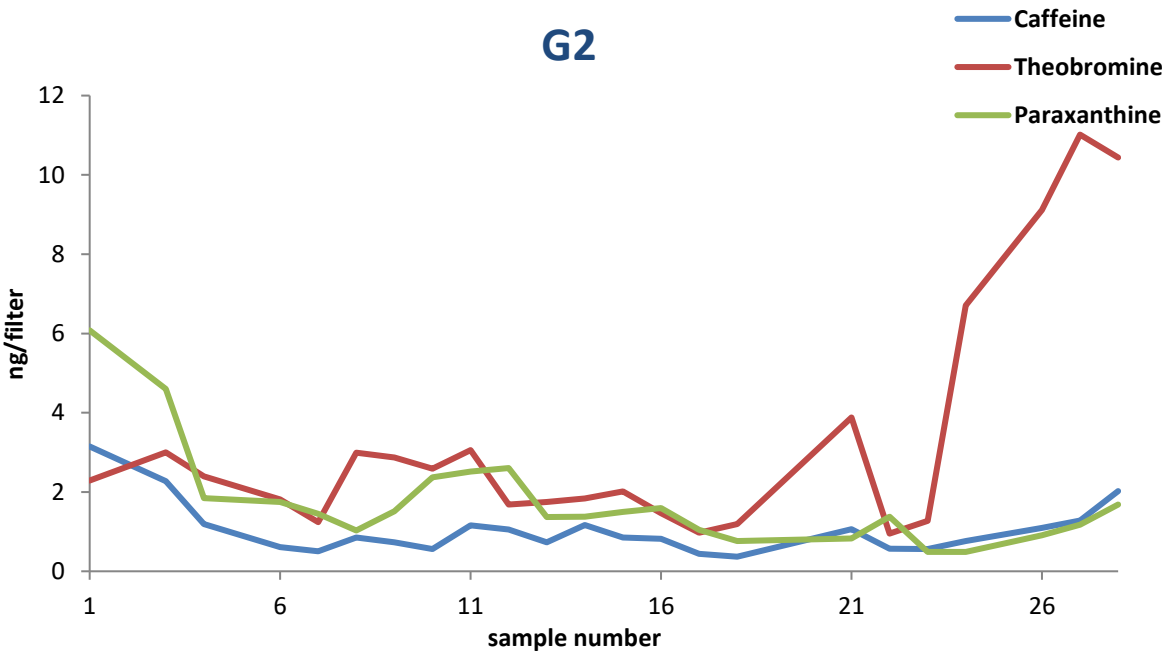

Figure 77: Time course of CF (blue) and its primary metabolites TB (red) and PX (green) quantified in sweat samples of subject G during phase 2 of the double-blind study.

Although increasing PX levels in samples 23 to 27 in set G3 brought some ambiguity into the dataset obtained from subject four, phase three of the experiment could be clearly associated with the withdrawal phase based on the clear trend towards decreasing CF levels during the second half of the experiment, especially when compared to the time courses of CF and PX within G1. Elevated PX levels were accompanied with an intense TB peak in sample 25. Time courses of all four analytes during experiment G3 can be obtained from Figure 78.

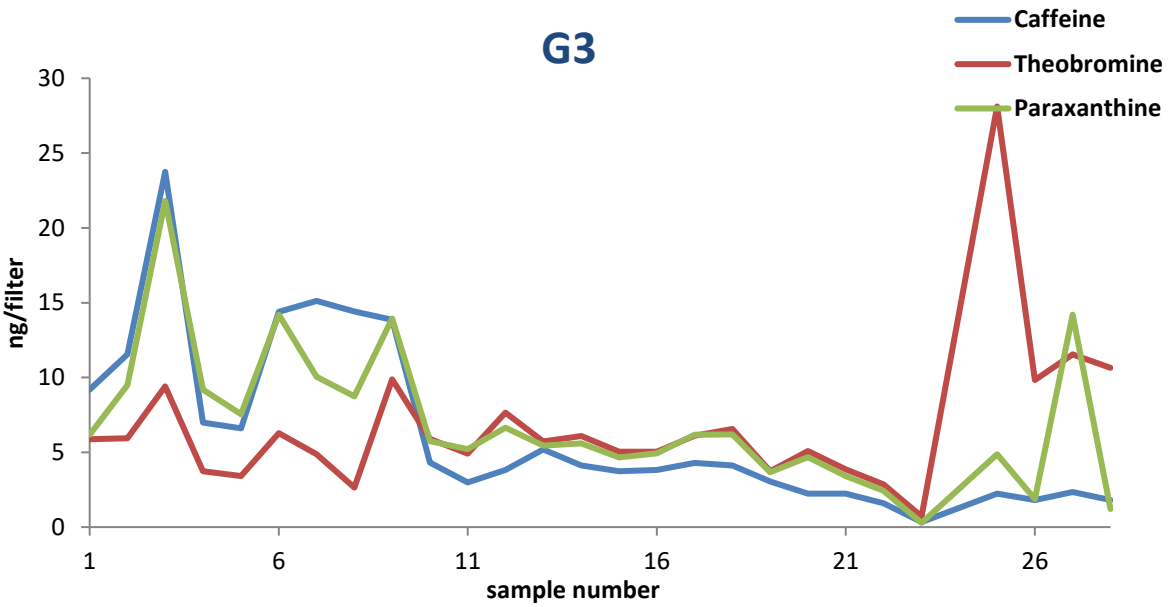

Figure 78: Time course of CF (blue) and its primary metabolites TB (red) and PX (green) quantified in sweat samples of subject G during phase 3 of the double-blind study.

Table of abbreviations:

5-CQA	5-O-Caffeoylquinic acid
AUC	Area under curve
CE	Capillary electrophoresis
CF	Caffeine
CFTCR	Cystic fibrosis transmembrane conductor regulator
CGA	Chlorogenic acid
CID	Collision induced dissociation
CQA	Caffeoylquinic acid
CV	Coefficient of variation
CYP	Cytochrome P450
dd	Data dependent
EDTA	Ethylendiaminetetraacetic acid
ESI	Electro spray ionization
FA	Formic Acid
GC	Gas chromatography

HCD	High energy collision induced dissociation
HILIC	Hydrophilic interaction liquid chromatography
HMDB	Humane metabolome database
HPLC	High performance liquid chromatography
IS	Internal standard
LC	Liquid chromatography
LOD	Limit of detection
LOQ	Limit of quantitation
m/z	Mass -to-charge ratio
MeOH	Methanol
MS	Mass spectrometry
MS^n	Tandem mass spectrometry
MX	Methylxanthine
NAT 2	N-acetyltransferase 2
NCE	Normalized collision energy
NMF	Natural moisturizing factor
NP	Normal phase
PEG	Polyehtylenglycol
PX	Paraxanthine
R^2	Coefficient of determination
rAUC	Relative area under curve
RP	Reversed Phase
RT	Retention time
SC	Stratum corneum
TB	Theobromine
TP	Theophylline
UPLC	Ultra performance liquid chromatography

Table 8: Table of abbreviations

Table of Figures:

Index of Tables:

Literature:

1. **Álvarez-Sánchez, B., Priego-Capote, F. and Luque de Castro, M.D.** Metabolomics analysis I. Selecetion of biological samples and practical aspects preceding sample preparation. *Trends in Analytical Chemistry.* 2010, Vol. 29, 2, pp. 111-119.

2. **Wishart, David S.** Emerging applications of metabolomics in drug discovery and precision medicine. *Nature Reviews Drug Discovery.* 2016, 15, pp. 473-484.

3. **Dettmer, Katja, Aronov, Pavel A. and Hammock, Bruce D.** Mass spectrometry-based metabolomics. *Mass Spectrometry Reviews.* 2007, Vol. 26, 1, pp. 51-78.

4. **Ghaste, Manoj, Mistrik, Robert and Shulaev, Vladimir.** Applications of Fourier Transform Ion Cyclotron Resonance (FT-ICR) and Orbitrap Based High Resolution Mass Spectrometry in Metabolomics and Lipidomics. *International Journal of Molecular Sciences.* 2016, 17, pp. 816-837.

5. **Suhre, Karsten, et al.** Human metabolic individuality in biomedical and pharmaceutical research. *Nature.* 2011, 477, pp. 54-60.

6. **Wishart, David S., et al.** HMDB 3.0—The Human Metabolome Database in 2013. *Nucleic Acids Research.* 2013, 41, pp. D801-D807.

7. **Scalbert, Augustin, et al.** The food metabolome: a window over dietary exposure. *The American Journal of Clinical Nutrition.* 2014, 99, pp. 1286–1308.

8. **Hooton, Kevin, Han, Wei and Li, Liang.** Comprehensive and Quantitative Profiling of the Human Sweat Submetabolome Using High-Performance Chemical Isotope Labelling LC-MS. *Analytical Chemistry.* 2016, 88, pp. 7378-7386.

9. **Nicholson, Jeremy K., Holmes, Elaine and Wilson, Ian D.** Gut microorganisms, mammalian metabolism and personalized health care. *Nature Riviews Microbiology.* 2005, 3, pp. 431-438.

10. **HMDB - The Human Metabolome Database. [Online] The Metabolomics Innovation Center. [Cited: 11 20, 2017.] http://www.hmdb.ca/metabolites?utf8=%E2%9C%93&filter=true&quantified=1&detected=1&filter=true.**

11. Nassar, Ala F., et al. UPLC-MS for metabolomics: a giant step forward in support of pharmaceutical research. *Drug Discovery Today.* 2017, Vol. 22, 2, pp. 463-470.

12. Wang, Thomas J., et al. Metabolite profiles and the risk of developing diabetes. *Nature Medicine.* 2011, Vol. 17, 4, pp. 448-454.

13. Koeth, Robert A., et al. Intestinal microbiota metabolism of L-carnitine, a nutrient in red meat, promotes atherosclerosis. *Nature Medicine.* 2013, Vol. 19, 5, pp. 576–585.

14. Chen, Rui, et al. Personal Omics Profiling Reveals Dynamic Molecular and Medical Phenotypes. *Cell.* 2012, 148, pp. 1293-1307.

15. Stewart, Nicolas A., et al. A UPLC-MS/MS assay of the "Pittsburgh Cocktail": six CYP probe-drug/metabolites from human plasma and urine using stable isotope dillution. *Analyst.* 2011, 136, pp. 605–612.

16. Miller, James M. *Chromatography: Concepts and Contrasts.* 2. New York : Wiley, 2005.

17. Lottspeich, Friedrich. *Bioanalytik.* [ed.] Joachim W. Engels. 3. Heidelberg : Springer Spektrum, 2012.

18. Swartz, Michael E. UPLC: An Introduction and Review. *Journal of Liquid Chromatography & Related Technologies.* 2005, 28, pp. 1253–1263.

19. Ho, C.S., et al. Electrospray Ionisation Mass Spectrometry: Principles and Clinical Applications. *The Clinical Biochemist Reviews.* 2003, 24, pp. 3-12.

20. Adaway, Joanne E., Keevil, Brian G and Owe, Laura J. Liquid chromatography tandem mass spectrometry in the clinical laboratory. ***Annals of Clinical Biochemistry.*** **2015, Vol. 52, 1, pp. 18–38.**

21. Vogeser, Michael and Seger, Christoph. A decade of HPLC–MS/MS in the routine clinical laboratory — Goals for further developments. ***Clinical Biochemistry.*** **2008, 41, pp. 649-662.**

22. Wilm, Matthias. Principles of Electrospray Ionization. ***Molecular & Cellular Proteomics.*** **2011, 10(7), pp. 1–8.**

23. PLANET ORBITRAP. [Online] Thermo Fisher Scientific. [Cited: 04 23, 2017.] http://planetorbitrap.com/q-exactive-hf#tab:schematic.

24. PLANET OBRITRAP. [Online] Thermo Fisher Scientific. [Cited: 04 23, 2017.] http://planetorbitrap.com/q-exactive-hf#tab:features.

25. Kind, Tobias, et al. Identification of small molecules using accurate mass MS/MS search. ***Mass Spectrometry Reviews.*** **2017, 9999, pp. 1-20.**

26. Grosso, Giuseppe, Godos, Justyna and Galvano, Fabio. Coffee, Caffeine, and Health Outcomes: An Umbrella Review. ***Annual Reviews of Nutrition.*** **2017, 37, pp. 131-156.**

27. Ludwig, Iziar A., et al. Coffee: biochemistry and potential impacts on health. ***Food and Function.*** **2014, 5, pp. 1695-1717.**

28. Zulli, Anthony, et al. Caffeine and cardiovascular diseases: critical review of current research. ***European Journal of Nutrition.*** **2016, 55, pp. 1331-1343.**

29. Butt, Masood Sadiq and Sultan, M. Tauseef. Coffee and its Consumption: Benefits and Risks. ***Critical Reviews in Food Science and Nutrition.*** **2011, 51, pp. 363-373.**

30. Muqaku, Besnik, et al. Coffee consumption modulates inflammatory processes in an individual fashion. ***Molecular Nutrition & Food Research.*** **2016, Vol. 60, 12, pp. 2529-2541.**

31. Boettler, Ute, et al. Induction of antioxidative Nrf2 gene transcription by coffee in humans: Depending on the genotype? ***Molecular Biology Reports.*** **2012, 39, pp. 7155–7162.**

32. Lang, Roman, et al. Bioappearance and pharmacokinetics of bioactives upon coffee consumption. ***Analytical and Bioanalytical Chemistry.*** **2013, 405, pp. 8487-8503.**

33. Selby-Pham, S.N., et al. Modelling passive absorption properties of phytochemicals using phytochemical properties. ***Acta horticulturae.*** **2015, 1106, pp. 211-218.**

34. Kim, Jiyoung, et al. Cocoa Phytochemicals: Recent Advances in Molecular Mechanisms on Health. ***Critical Reviews in Food Science and Nutrition.*** **2014, 54, pp. 1458-1472.**

35. Lang, Roman, et al. Development of a Hydrophilic Liquid Interaction Chromatography-HPLC-Tandem Mass Spectrometry Based Stable Isotope Dilution Analysis and Pharmacokinetic Studies on Bioactive Pyridines in Human Plasma and Urine after Coffee Consumption. ***Analytical Chemistry.*** **2010, 82, pp. 1486–1497.**

36. McShae, Andy, Leissle, Kristy and Smith, Mark A. The essence of chocolate: A rich, dark, and well-kept secret. ***Nutrition.*** **2009, 25, pp. 1104-1105.**

37. Rein, Dietrich, et al. Cocoa inhibits platelet activation and function. *The American Journal of Clinical Nutrition.* 2000, 72, pp. 30-35.

38. Ashihara, Hiroshi, Sano, Hiroshi and Crozier, Alan. Caffeine and related purine alkaloids: Biosynthesis, catabolism, function and genetic engineering. *Phytochemistry.* 2008, 69, pp. 841-856.

39. Schroeter, Hagen, et al. (-)-Epicatechin mediates beneficial effects of flavanol-rich cocoa on vascular function in humans. *PNAS.* 2006, Vol. 106, 4, pp. 1024-1029.

40. Agewall, S., et al. Does a glass of red wine improve endothelial function? *European Heart Journal.* 2000, 21, pp. 74–78.

41. Duffy, Stephen J., et al. Short- and Long-Term Black Tea Consumption Reverses Endothelial Dysfunction in Patients With Coronary Artery Disease. *Circulation.* 2001, 104, pp. 151-156.

42. Stein, James H., et al. Purple Grape Juice Improves Endothelial Function and Reduces the Susceptibility of LDL Cholesterol to Oxidation in Patients With Coronary Artery Disease. *Circulation.* 1999, 100, pp. 1050-1055.

43. Magrone, Thea, Russo, Matteo Antonio and Jirillo, Emilio. Cocoa and Dark Chocolate Polyphenols: From Biology to Clinical Applications. *Frontiers in Immunology.* 2017, Vol. 8, 677, pp. 1-13.

44. Ludovic, Valeria, et al. Cocoa, Blood Pressure, and Vascular Function. *Frontiers in Nutrition.* 2017, Vol. 4, 36, pp. 1-12.

45. Alkerwi, Ala'a, et al. Daily chocolate consumption is inversely associated with insulin resistance and liver enzymes in the Observation of Cardiovascular Risk Factors in Luxembourg Study. *British Journal of Nutrition.* 2016, 115, pp. 1661–1668.

46. Arnaud, M. J. Pharmacokinetics and Metabolism of Natural Methylxanthines in Animal and Man. *Handbook of experimental phramacology.* 200. Heidelberg : Springer-Verlag, 2011, pp. 33-91.

47. Kot, Marta and Daniel, Wladyslawa A. Caffeine as a marker substrate for testing cytochrome P450 activity in human and rat. *Pharmacological Reports.* 2008, 60, pp. 789-797.

48. Daly, J.W., Jacobson, K.A. and Ukena, D. Adenosine receptors: development of selective agonists and antagonists. *Progress in clinical and biological research.* 1987, 230, pp. 41-63.

49. Kolahdouzan, Mahshad and Hamadeh, Mazen J. The neuroprotective effects of caffeine in neurodegenerative diseases. *CNS Neuroscience & Therapeutics.* 2017, 23, pp. 272–290.

50. Landi, M.T., Lang, N.P. and Kadlubar, F.F. Human cytochrome P4501A2. *IARC Scientific Publications.* 1999, 148, pp. 173-195.

51. Kuwayama, Kenji, et al. Time-course measurements of caffeine and its metabolites extracted from fingertips after coffee intake: a preliminary study for the detection of drugs from fingerprints. *Analytical and Bioanalytical chemistry.* 2013, Vol. 405, 12, pp. 3945-52.

52. Langbauer, Clemens. Time-course measurements of caffeine and its primary metabolites extracted from fingertips after coffee intake. *Master Thesis, University of Vienna.* 2014.

53. Lang, Roman, et al. Urinary N-methylpyridinium and trigonelline as candidate dietary biomarkers of coffee consumption. *Molecular Nutrition & Food Research.* 2011, 55, pp. 1613-1623.

54. Makowskaa, Joanna, et al. Preliminary studies on trigonelline as potential anti-Alzheimerdisease agent: Determination by hydrophilic interaction liquid chromatography and modeling of interactions with beta-amyloid. *Journal of Chromatography B.* 2014, 968, pp. 101–104.

55. Monteiro, Mariana, et al. Chlorogenic Acid Compounds from Coffee Are Differentially Absorbed and Metabolized in Humans. *The Journal of Nutrition.* 2007, 137, pp. 2196-2201.

56. Clifford, Michael N. Chlorogenic acids and other cinnamates- nature, occurance and dieatary burden. *Jornal of the Science of Food and Agriculture.* 1999, 79, pp. 362-372.

57. Renouf, Mathieu, et al. Dose–response plasma appearance of coffee chlorogenic and phenolic acids in adults. *Molecular Nutrition & Food Research.* 2014, 58, pp. 301–309.

58. Baroni, Adone, et al. Structure and function of the epidermis related to barrier properties. *Clinics in Dermatology.* 2012, 30, pp. 257–262.

59. Bouslimani, Amina, et al. Molecular cartography of the human skin surface in 3D. *PNAS.* 2015, Vol. 112, 17, pp. E2120-E2129.

60. Menon, Gopinathan K., Cleary, Gary W. and Lane, Majella E. The structure and function of the stratum corneum. *International Journal of Pharmaceutics.* 2012, 435, pp. 3– 9.

61. Taylor, Nigel A. S. and Machado-Moreira, Chrisitano A. Regional variations in transepidermal water loss, eccrine sweat gland densitiy, sweat secretion rates and electrolyte composition in resting and exercising humans. *Extreme Physiology & Medicine.* 2013, Vol. 2, 4, pp. 1-29.

62. Sato, K., et al. Biology of sweat glands and their disorders. I. Normal sweat gland function. *Journal of the American Academy of Dermatology.* 1989, Vol. 20, 4, pp. 537-563.

63. Wilke, K., et al. A short history of sweat gland biology. *International Journal of Cosmetic Science.* 2007, 29, pp. 169–179.

64. Coulson, I.H. Disorders of Sweat Glands. [book auth.] Tony Burns, et al. *Rook's Textbook of Dermatology.* 8. s.l. : Blackwell Publishing Ltd., 2010, Vol. 1.

65. Layton, A.M. Disorders of the Sebaceous Glands. [book auth.] Tony Burns, et al. *Rook's Textbook of Dermatology.* 8. s.l. : Blackwell Publishing Ltd., 2010, Vol. 1.

66. van Dam, Annemieke, et al. Techniques that acquire donor profiling information from fingermarks- A review. *Science and Justice.* 2016, 56, pp. 143-154.

67. Ogawa, Tokuo and Bullard, Robert W. Characteristics of subthreshold sudomotor neural impulses. *Journal of Applied Physiology.* 1972, Vol. 33, 3, pp. 300-305.

68. Ando, H. and Noguchi, R. Dependence of palmar sweating response and central nervous system activity on the frequency of whole-body vibration. *Scandinavian Journal of Work, Environment and Health.* 2003, Vol. 29, 3, pp. 216-219.

69. Park, Soon Ja and Tamura, Teruko. Distribution of Evaporation Rate on Human Body Surface. ***The Annals of Physiological Anthropology.*** **1992, Vol. 11, 6, pp. 593-609.**

70. Mena-Bravo, A. and Luque de Castro, M.D. Sweat: A sample with limited present applications and promising future in metabolomics. ***Journal of Pharmaceutical and Biomedical Analysis.*** **2014, 90, pp. 139-147.**

71. Shibasak, Manabu and Crandall, Craig G. Mechanisms and controllers of eccrine sweating in humans. ***Frontiers in Bioscience (Scholar Edition).*** **2011, 2, pp. 685-696.**

72. Sonner, Z., et al. The microfluidics of the eccrine sweat gland, including biomarker partitioning, transport, and biosensing implications. ***Biomicrofluidics.*** **2015, Vol. 9, 031301, pp. 1-19.**

73. Cui, Chang-Yi and Schlessinger, David. Eccrine sweat gland developement and sweat secretion. ***Experimental Dermatology.*** **2015, 24, pp. 644-650.**

74. Papanas, N., et al. A simple new non-invasive sweat indicator test for the diagnosis of diabetic neuropathy. ***Diabetic Medicine.*** **2012, pp. 525-534.**

75. Tsunada, Makoto, et al. Noninvasive monitoring of plasma L-dopa concentrations using sweat samples in Parkinson's disease. ***Clinica Chimica Acta.*** **2015, 442, pp. 52-55.**

76. Harker, Mark and Harding, Clive R. Amino acid composition, including key derivatives of eccrine sweat: potential markers of certain atopic skin conditions. ***International Journal of Cosmetic Sciences.*** **2013, 35, pp. 163-168.**

77. Calderón-Santiago, Mónica, et al. Human sweat metabolomics for lung cancer screening. ***Analytical and Bioanalytical Chemistry.*** **2015, 407, pp. 5381-5392.**

78. Kutyshenko, Viktor P., et al. Analyzing and Mapping Sweat Metabolomics by High-Resolution NMR Spectroscopy. ***PLoS ONE.*** **2011, Vol. 6, 12, pp. 1-9.**

79. Rafeeq, Misbahuddin M. and Murad, Hussam Aly Sayed. Cystic fibrosis: current therapeutic targets and future approaches. ***Journal of Translational Medicine.*** **2017, Vol. 15, 84, pp. 1-9.**

80. HMDB-The Human Metabolome Database. [Online] The Metabolomic Innovation Center. [Cited: 11 20, 2017.] http://www.hmdb.ca/metabolites?utf8=%E2%9C%93&filter=true&quantified=1&detected=1&sweat=1&endogenous=1&filter=true.

81. de la Torre, Rafael and Pichini, Simona. Usefulness of Sweat Testing for the Detection of Cannabis Smoke. ***Clinical Chemistry.*** **2004, Vol. 50, 11, pp. 1961-1962.**

82. Brunet, Bertrand R., et al. Development and validation of a solid-phase extraction gas chromatography–mass spectrometry method for the simultaneous quantification of methadone, heroin, cocaine and metabolites in sweat. ***Analytical and Bioanalytical Chemistry.*** **2008, 392, pp. 115–127.**

83. De Alcaraz-Fossoul, Josep, et al. Determination of latent fingerprint degradation patterns- a real fieldwork study. ***International Journal of Legal Medicine.*** **2013, 127, pp. 857–870.**

84. Atherton, Tom, et al. Analysis of amino acids in latent fingerprint residue by capillary electrophoresis-mass spectrometry. *Journal of Separation Sciences.* 2012, 35, pp. 2994-2999.

85. Bouslimani, Amina, et al. Lifestyle chemistries from phones for individual profiling. *PNAS.* 2016, Vol. 113, 48, pp. E7645-E7654.

86. Kuwayama, K., et al. Effectiveness of saliva and fingerprints as alternative specimens to urine and blood in forensic drug testing. *Drug Testing and Analysis.* 2016, 8, pp. 644-651.

87. Cadd, Samuel, et al. Fingerprint composition and aging: A literature review. *Science and Justice.* 2015, 55, pp. 219–238.

88. Sears, V.G., et al. A methodology for finger mark research. *Science and Justice.* 2012, Vol. 52, 3, pp. 145-160.

89. Croxton, Ruth S., et al. Variation in amino acid and lipid composition of latent fingerprints. *Forensic Science International.* 2010, 199, pp. 93-102.

90. Girod, Aline, Ramotowski, Robert and Weyermann, Céline. Composition of fingermark residue: A qualitative and quantitative review. *Forensic Science International.* 2012, 223, pp. 10–24.

91. de Pruit, Marcel, Ismail, Mahado and Xu, Xiaoma. LCMS Analysis of Fingerprints, the Amino Acid Profile of 20 Donors. *Journal of Forensic Sciences.* 2014, Vol. 59, 2, pp. 364-370.

92. Hauser, Christoph. Messung von Koffein und seiner primären sowie sekundären Metaboliten im Zeitverlauf aus dem Fingerabdruck. *Bachelor Thesis, University of Applied Sciences Vienna.* 2015.

93. Langer, Tobias Fridtjof. Zeitabhängige Bestimmung von Koffein und seinen Metaboliten in Fingerabdrücken. *Bachelor Thesis, University of Vienna.* 2015.

94. Bradley, E. L., et al. Method of test and survey of caprolactam migration into foods packaged in nylon-6. *Food Additives & Contaminants.* 2004, 21, pp. 1179-1185.

95. Raiszadeh, Michelle M., et al. A Proteomic Analysis of Eccrine Sweat: Implications for the Discovery of Schizophrenia Biomarker Proteins. *Journal of Proteome Research.* 2012, 11(4), pp. 2127-2139.

96. Schwarz, Thomas. Mechanisms of UV-induced immunosuppression. *The Keio Journal of Medicine.* 2005, 54, pp. 165-171.

97. mzCloud - Advanced Mass Spectral Database. [Online] HighChem LLC, Slovakia. [Cited: 04 23, 2017.] https://www.mzcloud.org/Features.